uOttawa

Modeling Human Dynamics for Powered Exoskeleton Control

Andrew James John Smith

Thesis submitted to the
Faculty of Graduate and Postdoctoral Studies
In partial fulfilment of the requirements
for the Doctorate in Philosophy of Health Science
University of Ottawa

Abstract

Lower extremity powered exoskeletons (LEPE) are powered orthoses that enable persons with spinal cord injury (SCI) to ambulate independently. Since locomotor therapy must be specific and resemble natural gait patterns, to promote motor recovery, current LEPE control architectures may be inappropriate since they typically use able-bodied, pre-recorded reference position and force data, at normal walking speeds, to define exoskeleton motion and predict torque assistance. This thesis explored two aspects: a) able-bodied walking dynamics between 0.2 m/s and the person's self-paced speed to provide a biomimetic basis for LEPE control and b) musculoskeletal modelling of LEPE-human dynamics. For walking dynamics, appropriate regression equations were developed for stride, kinematic, and kinetic parameters. These equations can be used by LEPE designers when constructing angular trajectories and forces for LEPE control at any given speed. An inflection point at 0.5 m/s was identified for temporal stride parameters; therefore, different walking strategies should be considered for walking above and below this point. The full body musculoskeletal model (Anybody) of persons with SCI using the ARKE LEPE incorporated all external contact forces and inertial properties (exoskeleton and person) and was driven using real LEPE SCI user kinematics and kinetics. For the lower extremity, large dorsiflexion range of motion, large device anterior tilt, incomplete knee extension, and uncontrolled center of pressure forward progression lifted the heel during stance. This triggered step termination before trajectory tracking at the knee and hip was complete, thereby reducing hip extension, increasing knee flexion through stance, increasing knee and hip support moments, and increasing thigh and shank strap reaction forces. This also shortened effective participant limb-length, further shortening step-length and LEPE walking speed. For the upper-limbs, LEPE users walked with more anterior trunk tilt and twice the shoulder flexion angle, compared with persons with incomplete SCI. This increased forces and moments at the crutch, shoulder, and elbow. Crutch floor contact periods were 30-40% longer, resulting in upper-extremity joint impulses 5 to 12 times greater than previously reported. Improved step-completion and upright posture would reduce support loads on the crutches and upper-limbs, and would further improve LEPE-human lower limb interaction forces. Improved upright posture and LEPE-human interaction forces would enhance mobility and quality of movement for people with SCI.

Table of Contents

List of tables

List of figures

List of abbreviations

3D: Three dimensional
AB: Able-bodied
ABD: Abduction
ABS: Absorption
ADD: Adduction
AFO: Ankle foot orthosis
AMS: AnyBody Modeling System
ANOVA: Analysis of variance
ANT: Anterior
BW: Body weight
CAREN: Computer assisted rehabilitation environment
COP: Center of pressure
CV: Coefficient of variability
DF: Dorsiflexion
DOF: Degrees of freedom
DST: Double-support-time
EMG: Electromyography
ER: External rotation
Ext: Extension
Flx: Flexion
GC: Gait cycle
GEN: Generation
GFB: GaitFullBody
GH: Glenohumeral
GRF: Ground reaction force
HAL: Hybrid Assistive Lim
INF: Inferior
IR: Internal rotation
IRGO: Isocentric reciprocating gait orthosis
iSCI: Incomplete spinal cord injury
Kmat: Kinematics
Knet: Kinetics
LAT: Lateral
LC: Left crutch
LCL: Left-crutch-loading
LCOFF: Left-crutch-on
LCR: Left-crutch-repositioning
LEPE: Lower extremity powered exoskeleton
LF: Left Foot
LFON: Left-foot-ground-contact
MED: Medial
NR: Not reported
PF: Plantarflexion
POS: Posterior
Q2: Second order quadratic
Q3: Third order quadratic
R^2: Coefficient of Determination
RC: Right crutch
RCL: Right-crutch-loading
RCOFF: Right-crutch-off
RCOFF: Right-crutch-on
RCR: Right-crutch-repositioning
Reg: Regression
RF: Right Foot
RFON: Right-foot-on
ROM: Range of motion
SCI: Spinal cord injury
SD: Standard deviation
SP: Self-pace
SS: Single-support-time
SUP: Superior
SWR: slow walking specific regression equations
TOHRC: The Ottawa Hospital Rehabilitation Centre
UE: Upper-extremity
WPAL: Wearable power assist locomotor

Acknowledgments

First, I would like to acknowledge and thank my supervisors, Edward Lemaire and Julie Nantel, for their support and guidance. Second I would like to thank my friend and colleague Brandon Fournier, for all his work in the development of the LEPE-human SCI model. Additionally, I would like to thank Jamie MacDougal and Dorothyann Curran at the Ottawa Hospital Research Institute's Center for Rehabilitation Research and Development for their continued support. I would as well like to thank the Ontario Centres of Excellence, Bionik Laboratories, and Natural Sciences and Engineering Research Council of Canada for funding the research in this thesis.

I would also like to thank the following individuals:

Staff of The Ottawa Hospital Rehabilitation Centre

Andrew Herbert-Copley
Courtney Bridgewater
Joao Tomas
Louis Goudreau

Bionik Laboratories Incorporated

William Song
Aleksander Wyszynski
Amir Takhmar

Students at The Ottawa Hospital Rehabilitation Centre

Johnny Farah
Kyle Daines

Finally, I would like to sincerely thank the volunteers who donated their time to participate in this research.

Thesis outline

Chapter 1 delivers a general introduction, thesis rational, objectives, and thesis contributions.

Chapter 2 provides a literature review of lower extremity powered exoskeletons (LEPE). The first part contains background knowledge on LEPE. The second and third parts provide background on LEPE control and motor adaptation to different gait speeds. The fourth part provides a methodological review of LEPE-human interaction models.

Chapters 3 to 6 contain articles from this research that were published or submitted for publication.

Chapter 7 summarises thesis findings, discussions, limitations, future directions, and conclusions.

Chapter 1. Introduction

Over the last decade, advances have been made in lower extremity powered exoskeletons (LEPE). A number of LEPE devices designed specifically for people with paraplegia have emerged on the market and research into their use continues. LEPE for persons with paraplegia typically use onboard sensor technology to determine a user's movements, such as leaning forward or side-to-side. This sensor technology allows the exoskeleton to determine the intended activity, including when the user wants to walk or stop. The activity is carried out by LEPE actuators in parallel with the user's joints. Built-in controllers calculate joint angles and assistive torques for the intended activity, typically based on able-bodied trajectories, and then the LEPE provides all moments and forces to move the person.

According to motor control and learning theory, recovery of motor function following neurological injury requires user involvement (effort) and therapeutic interventions that mimic activities of daily living (biomimetic) (Dobkin et al., 2006; Harkema, 2001; Harkema et al., 2012; Kaelin-Lane, Sawaki, & Cohen, 2005; Moseley, Stark, Cameron, & Pollock, 2005). However, robotically guided movement with minimal variability can reduce the required effort on the learner's motor system to rediscover the principles needed to complete the task (Marchal-Crespo & Reinkensmeyer, 2009). This "slacking" may actually decrease motor adaptation and harm a patient's recovery (Claros, Soto, Gordillo, Pons, & Contreras-Vidal, 2016; Crespo & Reinkensmeyer, 2008; Huo, Mohammed, Moreno, & Amirat, 2016; Marchal-Crespo & Reinkensmeyer, 2009; Schmidt & Bjork, 1992).

Impedance or adaptive control, based on the principles of assist-as-needed, have been used to control LEPE and may prevent slacking by tuning LEPE assistance to the user's ability (Emken, Benitez, & Reinkensmeyer, 2007; Reinkensmeyer, Akoner, Ferris, & Gordon, 2009). This control strategy changes LEPE assistance based on user deviation from desired LEPE-human interaction torque and position trajectories (Ibarra, Santos, Krebs, & Siqueira, 2014; Rajasekaran, Aranda, & Casals, 2015b, 2015a, 2016; Sup, Bohara, & Goldfarb, 2008). However, to assist gait at different walking speeds and user abilities, position and interaction torque trajectories need to be tuned to speed dependent gait cycle parameters. This requires multiple reference trajectories and joint torques at a variety of speeds to accommodate LEPE user needs and ability.

The wealth of literature on walking speed effects on gait biomechanics could be used to define position and force inputs for LEPE control (Borghese, Bianchi, & Lacquaniti, 1996; Bovi, Rabuffetti, Mazzoleni, & Ferrarin, 2011; Han & Wang, 2011; Lelas, Merriman, Riley, & Kerrigan, 2003; Li, Haddad, & Hamill, 2005; Murray, Mollinger, Gardner, & Sepic, 1984; Tommy Oberg & Karsznia, 1994; Schwartz, Rozumalski, & Trost, 2008). However, nearly all biomechanics literature involves faster speeds than LEPE users, who typically walk at 0.1 m/s to 0.55 m/s (Aach et al., 2014; Arazpour et al., 2013, 2012; Benson, Hart, Tussler, & Middendorp, 2016; Farris et al., 2014; Fineberg et al., 2013; Kressler et al., 2014; Neuhaus, 2011; Ohta et al., 2007; Tanabe, Hirano, & Saitoh, 2013; Zeilig et al., 2012). Therefore, the majority of gait parameter data from earlier studies are inappropriate for defining LEPE control parameters. An improved understanding of slow walking (<0.5 m/s) stride parameters, kinematics, and kinetics at speeds achievable by device users would provide the necessary information to develop an effective LEPE control strategy (Rajasekaran, 2015).

To improve LEPE control, research could involve iterative device testing on users, which require expensive and intensive user training. A modelling framework could improve LEPE design efficiency, safety, and provide a means to better understand human-machine interaction when developing LEPE control architecture. Musculoskeletal modeling can calculate underlying human variables (forces, muscle-lengths, reactions of joints, bone, muscle, and tendon) and, when combined with CAD modeling software, allow for human-machine interaction analysis. However, existing models are insufficient to achieve these evidence-based design goals.

Within the sparse literature on LEPE-human models, no LEPE-human model has been driven with realistic slow walking joint trajectories and ground reaction forces (GRF). As well, due to the lack of available biomechanical data on LEPE users, no LEPE-human model has simulated LEPE use with real LEPE user kinematic data. Though most exoskeletons require crutches to remain upright, no model has simulated LEPE use with instrumented crutches that measure axial load during device use.

Since walking slowly is considered to be more complex (Schablowski-Trautmann & Gerner, 2006) and uses different locomotor and postural control strategies (Holden, Chou, & Stanhope, 1997; Nymark, Balmer, Melis, Lemaire, & Millar, 2005; Otter, Geurts, Mulder, & Duysens, 2004), LEPE controls may be improved with appropriate slow gait biomechanics. Up to this point LEPE have been developed without taking into account the needs and characteristics of LEPE users. “Research and practical experience show that systems which neglect ergonomics, particularly human-machine interaction, are more likely to give rise to occupational diseases, operating errors and accidents” (Flaspöler, Hauke, Pappachan, & European Agency for Safety and

Health at Work, 2010). LEPE share an intimate mechanical interaction with humans. Gaps in our understanding of human dynamics with LEPE control, and in our ability to measure human-machine interaction, should not be neglected and merit further investigation.

1.1 Rational

In this early stage of LEPE development, LEPE require users to adapt to the device, versus adapting the device to the user. In part, this is due to limited biomechanical data characterising speed dependent gait parameters of able-bodied persons walking at very slow speeds and limitations in our ability to appropriately measure human-machine interaction. To improve LEPE performance, safety, and design, a framework for measuring and tuning LEPE slow walking dynamics and human-machine interactions are required.

1.2 Thesis Objective

The main goal of this thesis was to advance LEPE control by studying human dynamics. The first objective was to define how able-bodied persons walk at very slow speeds, consistent with LEPE use. The second objective was to develop and apply a comprehensive LEPE-human spinal cord injured (SCI) musculoskeletal model to solve human-machine dynamics based on real LEPE user biomechanics. This research is relevant to LEPE developers who should accommodate speed dependent gait biomechanics into LEPE control.

1.3 Thesis Contributions

1. A consistent stride parameter inflection point at 0.5 m/s was discovered, identifying a change in gait strategy at very slow walking speeds that favours greater ground contact time. Implementing this strategy into LEPE control could improve dynamic stability.
2. Regression equations were published to compute stride parameters, sagittal gait kinematics, and sagittal gait kinetics across a wide range of walking speeds. These equations are valuable to LEPE designers since they are comprehensive and easy to apply, and remove the need for multiple speed specific walking trajectories in a LEPE control system.
3. Evidence was provided that non-linear models are more robust for calculating step-length, stride-length, and stride frequency, previously considered as linear for model simplicity. The majority of sagittal kinematic and kinetic gait parameters were also non-linear across slow speeds.
4. The first LEPE-human SCI model driven by real device trajectories with real external forces, captured with force plates and instrumented forearm crutches, was produced. This model

presents a framework to test how the human body interacts with different LEPE or powered orthoses. Model output could be used as input to drive adaptive controllers, providing interaction torques customisable to user ability. These data could be used to better tune LEPE in-silico vs in-situ, as well answer questions about LEPE safety by providing estimates of contact forces between the device and user.

5. This research presented the first LEPE-human musculoskeletal model to estimate upper-extremity biomechanics, driven by 3D motion data of persons with complete SCI walking with LEPE and crutch assistance. A quantitative understanding of upper-extremity dynamics during LEPE walking can be used to improve device training, rehabilitation, and design. Reducing upper-extremity load is important to reduce ambulatory assistive device overuse injuries and allow people with reduced upper-limb function to use these powered assistive devices.

Chapter 2. Literature Review

LEPE control requires efficient and intelligent hardware, an interactive control strategy, and an understanding of the human dynamics involved in LEPE assisted gait. Therefore, this chapter reviews literature on assistive LEPE, LEPE performance, assistive device control strategies, and human dynamics.

2.1 Exoskeletons

The term exoskeleton has been used to describe a broad range of wearable devices that assist individuals with limb pathology, augment intact limb function, enhance strength, and increase endurance. Device design is equally broad. Exoskeletons can act in series with the human body to increase limb-length and displacement or in parallel with a human limb to augment load transfer to the ground for moment and work augmentation (Herr, 2009). Devices also vary by the number of joints with moment-augmentation. Partial exoskeletons typically act on one or two joints. Full lower limb exoskeletons have joints parallel to the hip, knee, and ankle. Exoskeletons can be further divided into rehabilitation exoskeletons and assistive exoskeletons (Viteckova, Kutilek, & Jirina, 2013).

2.1.1 Rehabilitation Exoskeletons

Rehabilitation exoskeletons (e.g., Lokomat, Auto-Ambulator, ALEX, LOPES) are LEPE suspended over a treadmill and secured to a patient’s legs. A body weight support system provides total or partial support, preventing collapse and managing forces applied to load bearing joints during therapy. For neurorehabilitation locomotor training, therapies are based on the principles of neuroplasticity and motor learning to encourage motor recovery through consistent repeated exercise, designed to engage the neuromuscular system below the level of injury (Behrman, Bowden, & Nair, 2006; Harkema, 2001). This training should stimulate central pattern generator neural activity, promoting gait recovery (Molinari, 2009; Winchester et al., 2005) and quality (Nooijen, Ter Hoeve, & Field-Fote, 2009). Rehabilitation exoskeletons have effectively reduced the laborious effort of active assist neurorehabilitation and improved therapist ability to generate precise reproducible joint motions, thereby increasing the duration and efficiency of physical therapy sessions (Reinkensmeyer, Emken, & Cramer, 2004). Rehabilitation exoskeletons can also enhance clinical assessment of motor recovery and injury level as well by measuring impedance and movement between the rehabilitation LEPE and the user (Low, 2011).

2.1.2 Assistive Exoskeletons

Assistive exoskeletons are autonomous walking devices, designed for persons with lower limb weakness or paralysis to perform activity of daily living. User inclusion criteria typically includes height (1.45 m to 2.0 m) and weight (generally less than 113 kg) (Louie, Eng, & Lam, 2015). LEPE systems generally consist of the exoskeleton, a user interface or GUI (smart phone, watch, or tablet), and a support aid (crutches). Since most LEPE require crutches, few studies report users with SCI higher than the fifth cervical vertebra (Kozlowski, Bryce, & Dijkers, 2015). To don a LEPE, users generally transfer from a wheelchair into a device seated adjacent to them. This pivot transfer can produce high reaction forces on shoulder and elbow joints (D. Gagnon, Nadeau, Noreau, Dehail, & Gravel, 2008; D. Gagnon, Nadeau, Noreau, Dehail, & Piotte, 2008); thus, some LEPE like the Indego from Vanderbilt University's (Nashville TN) are modular, allowing the user to strap foot and shank, thigh, and pelvis segments onto their body one at a time and then snap adjacent segments together. Devices are secured to the user via strapping at the feet, shanks, thighs, and torso. LEPE sensors monitor a user's movements to determine the intended activity, including when the user wants to take a right or left step. During LEPE training, users learn to shift the majority of their weight (including LEPE mass) onto the stance limb unload and clear the swing limb. This triggers swing limb hip flexion and stance limb hip extension. The upper-extremity connects with the ground via support aids (crutch or walker) to prevent the user from falling and aid forward progression.

Learning to walk with a LEPE requires a supervised, graduated training process. In general, users advance from walking with LEPE assistance within parallel bars, supported by an overhead suspension system and a therapist to walking independently with crutches. LEPE users could adopt a three point swing through crutch approach during training, where both forearm crutches move forward simultaneously after each foot strike. Four point crutch gait can also be used, and involves moving one crutch after foot strike and only swinging the other limb and crutch after the initial crutch has contacted the ground. LEPE training duration varies in the literature. For example, ReWalk training to independent walking required 12-13, 60–90 minute sessions (Zeilig et al., 2012) and Parker-Indigo reported 5, 1.5 hour sessions (Hartigan et al., 2015). Level of injury influenced LEPE walking, where rehabilitation professionals and users can expect a shorter training period and greater walking proficiency for individuals with lower SCI (Lemaire, Smith, Herbert-Copley, & Sreenivasan, 2017). A comprehensive systematic review and correlational study of LEPE gait speed reported that persons with complete SCI who were older, had a lower in injury level, and who were able to train longer achieved greater waking speeds and therefore better LEPE utility (Louie et al., 2015).

LEPE have created a new paradigm in both neurorehabilitation and health promotion for persons previously restricted to wheelchairs for mobility and seated exercise. For seated mobility and exercising, repetitive motion injuries can occur on unaffected limbs and joints. LEPE are less energy intensive than rigid orthoses (Arazpour, Hutchins, & Bani, 2015) and, as devices become more accessible, LEPE will help persons with lower-limb paralysis to re-enter upright society, influencing both community and social participation (Louie et al., 2015). Adapted robotic assisted exercise using LEPE can provide the benefits of upright exercise under full body weight and reduce the risk of upper-limb overuse injuries, while also engaging the neuromuscular system below the level of injury. Thus, under this new paradigm LEPE can be used for health promotion, adapted physical activity, neurorehabilitation, or a powered orthosis to aid walking.

2.1.3 Existing Assistive exoskeleton

Advances have been made over the last decade in assistive exoskeletons. Emerging commercial devices for people with paraplegia include ReWalk by Argo Medical Technologies (Esquenazi, Talaty, Packel, & Saulino, 2012; Zeilig et al., 2012), Ekso by Berkeley Bionics (Strickland, 2012), Hybrid Assisted Leg (HAL) by CYBERDYNE Inc. (Kubota et al., 2013; Suzuki, Mito, Kawamoto, Hasegawa, & Sankai, 2007; Tsukahara, Hasegawa, & Sankai, 2009; Tsukahara, Kawanishi, Hasegawa, & Sankai, 2010), Indigo by Parker Hannifin. (Farris, Quintero, & Goldfarb, 2011; Farris et al., 2014), and REX by REX Bionics (Birch et al., 2017).

Figure 2-1 : ReWalk.

ReWalk (Figure 2-1) attaches to the person’s torso and legs and forearm crutches are required for balance and safe movement. Torso mounted tilt sensors are used to initiate alternating limb movement by recognising sagittal plane changes in torso angle as the user leans forward and frontal plane movement as the person offloads the swing leg. Hip and knee joints are actuated in flexion and extension. A passive double action ankle joint, with limited motion, is spring loaded to assist dorsiflexion. Participants interact with the system via a wrist watch to select walking, sit-to-stand, or stair modes. Data have been published on ReWalk’s safety and performance during level ground walking with SCI (T4-T12) participants (Zeilig et al., 2012). Participants walked more than 100m following an average of 13-14 training sessions that lasted 60-90 minutes. Average speed in performance testing was 0.25 m/s, ranging between 0.03 m/s and 0.45 m/s (Esquenazi et al., 2012). In a recent study (Yang, Asselin, Knezevic, Kornfeld, & Spungen, 2015), a participant with a motor-incomplete injury walked at 0.71 m/s, which is higher than the max speed of 0.55 m/s reported in the ReWalk User Guide (ReWalk™ Personal System User Guide, ReWalk Robotics, Israel).

Figure 2-2 Ekso.

After an evolving series of exoskeletons from Berkeley Bionics designed to improve load carrying capacity and endurance of able-bodied soldiers, beginning with the ExoHiker and HULC (Mertz, 2012), the Ekso device was released (Figure 2-2). This knee and hip powered exoskeleton was the second generation of eLEGS (Strausser, Swift, Zoss, & Kazerooni, 2010; Swift, Strausser, Zoss, & Kazerooni, 2010), designed for a paraplegic population. Ekso was tested for safety on people with complete SCI, achieving walking velocities 0.28 m/s after six weeks of training (Kolakowsky-Hayner, 2013; Kressler et al., 2014). Ekso also requires forearm crutches and has a spring loaded ankle to avoid drop foot. Three walking modes are available: First Step, where the therapist actuates step; ActiveStep, where the user activates their own step with buttons on the walker or crutches; ProStep, where users initiate their steps by moving their hips forward and shifting laterally. ProStep control is mediated through foot pressure switches and hip, knee, and torso potentiometers, accelerometers, gyroscopes, and digital encoders to determine absolute joint and torso angle in the sagittal plane.

Figure 2-3: HAL: Hybrid Assistive Limb.

The Hybrid Assistive Limb (HAL) (Figure 2-3) was designed to assist mobility for able-bodied persons and those with lower limb disabilities. HAL uses electromyographic signals from the legs and on-device sensors to control ankle, knee, and hip actuators. HAL enables users to lift loads 40kg heavier than they would be able to otherwise. HAL-5 LB (type C) targets the paraplegic population (Suzuki et al., 2007) and estimates the user's desire to sit, stand, or to walk using intention estimation algorithms, changes in body inclination, and centre of pressure (COP). In a trial with 38 people (12 stroke, 8 SCI, 4 muscular disorders, and 14 other) (Kubota et al., 2013), speed (pre 0.52 ± 0.40, post 0.61± 0.43 m/s), number of steps, and step-frequency improved during the 10 Minute Walk Test.

Figure 2-2: Indigo.

Indigo (Figure 2-4), the commercial form of Vanderbilt University's (Nashville TN) exoskeleton, has been evaluated in a number of device design and control articles (Farris, Quintero, Withrow, & Goldfarb, 2009; Quintero, Farris, & Goldfarb, 2011). This exoskeleton assists the hip and knee in the sagittal plane but has no ankle, attaching to the users shank or the shoe with a standard foot orthosis to prevent drop-foot. This device is equipped with similar sensors as other commercial exoskeletons and is controlled by torso inclination. A single user with paraplegia (T10) walked with near healthy hip and knee joint angles and amplitude, with 0.22 m/s max walking velocity (Farris et al., 2011).

The REX Bionics (London, United Kingdom) exoskeleton was designed for both paraplegic and quadriplegic users ("REX BIONICS," 2017). Unlike the models described previously, Rex requires no balance supporting device (crutches, etc.) and has hip, knee, and ankle actuators (Figure 2-5). The operator uses a joystick on an upper-limb railing to control sit-to-stand, level walking, side stepping, and stair assent. A recent publication found 18 persons with complete and incomplete tetraplegia or paraplegia could safely participate in a functional exercise program and complete a TUG within 313s (Birch et al., 2017).

Figure 2-3: REX.

Additional exoskeletons still in the research phase include the SUBAR (Kong, Moon, Hwang, Jeon, & Tomizuka, 2009; Kong, Moon, Jeon, & Tomizuka, 2010), Saga (He & Kiguchi, 2008; Kiguchi & Imada, 2009) and MINA (Figure 2-6) (Kwa et al., 2009; Neuhaus, 2011; Srikanth et al., 2005). These exoskeletons have similar capabilities to the devices above, achieving walking speeds around 0.2 m/s. Actuators in these models are back-drivable, allowing the therapist to control the amount of assistance provided by the device. This capability is important for those with some residual walking capacity, like the physically weak or those with incomplete SCI. Literature is lacking on SUBAR and Saga performance with a pathologic population. A proof of concept study was conducted with MINA prototype with two persons with SCI (Neuhaus, 2011).

A unique LEPE called "ABLE" (Mori, Maejima, Inoue, Shiroma, & Fukuoka, 2011; Mori, Okada, & Takayama, 2006; Mori, Takayama, & Zengo, 2008) combines mobile foot platforms and telescoping crutches with actuators at the hip and knee joints. With the telescoping crutches, this device was tested on both level and unlevel ground, and can perform sit-to-stand and stair ascent. No outcomes have been published with pathologic populations.

Figure 2-4: Mina v2 with backpack.

The Wearable Power Assist Locomotor (WPAL) was developed by the Faculty of Rehabilitation and Health Sciences at the Fujita Health University in Japan to restore gait for people with complete paraplegia (Cao, Ling, Zhu, Wang, & Wang, 2009; Kagawa & Uno, 2009; Tanabe, Hirano, et al., 2013; Tanabe, Saitoh, et al., 2013). The device is actuated at the hip and knee, but attaches to the medial sides of the user's limbs and is used with an instrumented walker (Figure 2-7). This design facilitated sitting in a wheelchair by reducing hip width. The device has been tested with a paraplegic population (Tanabe, Saitoh, et al., 2013) and is capable of performing sit-to-stand as well as three gait modes (simple gait mode, turning mode, slow mode) with a reported maximal walking velocity of 0.4 m/s.

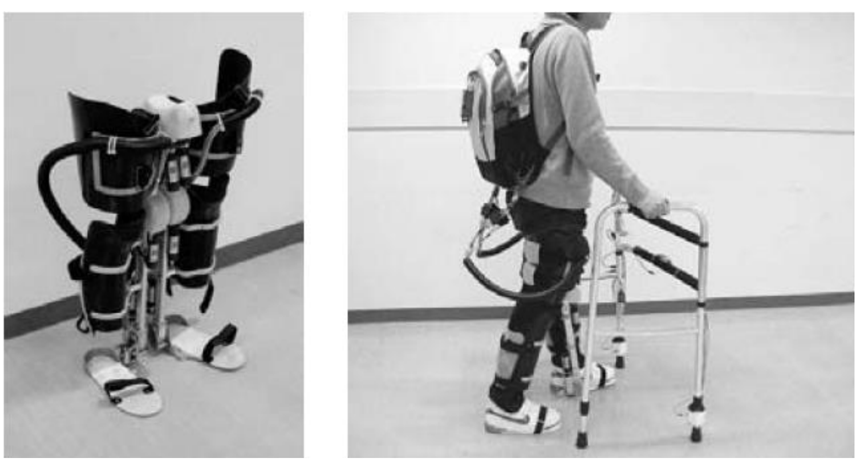

Figure 2-5: Wearable Power-Assist Locomotor (WPAL).

2.2 Position Control

Position control is the most used LEPE control strategy (Chen et al., 2016; Yang et al., 2015). Devices using this control architecture include eLEGS, ReWalk, Vanderbilt, WPAL, HAL, MINA and the Isocentric Reciprocating Gait Orthosis (IRGO). These devices are used by people with little to no voluntary use of their lower limbs, since positional control provides predefined trajectories to move the person's limbs. Onboard sensor technology constantly monitors a user's movements, such as leaning forward or side to side. This sensory technology allows the exoskeleton to determine the intended activity, including when the user wants to walk or stop.

Swift (2011) was among the first to present kinematic and temporal-spatial results of persons with SCI (N=7) walking with LEPE assistance (eLEGS). Under position control, joint angles were precalculated to match natural reciprocal gait kinematics, which were stored in a look up table within the eLEGS trajectory generator (Figure 2-8). The goal of this study was to provide users with natural reciprocal gait using step-time (T_D) and step-length (L_D) as input to determine the desired joint trajectories (θ_D). Based on the intended maneuver and input, the trajectory generator selected the desired trajectories for each joint from a look up table of angular joint trajectories. The controller generated the required electrical current to drive each joint through the desired motion, and the plant tracks the desired motor current and delivers current to the actuators. Resultant step-length (0.71 m) was consistent with natural gait at walking speeds between 1.3 m/s and 1.4 m/s; however, average walking speed with eLEGS assistance was 0.11 m/s, with a step-time of 5 s and 73 % of the GC in double support. These gait parameters were a factor of 10 different from natural gait.

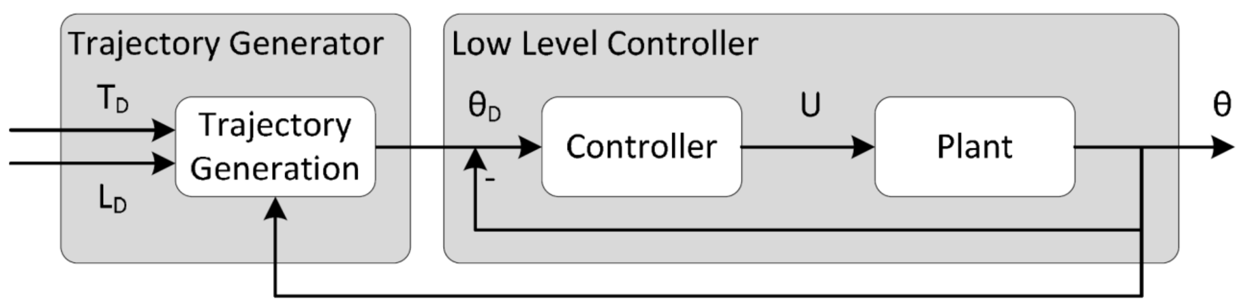

Figure 2-6: Example of position control architecture (Swift, 2011). T_D is the desired step-time, L_D is the desired step-length, and θ_D is the desired joint trajectory.

Present day LEPE are limited in their ability to provide reliable ambulation using trajectories similar to unimpaired persons at natural walking speeds. This is because today's devices are underpowered, limited in their degrees of freedom, or limited in sensor capacity for the target activities. The choice and or design of trajectories dictate the LEPE behaviour and, if inappropriate, lead to unstable movement. LEPE controllers should generate trajectories within the limits of the technology, and within the LEPE user's ability. Device walking speed not only influences LEPE trajectory generation and behaviour, but determines device utility.

LEPE that only walk slowly limits community utility and may regulate LEPE use to indoor activities like exercise and neurorehabilitation. Walking speed and distance requirements for persons living with pathology should be considered to ensure that LEPE users can safely ambulate within their community. These requirements vary based on age, injury severity, walking independence, and the community environment. From a systematic review of international community speed and distance requirements for able-bodied walking outside the home, walking speed and distance ranged from 0.44 m/s to 1.32 m/s and 16 m to 677 m (Salbach et al., 2014). For persons with incomplete SCI, criteria walking speed to cross a road safely ranged between 0.60 m/s and 1.06 m/s (Lapointe, Lajoie, Serresse, & Barbeau, 2001; Zörner, Blanckenhorn, Dietz, EM-SCI Study Group, & Curt, 2010). Functional walking distances for persons with incomplete SCI were set to 350 m, based on endurance (Du, Newton, Salamonson, Carrieri-Kohlman, & Davidson, 2009) or distance measured from accessible parking spaces to the entrance of frequently visited stores (342 m) like supermarkets (Lapointe et al., 2001).

The type of support aid can influence walking speed (Saensook et al., 2014). Ambulatory assistive devices that offered the most support resulted in significantly slower walking speed and shorter walking distance among incomplete SCI. Walkers provided the most support and had the slowest walking speed (0.3±0.1 m/s) and shortest distance (76.6±37.4 m), compared to crutches (0.4±0.2 m/s; 107.6±49.8 m), canes (0.6±0.2 m/s; 168.9±57.8 m), and unassisted (0.8±0.3 m/s; 242.0±74.9 m). The effect of support aid on walking speed is typically related to the injury severity and ambulatory ability. People with less severe injuries walked with less support (canes), versus people with higher grade injuries requiring more support (walkers). Similar walking speeds have been reported by people trained to use a LEPE who typically walk at 0.1 m/s to 0.55 m/s. People with SCI, with or without LEPE assistance, have difficulty reaching community ambulatory walking speeds and distance milestones. Understanding the limitations of these devices, and potential maximal walking speeds, will help determine LEPE utility and adjust user and clinician expectations (Benson et al., 2016).

As ambulatory persons with motor incomplete injuries typically walk at speeds below 0.5 m/s (Jonsdottir et al., 2009; Pepin, Norman, & Barbeau, 2003) and LEPE users typically walk very slowly, averaging 0.26 m/s (Louie et al., 2015), designing LEPE control architecture to generate joint angles similar to persons without impairment at normal walking speeds is unnatural. Basing LEPE controls on unimpaired slow-walking strategies would meet both LEPE and user ability, and may improve LEPE performance because able-bodied persons walking slowly use more complex locomotor and postural control strategies (Holden et al., 1997; Nymark et al., 2005; Otter et al., 2004) that could improve LEPE dynamic stability, device utility, and one day, help users reach community independence.

Slow walking strategies do not appear to have been incorporated into LEPE prototypes utilising position control. Persons walking with IRGO were reported to have achieved max walking speeds between 0.30 m/s and 0.40 m/s, with corresponding step-lengths greater than 0.41 m (Arazpour et al., 2013, 2012). From gait parameter data in the literature, step-lengths of this size are more consistent with walking speeds twice those achieved by participants. WPAL reported a maximum: walking speed around 0.4 m/s, stride-length of 0.7 m, and swing-time of 0.9 s; however, a maximum stride-length of 0.7 m should result in a maximum walking speed of 0.3 m/s, if swing-time could be set to 0.38 s (Nymark et al., 2005). Scaling device trajectories to kinematics at faster gait speeds may result in step-length and step-frequency inconsistencies for slow walking devices and unstable or unachievable gait. Initial gait trajectories calculated for the MINA exoskeleton (Neuhaus, 2011) resulted in step-lengths of 0.6 m, consistent with walking speeds greater than 0.9 m/s (Schwartz et al., 2008). With this trajectory, SCI users had to pull themselves forward using parallel bars to take a step and prevent falling. The solution was to shorten LEPE step-length to 0.28 m, which allowed their participants to walk at 0.2 m/s.

eLEGS artificially increased hip and knee range of motion (ROM) to peak at 49 and 76 degrees, respectively, to provide additional toe clearance in the absence of an actuated ankle. Similar ROM was reported for Mina v2 (Griffin et al., 2017). This accommodation does not appear in all LEPE with passive ankles (Arazpour et al., 2013, 2012). For example, a study of 12 persons with motor complete SCI walking with ReWalk assistance presented ankle, knee, and hip sagittal gait profiles at slow (0.22-0.31 m/s), medium (0.32 to 0.41 m/s), and fast (0.42 to 0.5 m/s) walking speeds (Talaty, Esquenazi, & Briceno, 2013). At matched slow and medium walking speeds, ankle, knee, and hip ROM were 25% to 50% smaller than what would be expected Even at fast walking speeds, knee ROM remained 20 degrees less than expected (Table 2-1).

Table 2-1: Sagittal joint angles (degrees) of persons with SCI walking with LEPE assistance and predicted values at matched speeds from Lelas et al., 2003 and Koopman, et al., 2014. Range of motion (ROM), flexion (Flx), extension (Ext), plantarflexion (PF), dorsiflexion (DF).

LEPE	Author, year	N	Gait speed (m/s)	Parameter	Angle (deg)	Lelias (2003)	Koopman (2014)
IRGO	Arazpour, (2012)	1	0.35	Hip Flx max	26.5	26.4	24.4
				Hip Ext max	-9.0	-5.6	4.7
				Hip ROM	35.5	32.0	27.5
				Knee Flx max	37.5	48.9	48.6
				Knee Ext max	0.0	1.6	2.4
				Knee ROM	37.5	47.3	51.1
	Arazpour, (2012)	4	0.40 (0.05)	Hip Flx max	18.8	26.8	23.1
				Hip Ext max	-7.8	-5.9	5.0
				Hip ROM	26.5	32.6	28.2
				Knee Flx max	37.0	49.5	49.9
				Knee Ext max	0.0	1.4	-2.4
				Knee ROM	37.0	48.1	52.3
ReWalk	Talaty, (2013)	12	0.22 to 0.31	Hip Flx max	18.0	25.4 to 26.1	21.9 to 22.6
				Hip Ext max	-3.0	-4.9 to -5.4	-3.7 to -4.4
				Hip ROM	21.0	30.4 to 31.5	25.6.7 to 27.0
				Knee Flx max	12.0	47.2 to 48.4	45.1 to 47.0
				Knee Ext max	-11.0	2.1 to 1.7	-2.4 to -2.4
				Knee ROM	23.0	45.1 to 46.7	47.6 to 50.3
				Ankle PF max	-3.0	13.1 to 12.9	
				Ankle DF max	17.0	-13.7 to 14.1	
				Ankle ROM	20.0	26.8 to 26.9	
			0.32 to 0.41	Hip Flx max	28.0	26.2 to 26.8	22.6 to 23.2
				Hip Ext max	8.0	-5.5 to -5.9	-4.4 to -5.1
				Hip ROM	20.0	31.6 to 32.8	27.0 to 28.3
				Knee Flx max	18.0	48.5 to 49.7	47.9 to 50.1
				Knee Ext max	-5.0	1.7 to 1.3	-2.4 to -2.4
				Knee ROM	23.0	50.2 to 51	50.3 to 52.5
				Ankle PF max	-4.0	-12.9 to 12.6	
				Ankle DF max	16.0	14.1 to 14.4	
				Ankle ROM	20.0	26.9 to 27.1	
			0.42 to 0.50	Hip Flx max	15.0	26.9 to 27.5	23.3 to 23.8
				Hip Ext max	-20.0	-6 to -6.4	-5.2 to -5.8
				Hip ROM	35.0	32.9 to 33.9	28.5 to 29.6
				Knee Flx max	23.0	49.8 to 50.7	50.3 to 52.1
				Knee Ext max	-9.0	-1.3 to -1.0	-2.4 to -2.4
				Knee ROM	32.0	51.1 to 51.8	52.8 to 54.5
				Ankle PF max	-.0	-12.6 to -12.4	
				Ankle DF max	17.0	14.5 to 14.8	
				Ankle ROM	29.0	27.1 to 27.2	
Mina v2	Griffin, (2017)	1	0.29	Hip Flx max	0.0	26.0	22.4
				Hip Ext max	-54.0	-5.3	-4.2
				Hip ROM	54.0	31.3	26.6
				Knee Flx max	80.2	48.1	47.1
				Knee Ext max	5.7	1.8	-2.4
				Knee ROM	74.5	46.3	49.5
				Ankle PF max	-28.6	-12.9	
				Ankle DF max	12.0	14.0	
				Ankle ROM	40.6	26.9	

2.3 Slacking

To promote motor learning and a therapeutic effect, training should be task specific, but must also require effort (Kaelin-Lane et al., 2005). Under these principles, locomotor training or active assist exercise has therapeutic value for improving gait patterns, speeds, and functional ability for those with neurological injuries (Dobkin et al., 2006; Harkema et al., 2012; Moseley et al., 2005). However, automating movement may promote users to become passive ("guidance hypothesis") (Crespo & Reinkensmeyer, 2008) and decrease motor adaptation. Evidence suggests that the human motor system adjusts to consistent external assistance by incorporating assistance into their motor plan by reducing muscle activation (Kao & Ferris, 2009). This property, coined as "slacking", suggests that the motor system, when physically assisted by a guiding movement, "greedily" optimises assistive forces to minimise effort while still effectively performing the task (Emken, Benitez, Sideris, Bobrow, & Reinkensmeyer, 2007). Robotically guiding movement thus alters the human dynamics of the task so that the burden on the learner's motor system to discover the principles needed to complete the task are reduced (Veneman, Ekkelenkamp, Kruidhof, van der Helm, & van der Kooij, 2006) and may actually decrease motor adaptation (Emken, Benitez, & Reinkensmeyer, 2007; Schmidt & Bjork, 1992). While position control via trajectory tracking may be acceptable for person with complete motor injuries, this type of control does not fulfill the necessities of motor recover therapy for persons with motor incomplete injuries. Moving forward, LEPE control must take into consideration the user ability and encourage the person to actively participate in LEPE movement.

2.4 Adaptive Control

The therapeutic goals of assistive robotic control are to provoke motor plasticity, adaptation, and improve motor recovery. Adaptive LEPE control models can engage users to initiate an activity, recruit muscles below their level of injury, and move their body with LEPE assistance. LEPE control strategies vary actuator assistance to work with the user, thereby helping to avoid slacking (Claros et al., 2016; Huo et al., 2016). Human centred interactive control requires additional user input (Marchal-Crespo & Reinkensmeyer, 2009), such as moments and joint orientation. Joint parameters are measured during device use and used by the adaptive controller to adjust a stiffness parameter that determines the amount of assistance transferred between the LEPE and the user.

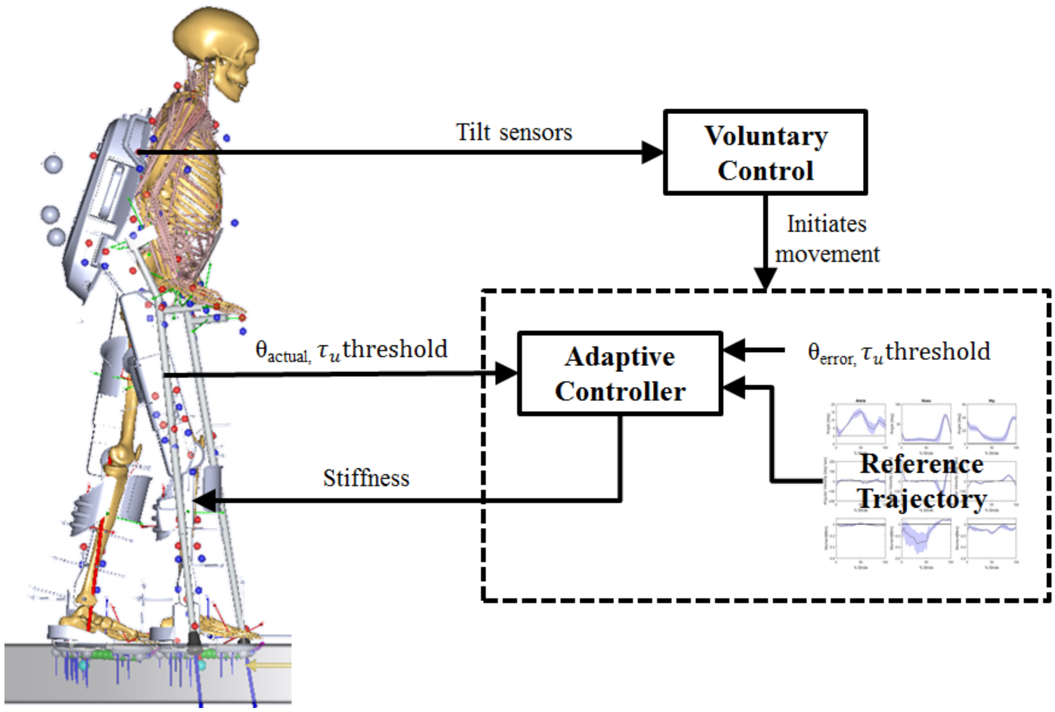

Figure 2-7: Adaptive control based predefined reference trajectories and interaction torque thresholds (modified figure from Rajasekaran et al., 2018).

Adaptive controllers model this interaction using equations of motion (2.1) (Pandy & Andriacchi, 2010; Rajasekaran et al., 2015b), where,

$$M(q)\ddot{q} + C(q,\dot{q}) + G(q) = \tau \qquad 2.1$$

M(q) is the mass matrix, C(q, q̇) are the Coriolis and centrifugal forces, G(q) is the gravitational force, and τ is the vector of generalized forces. Generalised forces include the actuator torque generated by the LEPE (τ_α), the torque generated by the user (τ_u), and the external forces acting on the user (τ_δ). Under adaptive control rotational stiffness is increased, decreased, or is maintained if position error or interaction torque is above, below, or within set thresholds. Stiffness is assistive or resistive, based on movement direction that is dynamically influenced by user movements.

Adaptive control has been applied to prosthetics (Sup et al., 2008; Sup, Varol, Mitchell, Withrow, & Goldfarb, 2009) and orthotics (Blaya & Herr, 2004; Hassani, Mohammed, Rifaï, & Amirat, 2014; Ibarra et al., 2014) to produce realistic walking patterns. Adaptive controlled LEPE were reported for neurologically intact users (Rajasekaran et al., 2015b, 2016) and users with neurological injury (Hassani et al., 2014; Rajasekaran et al., 2018). The adaptive controllers increased joint ROM and kept joint positions within a specified threshold of a healthy reference trajectory without forcing the user limb to track a predefined path (Rajasekaran et al., 2018; Swift, 2011; Swift et al., 2010). Interaction torques across all joints increased over time, signifying that the users provide greater joint torques and thereby required less adaptive assistance.

For position and force control, reference data are required to define the motion or set force thresholds to determine the amount of assistance. Generally, control reference patterns were developed from able-bodied volunteers walking in a passive or back-driveable device (Neuhaus, 2011; Rajasekaran et al., 2016; Tanabe, Hirano, et al., 2013) or generated online or in real-time using an unimpaired limb (Kahn, Lum, Rymer, & Reinkensmeyer, 2006; Vallery, Asseldonk, Buss, & Kooij, 2009). “Teach-and-replay” modes were used to generate reference trajectories from patients during manually assisted stepping with a LEPE passively attached (Aoyagi, Ichinose, Harkema, Reinkensmeyer, & Bobrow, 2007; Emken, Harkema, Beres-Jones, Ferreira, & Reinkensmeyer, 2008). While these methods provided device and patient specific profiles for control, they are device specific, walking speed specific, and require further tuning and manual support from a clinician. Since LEPE users’ walking speed varies, these approaches would require laborious collection and tuning of multiple trajectories based on speed to accommodate a wide array of users.

2.5 Reference trajectories

Input for position and force control could be based on speed appropriate reference data in the literature. Since most gait variables are affected by walking speed, several investigations have been conducted at slow, free, and fast walking speeds to characterise speed dependent changes to temporal-spatial stride parameters (Ardestani, Ferrigno, Moazen, & Wimmer, 2016; Gates, Darter, Dingwell, & Wilken, 2012; Murray, Kory, Clarkson, & Sepic, 1966; Nymark et al., 2005; Oberg, Karsznia, & Oberg, 1993; Pepin et al., 2003; Schwartz et al., 2008; Sekiya & Nagasaki, 1998; Shemmell et al., 2007; Silder, Heiderscheit, & Thelen, 2008; Stoquart, Detrembleur, & Lejeune, 2008) and kinematic and kinetic peak gait parameters (Borghese et al., 1996; Kerrigan, Todd, Della Croce, Lipsitz, & Collins, 1998; Murray et al., 1984; Nymark et al., 2005; Tommy Oberg & Karsznia, 1994; Pepin et al., 2003; Schwartz et al., 2008; Stansfield, Hillman, Hazlewood, & Robb, 2006; Stansfield, Hawkins, Adams, & Bhatt, 2018; Stoquart et al., 2008; van Hedel, Tomatis, & Müller, 2006). At slow walking speeds, hip, knee, and ankle kinematic and kinetic parameters decrease in amplitude. Changes in gait phase duration strongly influence temporal-spatial gait parameters, and the relative timing of gait kinematic and kinetics.

2.6 Temporal-spatial Parameters

Healthy able-bodied persons initiate walking by accelerating their centre of gravity ahead of their base of support, voluntarily initiating a forward fall. Humans make corrective responses to catch themselves using accurate foot placement, preventing destabilisation at each step (Bauby & Kuo, 2000). Temporal-spatial parameters (Table 2-2) that describe foot placements over the gait cycle include walking velocity, stride-length, stride-time, stride-width, and double-support-time (DST) (Winter, Patla, Frank, & Walt, 1990).

Table 2-2: Temporal-spatial stride parameter definitions.

Stride-time	Time (s) between successive foot contacts of the same foot
Step-time	Time (s) between successive contacts of each foot
Stance-time	Time (s) when the foot is in contact with the ground
Swing-time	Time (s) when the foot is not in contact with the ground
Double-support-time	Time between foot-off on one limb and foot contact on the opposite limb (% of stride-time)
Stride-length	Anterior-posterior distance (m) between the same heel marker over successive foot contacts
Step-length	Anterior-posterior distance (m) between heel markers at foot stride
Step-frequency	Number of steps per second (steps/s)

Walking can be subdivided into repetitive strides. The primary phases are stance and swing, which are further divided into initial contact, early stance, mid stance, terminal stance, initial swing, mid swing, and late swing (Figure 2-10). At natural walking speeds, stance phase occurs during the first 60% of the stride and swing is the remaining 40%. Increasing walking speed typically increases swing % and single leg stance duration, while stride-time and stance % and double support durations are reduced (Pepin et al., 2003; Schwartz et al., 2008; Shemmell et al., 2007).

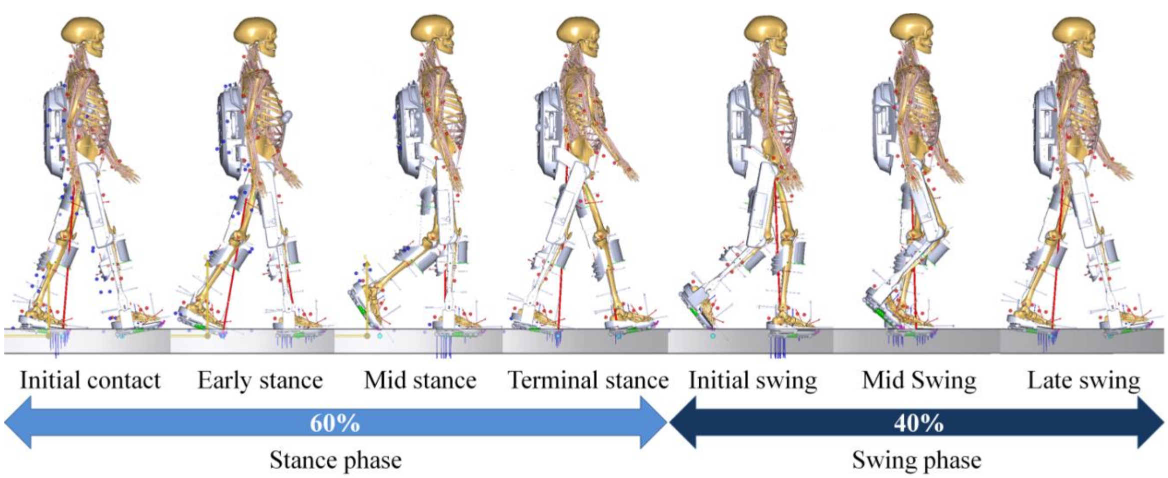

Figure 2-8: Gait cycle phases at normal walking speed.

The opposite is true with slower walking speed; however, changes to gait phase durations at speeds below 2.5 kph (0.56 m/s) are significantly greater than changes observed at faster walking speeds (Schwartz et al., 2008; Stansfield, Hawkins, Adams, & Bhatt, 2018; van Hedel et al., 2006). Reducing walking speed increases relative double limb support and stance phase. Changes in double support-time appear to happen more rapidly at lower speeds (Figure 2-11). At very slow speeds (0.14m/s) stance phase occupies as much as 80% of the gait cycle, with 60% spent in double support (van Hedel et al., 2006). For walking speeds less than 2.0 kph (0.44 m /s) left and right leg initiated double-support-times decreased and single support and swing time significantly increased between speed intervals as small as 0.1 m/s.

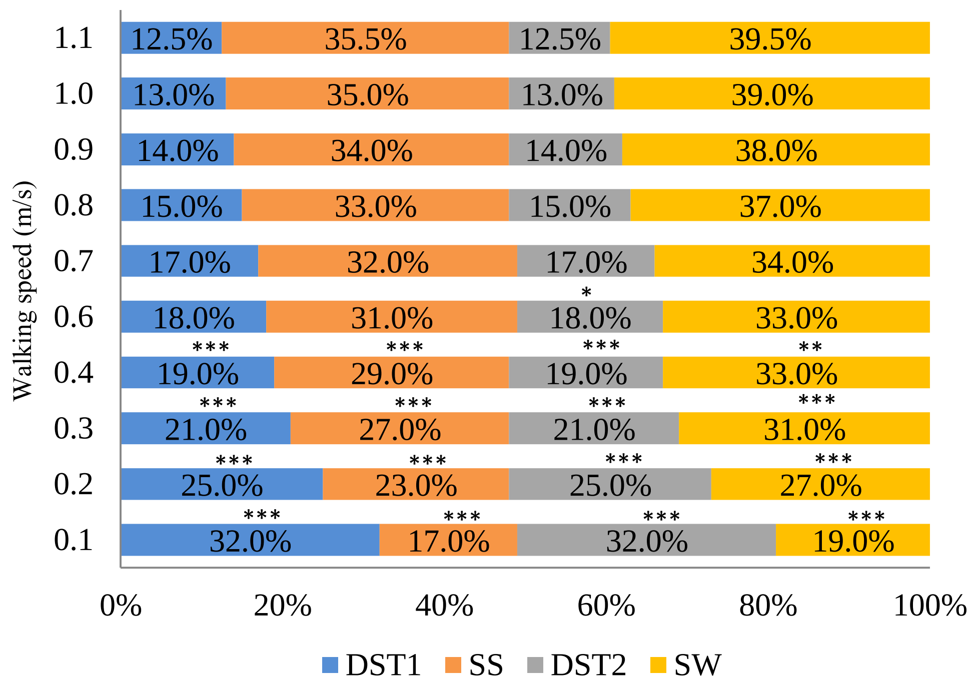

Figure 2-9: Percentage of gait phases. DST1, first double-support-time; SS, single stance time; DST2, second double-support-time; SW, swing time. *p<0.05, **p<0.01, ***p<0.001. Modified from van Hedel et al., (2006).

Walking speed influences all temporal-spatial parameters. Table 2-3 summarises temporal-spatial results in the literature for overground and treadmill walking at various walking speeds. Step-frequency and stride-length increase with speed, with more variability at walking speeds below 0.5 m/s (van Hedel et al., 2006). Variability and speed mediated changes to DST, step-frequency, and stride-length decrease with increased walking speed, indicating more consistent gait patterns at faster speeds (Nymark et al., 2005; van Hedel et al., 2006).

Table 2-3: Stride-parameters from overground and treadmill walking. NR is not reported.

Author, Year	N	Surface	Gait speed	Speed (m/s)	Step-frequency (steps/s)	Step-length (m)	Stride-length (m)	DST (%)	Stride-time (s)	Step-time (s)	Stance-time (s)	Swing-time (s)
Gates, 2012	13	Ground	Froude Number	0.71±0.03	NR	0.53±0.05	NR	NR	NR	0.73±0.05	NR	NR
				0.95±0.04	NR	0.61±0.04	NR	NR	NR	0.64±0.04	NR	NR
				1.19±0.05	NR	0.68±0.04	NR	NR	NR	0.58±0.04	NR	NR
				1.42±0.06	NR	0.75±0.05	NR	NR	NR	0.54±0.03	NR	NR
Shemmell, 2007	28	Ground	Slow	1.00±0.16	1.68±10.80	0.59±0.07	1.18±0.14	NR	1.20±0.14	NR	0.75±0.02	0.45±0.12
			Normal	1.32±0.14	1.97±8.70	0.67±0.07	1.35±0.14	NR	1.02±0.08	NR	0.62±0.02	0.40±0.06
			Fast	1.87±0.21	2.35±15.70	0.79±0.90	1.59±0.18	NR	0.86±0.09	NR	0.50±0.01	0.36±0.08
Ardestani, 2016	21	Ground	Normal	1.27±0.16	1.93±0.16	NR	1.31±0.10	NR	NR	NR	NR	NR
			Fast	1.50±0.19	2.10±2.10	NR	1.42±0.12	NR	NR	NR	NR	NR
Oberg, 1993	15	Ground	Slow	0.83±0.09	1.55±0.29	0.53±0.03	NR	NR	NR	NR	NR	NR
			Normal	1.23±0.11	1.98±0.13	0.62±0.04	NR	NR	NR	NR	NR	NR
			Fast	1.63±0.20	2.34±0.17	0.71±0.06	NR	NR	NR	NR	NR	NR
Murray, 1996	120	Ground	Free	1.21±0.20	NR	NR	1.56±0.13	43	0.87±0.06	NR	0.65±0.07	0.41±0.04
	120		Fast	2.18±0.25	NR	NR	1.86±0.16	39	1.06±0.07	NR	0.49±0.05	0.38±0.03
Schwartz, 2008	83	Ground	Slower	0.52±0.11	1.02±0.19	0.47±0.07	NR	36	NR	NR	NR	NR
			Slow	0.88±0.08	1.37±0.13	0.6±0.05	NR	24	NR	NR	NR	NR
			Free	1.30±0.08	1.71±0.11	0.71±0.04	NR	19	NR	NR	NR	NR
			Fast	1.69±0.09	2.00±0.16	0.79±0.05	NR	16	NR	NR	NR	NR
			Faster	2.10±0.14	2.29±0.19	0.86±0.07	NR	14	NR	NR	NR	NR
Stoquart, 2008	12	Treadmill	Set speed	0.28	0.87±0.2	NR	NR	NR	NR	NR	NR	NR
				0.56	1.27±0.12	NR	NR	NR	NR	NR	NR	NR
				0.83	1.55±0.12	NR	NR	NR	NR	NR	NR	NR
				1.11	1.80±0.10	NR	NR	NR	NR	NR	NR	NR
				1.39	2.02±0.08	NR	NR	NR	NR	NR	NR	NR
				1.67	2.20±0.12	NR	NR	NR	NR	NR	NR	NR
Pepin, 2003	7	Treadmill	Set speed	0.10	NR	NR	NR	NR	1.40±0.35	NR	1.16±0.31	0.25±0.05
				0.30	NR	NR	NR	NR	0.66±0.06	NR	0.47±0.06	0.18±0.02
				0.50	NR	NR	NR	NR	0.51±0.04	NR	0.34±0.04	0.16±0.01
				1.00	NR	NR	NR	NR	0.36±0.03	NR	0.23±0.03	0.13±0.01
Silder, 2008	20	Ground	Slow	1.06±0.10	1.65±0.17	1.27±0.10	NR	30±3	NR	NR	NR	NR
			Preferred	1.33±0.13	1.87±0.17	1.40±0.12	NR	28±3	NR	NR	NR	NR
			Fast	1.59±0.13	2.03±0.17	1.52±0.12	NR	26±3	NR	NR	NR	NR
Nymark, 2004	18	Ground	Natural	NR	1.87±0.16	NR	1.55±0.13	NR	NR	NR	2.32±0.09	NR
			Set speed	0.30	8.15±0.15	NR	0.74±0.16	NR	NR	NR	11.85±0.64	NR
				0.20	0.69±0.20	NR	0.65±0.16	NR	NR	NR	1.03±0.06	NR
	18	Treadmill	Natural	NR	1.96±0.12	NR	1.47±0.08	NR	NR	NR	2.48±0.09	NR
			Set speed	0.30	0.89±0.00	NR	0.71±0.12	NR	NR	NR	1.27±0.06	NR
				0.20	0.68±0.17	NR	0.63±0.23	NR	NR	NR	1.00±0.07	NR
Sekiya, 1998	25	Ground	Slowest	0.77±0.19	1.39±0.15	0.55±0.11	NR	NR	NR	NR	NR	NR
			Slow	1.01±0.14	1.61±0.10	0.65±0.06	NR	NR	NR	NR	NR	NR
			Preferred	1.20±0.12	1.81±0.13	0.66±0.05	NR	NR	NR	NR	NR	NR
			Fast	1.43±0.11	1.93±0.11	0.74±0.04	NR	NR	NR	NR	NR	NR
			Fastest	1.96±0.27	2.22±0.14	0.88±0.81	NR	NR	NR	NR	NR	NR

Slower walking speeds, with shorter step-lengths, faster step-times, and longer DST are often characterised as a cautious, protective gait pattern (Menz, Lord, & Fitzpatrick, 2003; Winter et al., 1990). These changes indicate a change in step strategy toward a safer, more stable gait pattern (Borghese et al., 1996; Bovi et al., 2011; Han & Wang, 2011; Li et al., 2005; Murray et al., 1984; Nymark et al., 2005; Schwartz et al., 2008; Stoquart et al., 2008) which, if incorporated into LEPE control architecture, could improve dynamic stability and LEPE performance.

2.7 Kinematic and kinetic peak sagittal gait parameters

The hip, knee, and ankle joints contribute to forward acceleration, absorb energy, ensure foot clearance, and decelerate the lower limb in terminal swing. At slow walking speeds, demands on hip (Figure 2-12), knee (Figure 2-13), and ankle (Figure 2-14) segments are diminished with associated decreases in all lower limb segments angles and moments (Nymark et al., 2005).

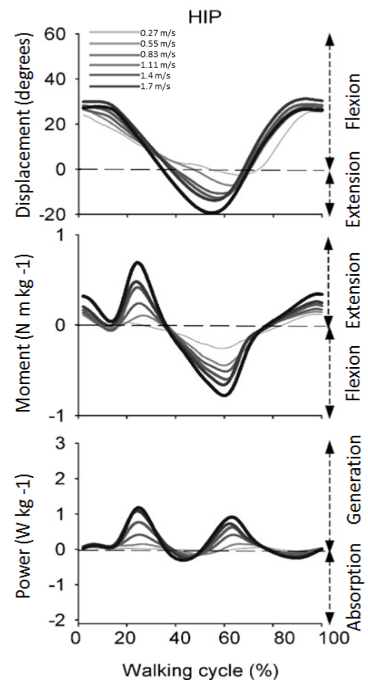

Figure 2-10: Hip kinematics and kinetics (Stoquart et al., 2008).

2.7.1 Hip kinematics and kinetics

At normal walking speeds, the hip undergoes a ROM of 40° with three peak kinematic and kinetic values commonly reported in the literature. Hip flexion angle and extension moments in stance and swing increase with walking speed, with little change in peak relative timing within the gait cycle. Peak hip extension and flexion moment increase with speed, and occur earlier in the gait cycle due to reduced DST and relative stance-time (Kirtley, Whittle, & Jefferson, 1985; Oberg et al., 1993; Schwartz et al., 2008; Stoquart et al., 2008). At slower walking speeds, hip acceleration and deceleration are reduced, with associated losses in hip flexion and extension moment and peak angles, reducing overall hip ROM to less than 30° at speeds below 0.3 m/s (Pepin et al., 2003; Stoquart et al., 2008).

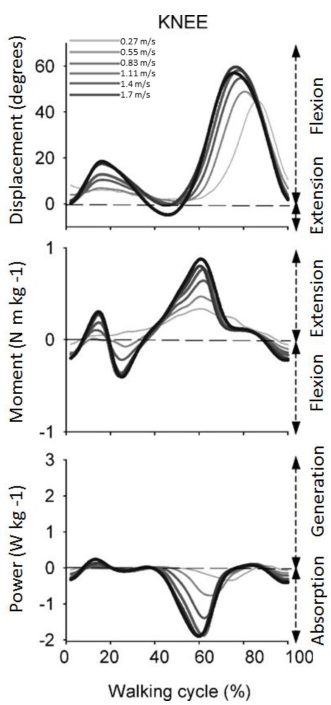

Figure 2-11: Knee kinematics and kinetics (Stoquart et al., 2008).

2.7.2 Knee kinematics and kinetics

At normal walking speeds, knee ROM is around 55º with two knee flexion peaks commonly reported in the literature. During stance, a knee flexion peak during loading response acts as a shock absorber (Perry & Burnfield, 2010; Stoquart et al., 2008). The knee flexion peak during swing increases with speed. Swing is considered a passive process at optimum walking velocities (Shemmell et al., 2007) and is the least constrained motion in the gait cycle. Increased and earlier peak knee flexion at faster walking speeds occurs ballistically due to increased moment of inertia and shortened stance phase duration (Perry & Burnfield, 2010). At slow walking speeds below 0.5 m/s, peak knee flexion angle and extension moment during stance are limited because the demand for shock absorption at the knee is reduced. Slow walking reduces the need to accelerate and decelerate the hip and knee joints, decreasing knee extension and flexion moments. This reduces lower limb inertia and decreases peak knee flexion.

2.7.3 Ankle kinematics and kinetics

Ankle joint ROM at normal walking speeds is approximately 30º. Ankle angle and moment trajectories have several peak values that change with walking speed. At initial contact a brief dorsiflexion moment prevents rapid plantarflexion and the foot slapping the ground. Forward progression stability comes from eccentric plantarflexion, until safe swing foot placement by the contralateral limb when dorsiflexion angle peaks at terminal stance (Winter, 1995). Peak plantarflexion increases and appears earlier with faster walking speed. Increased plantarflexion is thought to be related to ankle power. At normal and fast speeds, ankle plantarflexion pushes the body forward. Body weight is quickly transferred to the contralateral limb between mid-stance and toe-off. This results in a positive power peak that increases with speed (Perry & Burnfield, 2010). However, at walking speeds below 0.95 m/s, average ankle power is nearly zero as the ankle changes from an active system to a passive system, reducing plantarflexion (Han & Wang, 2011; Safaeepour, Esteki, Ghomshe, & Osman, 2014). Dorsiflexion during stance varies between publications, having been reported to both reduce (Schwartz et al., 2008; Stoquart et al., 2008; van Hedel et al., 2006), remain the same (Koopman, van Asseldonk, & van der Kooij, 2014), or increase at slower speeds (Nymark et al., 2005; Pepin et al., 2003; Stansfield, Hawkins, Adams, & Church, 2018).

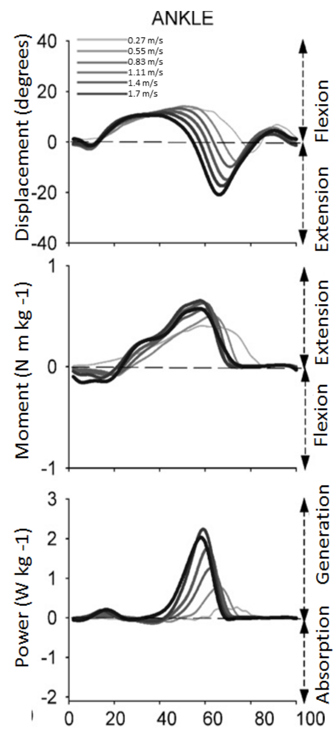

Figure 2-12: Ankle kinematics and kinetics (Stoquart et al., 2008).

Studies that involve multiple walking speeds average 0.91±0.10 m/s for slow, 1.30±0.12 m/s for free, and 1.70±0.26 m/s for fast (Table 2-4). Even studies reporting very slow speeds analysed gait characteristics at average walking speeds between 0.52 m/s and 0.77 m/s (Gates, Dingwell, Scott, Sinitski, & Wilken, 2012; Schwartz et al., 2008; Sekiya & Nagasaki, 1998). Most studies reporting gait parameter data characterise normal gait parameters at speeds above preferred walking speeds of potential LEPE users, between 0.1m/s and 0.55 m/s.

Table 2-4: Summary of studies reporting peak kinematic (Kmat) and kinetic (Knet), parameters at the ankle, knee, and hip. x=sagittal, y=frontal, z=transverse, F=female, M=male.

Author, Year	Biomechanical Data	Age	N	Surface	Walking	Speeds
Kerrigan, 1998	Hip Knet, Kmat: x Knee Knet, Kmat: x Ankle Knet, Kmat: x	65-84	10 F 10 M	Ground	Normal Fast	1.19±0.13 m/s 1.55±0.20 m/s
Van Hedel, 2006	Hip Kmat: x Knee, Kmat: x Ankle Kmat: x	19-32	10 F 10 M	Treadmill	10 set speeds	0.11-1.11 m/s
Stansfield, 2006	Hip Knet, Kmat: x Knee Knet, Kmat: x Ankle Knet, Kmat: x	7-12	8 F 8 M	Ground	Normal	0.80-1.90 m/s
Stoquart, 2008	Hip Knet, Kmat: x Knee Knet, Kmat: x Ankle Knet, Kmat: x	21-25	4 M 8 F	Treadmill	6 set speeds	0.23-1.33 m/s
Pepin, 2003	Hip Kmat: x Knee, Kmat: x Ankle Kmat: x	28-40	7 M	Treadmill	4 set speeds	0.10-1.00 m/s
Stansfield, 2018	Hip Kmat: x,y,z Knee, Kmat: x Ankle Kmat: x	22-44	10 F 10 M	Ground	Normal to as slow as comfortable	0.41-2.26 m/s
Schwartz, 2008	Hip Kmat: x,y,z Knee, Kmat: x,y,z Ankle Kmat: x,y,z	10	83	Treadmill	Very slow Slow Free Fast Vary Fast	0.52±0.11 m/s 0.88±0.08 m/s 1.30±0.08 m/s 1.69±0.09 m/s 2.10±0.14 m/s
Borghese,1996	Hip Kmat: x,y Knee, Kmat: x,y Ankle Kmat: x,y	21-40	6 M	Ground	Slow Moderate Fast	0.90 m/s 1.60 m/s 2.10 m/s
Murray, 1984	Hip Kmat: x Knee, Kmat: x Ankle Kmat: x	20-36	7	Ground	Slow Free Fast	0.80 m/s 1.40 m/s 1.90 m/s
Nymark, 2005	Hip Kmat: x Knee, Kmat: x Ankle Kmat: x	23-58	18	Treadmill Ground	2 set speeds and natural	0.20 m/s 0.30 m/s Natural m/s

A handful of studies recorded peak sagittal gait kinematics at speeds between 0.1 and 0.55 m/s (Nymark et al., 2005; Pepin et al., 2003; Stoquart et al., 2008; van Hedel et al., 2006). However, most presented a limited number of specific gait features. Studies that reported curves were typically grand ensemble averaged, which could result in lower peaks due to subject variability in peak timing. No study to our knowledge has published averaged peak kinematic and kinetic values over walking speeds ranging from 0.2-0.8 m/s.

2.8 Regression analyses

Consistent and predictable changes in temporal-spatial, kinematic, and kinetic parameters over a range of walking speeds have led to a general assumption that gait parameters follow consistent patterns of change in response to speed (Andriacchi, Ogle, & Galante, 1977; Ardestani et al., 2016; Kirtley et al., 1985; Oberg et al., 1993; Shemmell et al., 2007). This assumption has given rise to regression equations that estimate similar patterns of change in temporal-spatial, kinematic, and kinetic parameters based on walking speed, stride-length, step-frequency, and stride-time. Using regression equations to predict position and force are ideal since equations are easy to apply and may require only speed as input. Equations also eliminate the need for multiple speed-specific reference trajectories for position and adaptive control.

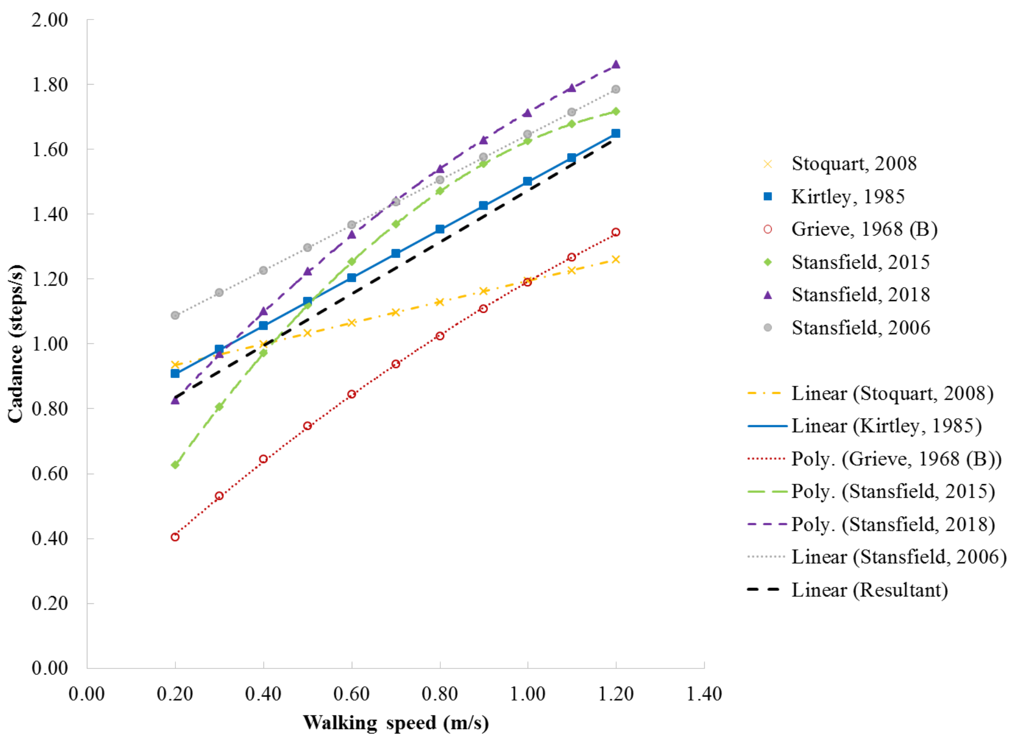

Figure 2-13: Estimated step-frequency relationships with speed.

2.8.1 Temporal-spatial reference equations

Temporal-spatial regression equations typically have moderate to high levels of agreement (Table 2-5). However, the relation between temporal-spatial parameters and speed described using regression analysis vary in the literature. For example, step-frequency relationship with speed has been estimated using a linear relationship with speed and step-length, and both polynomial and logarithmic relationships with speed. Estimated step-frequency using these regression equations are presented in Figure 2-15.

Table 2-5: Temporal-spatial parameters regression equations in the literature. Not reported (NR), *v*elocity (*v*), stride-length (*l*), cycle-time (*T*), cadence (*c*), * R^2.

Parameter	Author, year	Surface	Speed (m/s)	Equation	r
Step-frequency (steps/s)	Stoquart, 2008	Treadmill	0.28-1.67	$0.09v+.87$	0.98*
	Kirtley, 1985	Ground	NR	$0.74v+0.76$	0.95
				$1.26l-0.12$	0.81
	Grieve, 1968	Ground	0.40-1.40	$73.12v^{0.66}$	0.99
				$69.56v^{0.68}$	0.98
				$71.34v^{0.67}$	0.97
	Stansfield, 2015	Treadmill	0.10-1.00	$0.78v^2+2.20v+0.22$	1.00*
	Stansfield, 2018	Ground	0.40-2.26	$7.69v^3-10.51v^2+7.09v+0.5$	0.84*
Double support (%)	Kirtley, 1985	Ground	NR	$-3.6v+14.2$	-0.64
				$-8.0l+21.20$	-0.67
				$-0.058c+15.6$	-0.57
	Stansfield, 2018	Ground	0.40-2.26	$-130.2v^3+149.4v^2-76.2v+22$	0.57*
				$129.7v^3+1.46v^2+129.7v+1.46$	0.56*
	Koopman, 2014	Treadmill	0.14-1.40	$0.795v^2-7.23v+26.485$	NR
Single support (%)	Stansfield, 2018	Ground	0.40-2.26	$155.4v^3+-172.4v^2+82.9v+27.4$	NR
Swing-time (s)	Grieve, 1968	Ground	0.40-1.40	$0.749T-0.008$	0.99
				$0.682T-0.012$	0.99
				$0.16T-0.037$	0.99
Swing phase (%)	Stansfield, 2018	Ground	0.40-2.26	$110v^3-125.6v^2+67.8v+28.9$	0.58*
Stance phase (%)	Stoquart, 2008	Treadmill	0.28-1.67	$0.08v^2-2.25x+78.89$	0.98*
	Kirtley, 1985	Ground	NR	$-3.5v+64.2$	-0.71
				$1.89l-1.46$	-0.67
				$-0.073c+67.0$	-0.68
Stride-length (m)	Kirtley, 1985	Ground	NR	$0.47v+0.85$	0.95
				$0.0088c+0.58$	0.81
Step-length (m)	Stansfield, 2018	Ground	0.40-2.26	$-0.41v^2+0.94v+0.14$	0.87*

Estimated temporal-spatial parameters vary considerably between studies, despite strong and very strong correlations with speed. Table 2-6 summarises estimated temporal-spatial values from various regression equations, with velocity as the indeterminate variable, at speeds between 0.2 m/s and 1.0 m/s. When walking speed increased from 0.2 m/s to 1.0 m/s, a range of step-frequencies were calculated, between 0.26 steps/s to 1.00 steps/s. Differences were also observed for DST, stance-time, and stride-length. These discrepancies may be related to a number of factors including speeds and curve fitting. Recently, researchers studying treadmill and overground walking at speeds below 0.5 m/s showed that step-frequency, step-length, swing-time, stance-time, and DST were more variable at speeds below 0.5 m/s, and exhibit more rapid changes with speed (Koopman et al., 2014; Stansfield, Hajarnis, & Sudarshan, 2015; Stansfield, Hawkins, Adams, & Bhatt, 2018; van Hedel et al., 2006). These findings suggest that temporal-spatial gait parameters have a non-linear relationship with speed. Stoquart., et al (2008) did include two walking speed intervals below 0.50 m/s in their analysis. However, the authors chose to fit step-frequency and stance phase duration using a linear equation even though their figures clearly showed a non-linear relation with speed. Estimated step-frequency between 0.20 m/s and

1.00 m/s using Stoquart., et al (2008) linear equations resulted in an increase of 0.26 steps/s, less than half those of other published relationships (Table 2-6). For step-frequency, under-fitting these data resulted likely over estimated very slow and under estimated normal walking speeds.

Table 2-6: Estimated stride-parameters from published regression equations based on speed.

Temporal-spatial parameter	**Author, year**	**0.20**	**0.40**	**0.60**	**0.80**	**1.00**	**Range**
Step-frequency (steps/s)	Stoquart, 2008	0.93	1.00	1.06	1.13	1.19	**0.26**
	Kirtley, 1985	0.91	1.06	1.20	1.35	1.50	**0.59**
	Grieve, 1968 (B)	0.40	0.64	0.84	1.02	1.19	**0.78**
	Stansfield, 2015	0.63	0.97	1.25	1.47	1.63	**1.00**
	Stansfield, 2018	0.83	1.10	1.34	1.54	1.71	**0.89**
	Stansfield, 2006	1.09	1.23	1.37	1.51	1.65	**0.56**
Double-support-time (%)	Kirtley, 1985	13.48	12.76	12.04	11.32	10.60	**2.88**
	Stansfield, 2018	18.63	15.88	13.65	11.87	10.43	**8.20**
	Koopman, 2014	21.69	17.72	14.58	12.26	10.76	**10.93**
Stance-time (%)	Stoquart, 2008	77.31	75.82	74.40	73.07	71.83	**5.48**
	Kirtley, 1985	63.50	62.80	62.10	61.40	60.70	**2.80**
Stride-length (m)	Kirtley, 1985	0.94	1.04	1.13	1.23	1.32	**0.38**
	Stansfield, 2018	0.63	0.78	0.92	1.05	1.18	**0.55**

Authors have reported differences between treadmill and overground walking that may influence temporal-spatial parameters. Some studies reported slightly higher step-frequencies and shorter stride-lengths compared to overground walking (Alton, Baldey, Caplan, & Morrissey, 1998; Arsenault, Winter, & Marteniuk, 1986; Nymark et al., 2005), in contrast others found stride-length to decrease and cadence to increase (Wall & Charteris, 1981). Ardestani et al., (2016) defined habitual stepping strategies, where individuals only increased step-frequency or stride-length when progressing from normal to faster speeds.

Considerable variability between estimated temporal-spatial parameters exists, despite moderate to very strong correlations with speed. Large estimation differences show the importance of taking very slow walking speeds into account when characterising normal walking patterns, and suggest that temporal-spatial relationships with speed are curvilinear below 0.5 m/s. Greater variability and rapid changes in temporal-spatial parameters at walking speeds below 0.5 m/s may indicate a different walking strategy.

2.8.2 Kinematic and kinetic regression equations

From studies characterizing gait parameters over a range of walking speeds, linear and curvilinear relationships have been derived for several kinematic and kinetic peak gait parameters (Table 2-7). Though kinematic parameters have significantly correlated with increasing walking speed (Schwartz et al., 2008; Stansfield et al., 2006; van Hedel et al., 2006; Winter et al., 1990), kinematic relationships with speed are weak (Table 2-7). Contrary to kinematics, some peak kinetic parameters have very similar patterns of change and strongly correlate with speed. For example, at walking speeds between 0.5 and 2.5 m/s, Lelas et al., (2003) report moderate to strong coefficient of determination (R^2) between 0.73 to 0.92 for speed and peak knee moments during loading, pre-swing, and swing; and strong correlation coefficients between 0.80 and 0.89 for peak hip extension and flexion moments. Kirtley et al., (1985) as well report a strong correlation coefficient of 0.86 for knee flexion moment during swing. Not all published kinetic regression equations have strong correlations with speed. Stansfield et al., (2006) reported weak R^2 across all joint angles ($R^2 <0.09$), moments ($R^2<0.20$) and powers ($R^2<0.29$). The data in this study were over a narrow range of self-selected walking speeds (0.8-1.8 m/s). The authors acknowledged that, if a wider range of speeds were examined, gait parameter relationships would likely follow a different pattern and they cautioned use of their published equations for slower speeds.

Variable kinematic associations with speed and kinematic regression equation accuracy may be due to gait speed variability and experimental methods (Ardestani et al., 2016; Astephen Wilson, 2012). Considerable inter-subject kinematic variability, increasing as walking speed is reduced, have been reported by a number of studies (Kirtley et al., 1985; Koopman et al., 2014; Lelas et al., 2003; Tommy Oberg & Karsznia, 1994; Stansfield et al., 2006; Stansfield et al., 2015; Stansfield, Hawkins, Adams, & Bhatt, 2018). Methodological approaches to handle the effects of speed on biomechanical data have long been debated, including asking participants to walk at predetermined gait velocities (Hanlon & Anderson, 2006; Kirtley et al., 1985; Lelas et al., 2003; Stansfield et al., 2006). Treadmills can be used to provide a fixed walking pace; however, treadmill walking may not reflect a natural environment (Riley, Paolini, Della Croce, Paylo, & Kerrigan, 2007) and may artificially improve kinematic associations with speed (Stoquart et al., 2008). Recently, Koopman et al., (Koopman et al., 2014) collected kinematic data from 15 persons, aged 47-68, at seven treadmill walking speeds between 0.14 m/s to 1.4 m/s. Like previous studies, the majority kinematic gait parameters were speed related. However, unlike previous studies, R^2 between reconstructed and actual joint trajectories were strong for hip and knee flexion ($R^2 >0.93$), and moderate too strong for ankle flexion ($0.69 <R^2<0.89$). A strong correlation does not mean a regression equation will accurately estimate gait kinematics and kinetics at all speeds.

Table 2-7: Temporal-spatial parameters regression equations based on speed dependent gait characteristics. Dorsiflexion (DF), plantarflexion (PF), flexion (Flx), extension (Ext), R^2, root mean square error (RMSE), velocity (v) (m/s [1], kph [2], height normalized [3]).

Parameter	Author	Condition	Speed	Peak	Equation	R^2	RMSE
Ankle Angle	Koopman, 2014[1]	Treadmill	0.14-1.40	Foot contact	$0.55v^2+18.65v-13.25$		2.36
Min = Dorsiflexion				DF stance	$17.31v-14.17$		2.52
Max = Plantarflexion				DF swing	$-3.43v^2+21.98v^2-12.52$		4.85
				PF swing	$-0.66v+4.86$		2.69
	Lelas, 2003[2]	Ground	0.50-2.50	DF. stance	$-1.76v+9.19$	0.37	
				Max PF.	$-2.40v+13.62$	0.60	
				DF. swing	$3.78v+12.88$	0.06	
				PF. swing	$4.16v^2-10.75v+10.04$	0.44	
	Stansfield, 2006[3]	Treadmill	0.80-1.80	DF. stance	$-20.95v+23.84$	0.06	
				DF. swing	$-17.68v+-2.29$	0.01	
				PF. swing	$-14.88v+14.14$	0.00	
	Stansfield, 2018[3]	Ground	0.41-2.26	DF. stance	$41.56v^2-18.98v-5.26$	0.08	
				Max PF.	$-34.24v^2+13.23v+10.97$	0.11	
				DF. swing	$131.5v^2-121.4v+7.6$	0.27	
Knee Angle	Koopman, 2014[1]	Treadmill	0.14-1.40	Foot contact	$0.49v^3-4.31v^2+31.6-13.05$		3.60
Max =Flexion				Flx. stance	$3.03v+6$		3.48
Min = Extension				Ext. stance	$-10.04v+7.59$		2.29
				Flx. swing	$-1.11v^2+9.74v+38.11$		4.35
	Lelas, 2003[2]	Ground	0.50-2.50	Foot contact	$-11.0v^2+31.09v-22.44$	0.37	
				Flx. stance	$-2.84v^2+19.59v-4.00$	0.60	
				Ext. stance	$2.99v^2-6.03v+3.30$	0.06	
				Flx. swing	$-3.19v^2+14.92v+44.08$	0.44	
	Stansfield, 2006[3]	Treadmill	0.80-1.80	Flx. stance	$44.42v+9.12$	0.08	
				Ext. stance	$-10.46v+11.91$	0.01	
				Flx. swing	$24.26v+54.23$	0.03	
	Stansfield, 2018[3]	Ground	0.41-2.26	Flx. stance	$25.99v^2-62.97v+6.14$	0.44	
				Flx. swing	$74.36v^2-73.98v-39.72$	0.20	
	Kirtley, 1985[2]	Ground	NR	Flx. stance	$13.0v+ 4.7$	0.61	
				Flx. swing	$8.6v+49.6$	0.44	
Hip Angle	Koopman, 2014[1]	Treadmill	0.14-1.40	Foot contact	$1.93v+20.35$		3.60
Max = Flexion				Flx. stance	$2.58v+18.92$		3.48
Min = Extension				Max Ext.	$-2.09v-2.03$		3.56
				Flx. swing	$2.32v+21.45$		3.87
	Lelas, 2003[2]	Ground	0.50-2.50	Flx. stance	$7.382v+23.81$	0.24	
				Max Ext.	$5.11v+3.82$	0.14	
	Stansfield, 2006[3]	Treadmill	0.80-1.80	Foot contact	$37.61v+25.18$	0.09	
				Max Ext.	$-8.05v+-6.58$	0.00	
	Stansfield, 2018[3]	Ground	0.41-2.26	Foot contact	$33.03v+14.61$	0.26	
				Max Ext.	$14.993v^2-38.39v-1.41$	0.37	
Ankle Moment	Lelas, 2003[2]	Ground	0.50-2.50	Max PF.	$-0.0530v^2+0.28v+0.65$	0.48	
Max = Plantarflexion	Stansfield, 2006[3]	Treadmill	0.80-1.80	Max PF.	$0.04v+0.06$	0.00	
Knee Moment	Lelas, 2003[2]	Ground	0.50-2.50	Ext. stance	$0.33v-0.16$	0.73	
Min = Flexion				Flx. stance	$0.05v+0.22$	0.11	
Max = Extension				Ext swing	$0.15v-0.038$	0.89	
				Flx. swing	$-0.04v^2+0.34v-0.09$	0.92	
	Stansfield, 2006[3]	Ground	0.80-1.80	Ext. stance	$0.11v-0.003$	0.06	
				Flx. stance	$-0.05v+0.01$	0.03	
				Ext swing	$-0.04v+0.003$	0.03	
Hip Moment	Lelas, 2003[2]	Treadmill	0.50-2.50	Flx. stance	$0.11v^2+0.21v+0.01$	0.81	
Max = Flexion				Max Ext.	$0.059v^2+0.20v+0.12$	0.80	
Min = Extension				Flx. swing	$0.5741v-0.20$	0.89	
	Stansfield, 2006[3]	Ground	0.80-1.80	Flx. stance	$0.26v-0.024$	0.28	
				Max Ext.	$-0.10v-0.03$	0.18	
				Flx. swing	$0.12v+0.003$	0.08	

Hanlon et al., (2006) assessed the accuracy of methods for estimating lower limb kinematics. Liner regression models constructed from slow (0.93 to 1.38 m/s), normal (1.35 to 1.82 m/s), and fast (1.73 to 2.11 m/s) walking were tested for accuracy in estimating a person's joint angles. Regression models that produced the highest errors were based on regression data taken from speeds outside the regression model's speed range (i.e. using regressions based on fast data to predict slow walking parameters). Results from data within the regression models speed range worked well for predicting joint angles. These results emphasize the need for gait parameter prediction models to include a wide range of speeds in their development.

Regression equation accuracy varied according to population, between subject variability, speed range, speed variability, and experimental methods. No study to our knowledge has investigated published regression equation accuracy at estimating joint kinematics or kinetics at very slow walking speeds. Estimated kinematic result variability (standard deviation and coefficient of variability) from available regression equations were calculated and presented in Table 2-8. Greater variability between estimations appear to exist at slower walking speeds and suggest that error would be greater if these equations were used as references for LEPE control.

2.9 LEPE-human interaction

To improve LEPE adaptive control for rehabilitation based on the principle of assist as-needed, measuring LEPE-human interaction is central to determine the amount of assistance. Currently adaptive controllers model this interaction using reference joint position and forces from pre-recorded trajectories of AB users walking in the device in a passive mode, with low stiffness. This initialisation step determines the minimum interaction torque and position deviation in the determination of thresholds and adaptive behaviour of LEPE assistance. Deriving this information from pre-recorded trajectories of healthy individuals walking with a LEPE is limited as external forces acting on the user (τ_{δ}) do not include support from crutches. LEPE Impedance or residual stiffness while in passive mode do not as well reflect free walking and influence desired trajectories and both actuator (τ_{α}) and user (τ_{u}) joint torques. Pre-recorded trajectories are speed specific and do not simulate desired joint angles of users with motor incomplete injury. Reference data or regression estimates are limited as well because these data were generated without including device mass and inertia. Without accurate position and force data, methods for determining performance to scale stiffness will as well be inaccurate.

Table 2-8: Estimated peak sagittal joint angles using published regression equations.

Peak joint angle (degrees)	Speed (m/s)	Koopman, 2014	Leleas, 2003	Stansfield 2006	Stansfield, 2018	Kirtley, 1985	Mean	SD	CV
Ankle peak plantar-flexion	0.20	1.53	13.64	3.15	-2.00		-4.08	6.73	1.65
	0.40	12.02	14.39	4.01	2.97		-8.35	5.71	0.68
	0.60	18.95	15.15	4.87	7.32		-11.57	6.59	0.57
	0.80	22.33	15.91	5.73	11.05		-13.75	7.07	0.51
	1.00	22.15	16.66	6.59	14.15		-14.89	6.46	0.43
	Range	20.81	3.03	3.44	16.16		10.81	9.01	0.83
Knee peak flexing stance	0.20	8.18	-0.20	11.28	-3.14	7.30	-3.81	6.64	1.74
	0.40	10.36	3.38	13.45	-0.26	9.90	-6.62	6.20	0.94
	0.60	12.54	6.73	15.61	2.50	12.50	-9.33	5.86	0.63
	0.80	14.73	9.85	17.77	5.13	15.10	-11.96	5.62	0.47
	1.00	16.91	12.75	19.93	7.64	17.70	-14.51	5.47	0.38
	Range	8.73	12.94	8.65	10.78	10.40	10.69	1.76	0.16
Knee peak flexion swing	0.20	44.55	46.94	55.41	43.14	51.32	-49.2	5.32	0.11
	0.40	49.83	49.54	56.59	46.22	53.04	-51.35	4.47	0.09
	0.60	53.97	51.89	57.77	48.94	54.76	-53.34	3.79	0.07
	0.80	56.95	53.98	58.95	51.3	56.48	-55.18	3.29	0.06
	1.00	58.79	55.81	60.14	53.32	58.20	-56.87	2.95	0.05
	Range	14.24	8.87	4.72	10.17	6.88	7.66	2.38	0.31
Peak hip flexion	0.20	3.53	4.84	6.97	3.24		-4.65	1.70	0.37
	0.40	5.04	5.86	7.36	5.00		-5.82	1.10	0.19
	0.60	6.54	6.89	7.76	6.69		-6.97	0.54	0.08
	0.80	8.05	7.91	8.15	8.31		-8.11	0.17	0.02
	1.00	9.55	8.93	8.54	9.86		-9.22	0.6	0.06
	Range	6.02	4.09	1.57	6.62		4.57	2.28	0.50
Peak hip extension	0.20	20.78	25.29	27.01	16.22		-22.32	4.85	0.22
	0.40	22.64	26.77	28.84	17.82		-24.02	4.87	0.20
	0.60	24.49	28.24	30.67	19.43		-25.71	4.90	0.19
	0.80	26.35	29.72	32.5	21.04		-27.4	4.93	0.18
	1.00	28.21	31.19	34.34	22.65		-29.1	4.97	0.17
	Range	7.43	5.91	7.32	6.43		6.77	0.73	0.11

Therefore, a method for determining LEPE-human interaction and user performance is needed to better design adaptive controllers based on LEPE-human interaction torque and joint position input. A more formal biomechanical framework is needed for investigating how the human body interacts with a LEPE. This framework must include speed appropriate walking trajectories, the mass and inertia of both the user and the device, and all external forces including those from support aids. This framework is critical to improve LEPE design efficiency, safety, and to better understand human-machine interaction in the development of LEPE for use in physical rehabilitation.

2.10 Modeling

Virtual prototyping tools such as SolidWorks, ADAMS, and SimMechanics can be used by developers to iteratively refine a product design using computer based functional simulations (Agarwal, Narayanan, Lee, Mendel, & Krovi, 2010). Rapid quantification of design scenarios is advantageous in the exoskeleton design process since numerous design questions can be quickly answered, allowing for rapid refinement at a relatively low cost. Virtual prototyping tools have successfully solved engineering challenges by coupling parametric models with functional simulation and optimization. These tools have been used in LEPE design to provide theoretical foundations for kinematic and kinetic control strategies, describe exoskeleton component geometry, and determine mechanisms that describe device dynamics (Ying Li et al., 2013; Yang, Xu, Liu, He, & Xu, 2013). However, these advanced computational tools are insufficient for simulating the LEPE-human interaction (Agarwal et al., 2010).The need for more formal testing and experimentation on how the human body interacts with different LEPE designs is critical to better understand the human dynamics involved in LEPE assistance and device control, and a key piece missing in the exoskeleton design process.

Musculoskeletal analysis tools such as SIMM, OpenSim, AnyBody Modeling System, LifeModeler, and Virtual Interactive Systems (VIMS) perform dynamic kinematic and kinetic simulations of human musculoskeletal systems; including, forces, muscle-lengths, and joint reaction forces. Among other studies, anatomical models used in musculoskeletal simulations include joint degrees of freedom, limb segment inertial properties, and properties of muscle, tendon, cartilage, and bone. These models allow constraints to be applied on specific anatomical structures and musculoskeletal systems to describe complex conditions. Simulations can be driven using three dimensional motion data, where trajectories of surface markers linked to the anatomical model dictate kinematic parameters. Inverse dynamics can be used to calculate net joint reaction moments and forces. Muscle forces can as estimated though muscle recruitment optimization algorithms (Fluit, Andersen, Kolk, Verdonschot, & Koopman, 2014; Jung et al., 2016).

Some musculoskeletal modeling tools allow CAD files from virtual prototyping software to be integrated and kinematically constrained to the anatomical model. This feature incorporates LEPE inertial properties and degrees of freedom, to calculate kinetics. By combining virtual prototyping and musculoskeletal analysis tools, it is possible to apply external constraints and exoskeleton forces to analyse LEPE-human interactions. LEPE-human interaction kinetics could be used as input for adaptive control algorithms and iterative design of future LEPE. Musculoskeletal models have been applied by some LEPE developers and biomechanics researchers to overcome limitations of past CAD modeling tools.

Within the sparsely published literature on LEPE-human models, researchers examined the inertial effects of a LEPE on joint moments during natural human gait (Ferrati, Bortoletto, & Pagello, 2013), interaction forces of LEPE straps and their effect on joint moments (Cho, Kim, Jung, & Lee, 2012) and partial assist upper-limb devices (Agarwal, Kuo, Neptune, & Deshpande, 2013; Agarwal et al., 2010; Guan, Ji, Wang, & Huang, 2016). However, no published literature has modeled a person with paraplegia using an existing exoskeleton. Additionally, current models are not driven with realistic slow walking joint trajectories and ground reaction forces and do not include crutches, despite the majority of LEPE requiring support aids for device use (Figure 2-16). To our knowledge, no publication has reported simulated LEPE gait with crutches and therefore no study has adequately simulated device kinematics and kinetics for LEPE control purposes.

Authors, year	Model	Human model	LEPE	User	Baseline	N
A) Ferrati, 2013	OpenSim	OpenSim 23DOF, 91 muscle	Lower Limb (real)	SCI	Normal	0
B) Zhu, 2013	Life Mod	19 segment, 14 DOF, 0 muscles	Lower Limb (real)	SCI	Normal	0
C) Cho, 2012	AnyBody	AnyBody 37, segments, 69 DOF	Full Body (simplified)	AB	Normal	1
D) Pan, 2014	ADAMS	Simplified	Lower Limb (simplified)	AB	Normal	0
E) Li, 2015	ADAMS	Simplified	Lower Limb (simplified)	AB	Normal	0
F) Shi, 2008	ADAMS	Simplified	Lower Limb (simplified)	AB	Normal	0
G) Yali, 2008	ADAMS	None	Lower Limb (simplified)	AB	Normal	0

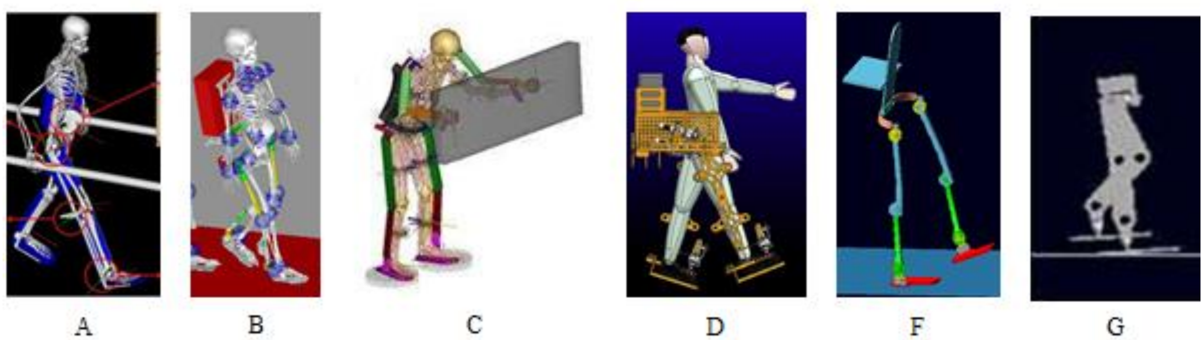

Figure 2-14: LEPE-human models characteristics. N=number of human participants.

2.11 LEPE-human models

Ferrati et al., (2013) designed a LEPE-human model (height 175 cm, weight 75 kg, 23 DOF, 91 muscles) in OpenSim using an existing exoskeleton prototype powered at the knee and hip. This model simulated operating forces required to move the thigh and shank segments along a desired trajectory, and the effect of adding a virtually prototyped actuated ankle. Model hip and knee angles closely followed OpenSim reference trajectories, with or without an actuated ankle, with minimal effects on hip and knee actuator forces. General forces calculated in this study did not include GRF between the LEPE-human model feet and the ground or contact forces between the LEPE-human model hands and parallel bars. Thus, reported forces only represented forces to overcome LEPE-human segment inertia. The author’s rational for negating external contact forces was that the system was designed as an assistive device, and only slow velocities would be involved. However, able-bodied kinematics, not slow speed, were used to drive the simulation and the assumption that slow walking forces are negligible is incorrect. This simulation also failed to reflect the contribution of a stabilisation aid (parallel bars or crutches).

Zue et al., (2013) also examined LEPE-human joint alignment by combined a human model anthropoid (19 segment, 14 DOF, 0 muscles) and a real exoskeleton using ADAMS (MSC Software Corporation). This study used LifeModeler (LifeModeler, Inc.) to generate natural human gait; however, like Ferrati et al., (2013), able-bodied kinematics were used and the authors did not include GRF. GRF were included in a full body, human-exoskeleton model to analyze an exoskeleton assisting an able-bodied person (Cho et al., 2012). However, GRF were simulated using predictive force plate modelling. Lifting movements were assessed with objects of increasing weight (0, 10, 20, 40 kg), with different strapping configurations that connected the user to the exoskeleton. A simplified CAD model of a full-body exoskeleton (upper and lower limb, 22 DOFs), was integrated with a full body musculoskeletal model (37 segments, 69 DOFs) from AnyBody's human model repository. Human joint moments and the interaction force between the human model and the exoskeleton were selected as performance measures. Not surprisingly, additional strapping resulted in better force distribution, reducing moments at the wrists and ankles. Additional strapping increased the stress on the human body (3.5 kPa); however, this stress was below values that could cause bodily harm (4.0 kPa) or skin damage (9.0 kPa) (Crenshaw & Vistnes, 1989).

Other studies have modeled LEPE to simulate LEPE control algorithms for stable LEPE walking, but these studies did not include a human model (Liao et al., 2015; Shi, Zhang, & Yang, 2008). LEPE simulations have also been used to estimate required joint torques of activities of daily living for joint control (Hicks & Ginis, 2008; Talaty et al., 2013) and to optimise LEPE hardware (Mooney & Herr, 2016) or joint trajectories (Ong, Hicks, & Delp, 2016). These studies used simplified human models or did not include device mass, simplifying the influence of LEPE-human interaction and segment inertia by multiplying normalised joint torques by the combined weight of the LEPE and user. While interesting and a first step in the development of LEPE-human models, results from these studies have limited ecological validity because they did not adequately simulate intended device use under realistic conditions. LEPE-human interactions are important for interactive LEPE control. A complete model incorporating these features is required to understand the human dynamics involved in LEPE assisted gait and act as input for LEPE interactive control strategies.

Chapter 3. Temporal-Spatial Gait Parameter Models of Very Slow Walking

The contents of this chapter were published in Gait and Posture:

Smith, A. J. J., & Lemaire, E. D. (2018). Temporal-spatial gait parameter models of very slow walking. Gait & posture, 61, 125-129.

3.1 Abstract

This study assessed the relationship between walking speed and common temporal-spatial stride-parameters to determine if a change in gait strategy occurs at extremely slow walking speeds. Stride-parameter models that represent slow walking can act as a reference for lower extremity exoskeleton and powered orthosis controls since these devices typically operate at walking speeds less than 0.4 m/s. Full-body motion capture data were collected from 30 health adults while walking on a self-paced treadmill, within a CAREN-Extended virtual reality environment. Kinematic data were collected for 0.2, 0.3, 0.4, 0.5, 0.6, 0.7, 0.8 m/s, and self-selected walking speed. Eight temporal stride-parameters were determined and their relationship to walking speed was assessed using linear and quadratic regression. Stride-length, step-length, and step-frequency were linearly related to walking speed, even at speeds below 0.4 m/s. An inflection point at 0.5 m/s was found for stride-time, step-time, stance-time, and double-support-time. Equations were defined for each stride-parameter, with equation outputs producing correlations greater than 0.91 with the test data. This inflection point suggests a change in gait strategy at very slow walking speeds favouring greater ground contact time.

3.2 Introduction

Humans naturally walk at different velocities, effortlessly increasing or decreasing step-frequency and stride-length to speed up or slowdown (Murray et al., 1966). Several investigations at slow, comfortable, and fast walking speeds have been conducted to characterise temporal-spatial stride-parameters (Andriacchi et al., 1977; Ardestani et al., 2016; Kirtley et al., 1985; Oberg et al., 1993; Shemmell et al., 2007). From these studies, simple linear relationships have been found between walking speed and stride-length and between walking speed and step-frequency. Curvilinear relationships were found between walking speed and stance-time, swing-time, and stride-time. Researchers that modelled temporal-spatial parameters and walking speed provided simple linear regression equations that predicted step-length and frequency, and approximated swing and stance-time, using quadratic polynomials or logarithmic formulas (Andriacchi et al., 1977; Grieve & Gear, 1966; Kirtley et al., 1985). These results and seminal works investigating walking speed (Winter, 1984) have led to a general assumption that stride-parameters follow a consistent pattern of change in response to speed, and that stride-parameter values can be predicted at a given walking velocity.

Numerous researchers have characterised the relationship between temporal-spatial parameters at slow, comfortable, and fast walking speeds. However, few studies have investigated these relationships with very slow walking speeds, below 0.4 m/s (Nymark et al., 2005; Stoquart et al., 2008), and no study has applied regression analyses to determine if very slow speeds follow a predictable pattern of change. Therefore a complete characterisation of stride-parameters at very slow speeds has yet to be realised.

At their preferred walking speeds, persons with lower limb pathology walk with visibly altered gait patterns compared to able-bodied people. Direct comparisons between these populations failed to identify stride-parameter differences independent of walking speed, where walking speed can differ by two to 10 times depending on the severity of pathology (Pepin et al., 2003). In this regard, clinicians should make allowances for walking speed when basing clinical decisions on stride-parameters. To do so, clinicians must know stride-parameter reference values across a wide range of walking velocities, including very slow walking (<0.4 m/s).

Slow walking is especially relevant for new lower extremity powered exoskeletons (LEPE), where users walk at speeds between 0.1 m/s and 0.55 m/s, with an average speed of 0.26 m/s (Louie et al., 2015). LEPE joint trajectories are from able-bodied individuals walking at speeds unattainable in use, including studies specifically conducted to provide slow walking joint trajectory data for exoskeleton development (Han & Wang, 2011).

Since individuals walking slowly use different locomotor and postural control strategies (Nymark et al., 2005; Otter et al., 2004), the relationship between speed and temporal-spatial parameters may change at slowing walking speed due to reduced underlying locomotor task demands on speed dependent muscle activation amplitude (Hof, Elzinga, Grimmius, & Halbertsma, 2002), time spent in double support (Murray et al., 1984), and altered neuromuscular control of the swing limb (Den Otter, Geurts, Mulder, & Duysens, 2007). An improved understanding of stride-parameters at speeds achievable by device users would provide a biomimetric basis for developers when designing LEPE gait trajectories. These data would provide a clearer picture of device parameters required to support users in the early stages of recovery following neurological injury, as well as those achievable within device parameter limitations (strength and speed of motors, number of joints, etc.).

This research extended temporal-spatial parameters models to very slow speeds that are common for exoskeleton users and those with incomplete spinal cord injury. Based on the assumption in the literature that parameters associated with walking speed follow a predictable pattern of change, we hypothesized that stride-parameters would fit simple linear and quadratic formulas at walking speeds below 0.4 m/s, but that these patterns may change predictably at very slow speeds. This analysis provides a more complete characterisation of stride-parameters at very slow speeds, a valuable tool for both clinicians and lower extremity powered orthosis developers.

3.3 Methods

3.3.1 Participants

A convenience sample of thirty able-bodied (AB) volunteers was recruited from staff, students, and volunteers at The Ottawa Hospital Rehabilitation Centre and University of Ottawa. (15 males, 15 females; mass=75.8±13.2 kg, height=1.73±0.12 m; age=30±10 years). Participants did not have gait or health issues that affected walking on level ground. Participant's leg-length was recorded for normalisation purposes. This study was approved by The Ottawa Hospital Research Ethics Board and all participants provided informed consent.

3.3.2 Equipment

The CAREN-Extended virtual environment (Motekforce Link, Amsterdam, NL) was used in this study. This system includes Vicon 3D motion capture (Vicon, Oxford, UK), 180° screen for 3D virtual world projection, and a six degree of freedom (6-DOF) moving platform with an embedded dual-track treadmill (Bertec Corp. Columbus, OH), with force plates under each track sampling at 1000 Hz. Full-body kinematics were tracked at 100 Hz, using a 6-DOF, 57 marker set (Wilken, Rodriguez, Brawner, & Darter, 2012). Platform position was tracked using three markers on the platform surface.

Participants were provided time to acclimate to the seven slow walking speeds (0.2-0.8 m/s, incremented by 0.1) and to self-paced treadmill walking. The self-paced (SP) algorithm used pelvis markers to determine the participant's anterior-posterior position on the treadmill, velocity, and acceleration, in relation to the participant's initial standing position (middle of the treadmill). As the participants walked, the system automatically changed treadmill speed to keep the person in the middle of the treadmill. Acclimation is required to ensure that the person does not try to walk at the front of the treadmill, where the treadmill would continue to speed up to bring the person back to their middle position. Following the acclimation period, at least 10 strides of level walking were collected for each speed while participants walked on a path through a virtual park scene (Sinitski et al., 2015) that provided realistic optic flow. Speeds were randomised to avoid learning bias. Total walking distance varied depending on acclimation period and time to complete 10 left and right strides with the left and right leg landing on their respective force plates.

3.3.3 Data analysis

Marker data were filtered with a dual pass, 4th order, low pass, dual pass Butterworth filter (10Hz). A 13-segment body model was created in Visual3D (C-Motion Inc., Germantown, MD). Foot on and foot off where determined using ground reaction force data, calculated at the first frame the vertical ground reaction force exceeded or dropped below 20 N respectively. Ground reaction force data were filtered with a zero phase shift 4th order Butterworth low pass filter with a cut off frequency of 20 Hz. Treadmill speed was determined from anterior-posterior foot marker velocity during midstance. Custom Matlab software (2016a, Mathworks, Matwick, MA) was used to calculate stride-time, step-time, stance-time, swing-time, double-support-time (DST), stride-length, step-length, and step-frequency (Table 3-1). These parameters were summarised for each person using mean, standard deviation, max, min, coefficients of variability, and 95% confidence interval. Repeated measures analysis of variance (ANOVA) was performed to determine the effect of walking speed and leg dominance, with p <0.05 considered statistically significant.

Group means for each parameter were calculated at each speed. Linear and quadratic regressions were performed to determine the relationship between walking speed and mean stride-parameter values. Pearson correlations were applied to determine the strength of association between speed and each stride-parameter. A coefficient of determination (R^2) greater than 0.90 was considered strong.

Table 3-1: Temporal-spatial stride parameter definitions.

Stride-time	Time (s) between successive foot contacts of the same foot
Step-time	Time (s) between successive contacts of each foot
Stance-time	Time (s) when the foot is in contact with the ground
Swing-time	Time (s) when the foot is not in contact with the ground
Double-support-time	Time between foot-off on one limb and foot contact on the opposite limb (% of stride-time)
Stride-length	Anterior-posterior distance (m) between the same heel marker over successive foot contacts
Step-length	Anterior-posterior distance (m) between heel markers at foot stride
Step-frequency	Number of steps per second (steps/s)

For parameters without a strong correlation, linear regressions were used to test for inflection points between faster and slower walking speeds. For each participant, linear regressions were performed across multiple walking speed sets, with data from the next slowest speed added to subsequent sets. Linear regression R^2 were determined for each speed set and a non-linear change was identified if R^2 dropped below 0.90 and remained so for subsequent sets. An inflection point was identified if a non-linear change occurred consistently at the same speed for the majority of participants. If an inflection point was found, linear and quadratic equations were fit to data before and after the defined point. To investigate leg-length effects, linear and quadratic curves were also calculated with speed normalised to leg-length.

Equations for parameters with strong linear and quadratic correlations were applied to each participant's data to assess how well the equations represented the participant's temporal-spatial gait. All statistics were calculated using Malab's Statistics and Machine Learning Toolbox.

3.4 Results

Temporal-spatial results for all speeds are shown in supplemental material (Appendix 8.1). No significant main effect was observed between limbs ($p = 0.247$), across all parameters. Linear and quadratic equations and R^2 values are presented in Table 3-2. As expected, stride-length (R^2 = 0.98±0.03), step-length (R^2 = 0.98±0.02), and step-frequency (R^2 = 0.94±0.04) had strong positive linear relationships with effect of walking speed. Correlations were marginally improved using a quadratic equation (R^2 = 0.99±0.02; R^2 = 0.99±0.02; R^2 = 0.95±0.05).

Stride, step, stance, and double-support-times all had a consistent inflection point at 0.5 m/s. Swing-time did not have a strongly linear relationship to speed and a consistent inflection point was not identified. Linear and quadratic equations fit before and after the 0.5 m/s inflection point had very strong negative correlations with speed (Table 3-3).

Table 3-2: Linear and quadratic equations from group means with coefficient of determination (R^2). ν = velocity (m/s).

Parameter	Linear Equation	R^2	Quadratic Equation	R^2
Stride-time (s)	-1.427ν + 2.615	0.73	$2.121v^2$ + -4.698ν + 3.575	0.76
Step-time (s)	-0.699ν + 1.292	0.72	$1.061v^2$ + -2.335ν + 1.773	0.75
Stance-time (s)	-1.260ν + 2.009	0.71	$1.964v^2$ + -4.290ν + 2.898	0.74
Swing-time (s)	-0.170ν + 0.606	0.87	$-0.173v^2$ + 0.436ν + 0.685	0.87
Double-support-time (s)	-0.533ν + 0.688	0.67	$0.894v^2$ + -1.912ν + 1.092	0.71
Stride-length (m)	0.712ν + 0.47	1.00	$-0.123v^2$ + 0.902ν + 0.414	1.00
Step-length (m)	0.355ν + 0.236	1.00	$-0.059v^2$ + 0.446ν + 0.209	1.00
Step-frequency (steps/s)	1.016ν + 0.659	0.95	$-0.630v^2$ + 1.988ν + 0.374	0.95

Equations for parameters with strong correlations were applied to each participant's data and mean R^2 results were calculated (Table 3-4). All equations had very strong correlations between calculated and measured results, for the majority of participants. Step-length R^2 range was 0.91-1.00 (0.98±0.02), stride-length was 0.88-1.00 (0.98±0.03), and step-frequency was 0.82-0.99 (0.94±0.40).

Table 3-3: Linear and quadratic equations with coefficient of determination (R^2) for gait parameters with an inflection point at 0.5 m/s. ν = velocity m/s.

Speed	Parameter	Linear Equation	R^2	Quadratic Equation	R^2
<0.5 m/s	Stride-time (s)	-4.102ν + 3.612	0.95	$10.49v^2$ + -11.328ν + 4.729	0.95
	Step-time (s)	-2.015ν + 1.785	0.95	$5.117v^2$ + -5.54ν + 2.33	0.95
	Stance-time (s)	-3.807ν + 2.952	0.94	$10.242v^2$ + -10.862ν + 4.044	0.95
	Double-support-time (s)	-1.728ν + 1.128	0.93	$5.125v^2$ + -5.259ν + 1.674	0.94
>0.5 m/s	Stride-time (s)	-0.691ν + 1.937	0.93	$0.891v^2$ + -2.37ν + 2.626	0.93
	Step-time (s)	-0.33ν + 0.953	0.91	$0.464v^2$ + -1.204ν + 1.312	0.92
	Stance-time (s)	-0.577ν + 1.381	0.93	$0.747v^2$ + -1.985ν + 1.958	0.93
	Double-support-time (s)	-0.223ν + 0.403	0.92	$0.295v^2$ + -0.778ν + 0.631	0.93

Regression analysis after normalizing gait speed to leg-length did not show an improvement in equation R^2. Therefore, normalised regression results were not presented. From repeated measures ANOVA of gait speed and leg dominance, for each parameter, speed significantly affected each parameter ($p<0.5$) but leg dominance did not. Therefore regression results for the dominant leg are only reported.

Table 3-4: Group means and standard deviations (in brackets) of coefficient of determination (R^2) between linear and quadratic equations results and parameters values from each participant across walking speeds.

Speed	Parameter	Linear R^2	Quadratic R^2
0.2 m/s to self-paced	Stride-length (m)	0.98 (0.03)	0.99 (0.01)
	Step-length (m)	0.98 (0.02)	0.99 (0.01)
	Step-frequency (m)	0.94 (0.04)	0.99 (0.01)
0.2 m/s to 5m/s	Stride-time (s)	0.99 (0.03)	0.98 (0.02)
	Step-time (s)	0.98 (0.03)	0.98 (0.02)
	Stance-time (s)	0.98 (0.06)	0.99 (0.02)
	Double-support-time (s)	0.97 (0.08)	0.98 (0.02)
0.5 m/s to SP	Stride-time (s)	0.92 (0.04)	0.98 (0.02)
	Step-time (s)	0.91 (0.03)	0.98 (0.02)
	Stance-time (s)	0.92 (0.04)	0.99 (0.02)
	Double-support-time (s)	0.91 (0.05)	0.98 (0.02)

3.5 Discussion

Consistent with the general assumption that stride-parameters associated with walking speed are linear and predictable, simple linear relationships were found between walking speed and stride-length, step-length, and step-frequency. These relationships were strongly correlated ($R^2 > 0.9$); therefore, linear equations can be used to describe the relationships between walking speeds and these temporal-spatial parameters, even at speeds below 0.5 m/s. However, this linear approach was not the best solution for other temporal-spatial measures.

While linear regression was acceptable for stride-length, step-length, and step-frequency, quadratic model R^2 were slightly better, when applied to each participant's data (Table 3-3). In the literature, linear models were promoted due to their simplicity. However, powered orthoses may benefit from more robust models, where even 1% improvement in device control could improve a person's assisted mobility and avoid stumbles.

Swing-time was not well represented by linear or quadratic equations, and presented no inflection point. Few studies have investigated swing-time in relations to very slow walking speeds. Grive and Gear (Grieve & Gear, 1966) reported no simple relationship with swing and gait speed, since people of similar stature varied swing-time more predictably with respect to cycle duration but did so as "a matter of individual choice". We found that swing-time was inversely proportional to speed, and better fit our sample population using a quadratic polynomial ($R^2 = 0.85 \pm 0.15$) versus a linear model ($R^2 = 0.73 \pm 0.18$). While an R^2 of 0.85 could be considered strong, neither regression met the conservative criterion we placed on temporal-spatial parameter correlations.

Swing is considered a passive process at optimum walking velocities (Shemmell et al., 2007), and is the least constrained motion in the gait cycle. Modelling swing-phase parameters may be more difficult at slower walking speeds (Grieve & Gear, 1966) because muscle activity at foot off varies and momentum changes during pre-swing at non-optimal speeds may affect limb advancement. Muscle activation patterns can vary between individuals but remain fairly consistent with respect to speed, with activation patterns phase shifting within the gait cycle in the direction of swing-phase onset (Ivanenko, Poppele, & Lacquaniti, 2004). Thus, while determining when swing is passive or active may be difficult at slower speeds, without EMG data, muscle activation patterns in the literature were consistent despite speed changes. However, our lower swing-time correlation results supported the idea that swing and stance are not controlled by the same mechanisms (Frenkel-Toledo et al., 2005). This has implications for the relative priority of these periods in relation to stability and should be investigated in future research.

While spatial measures (stride-length, step-length) decreased linearly with reduced waking speed, all temporal parameters (stride, step, stance, and double-support-times) had an inflection point at 0.5 m/s. Several studies described curvilinear relationships with proportional changes for these temporal parameters and speed (Andriacchi et al., 1977; Grieve & Gear, 1966; Kirtley et al., 1985; Murray et al., 1966, 1984; Pepin et al., 2003; Stoquart et al., 2008); however, many of these studies included speeds greater than participant's comfortable walking pace, did not include data at speeds below 0.4 m/s, did not apply regression analysis, or applied a regression model without previously identifying consistent deviations from the linear model. We also found a non-linear change in relation to speed for these temporal measures, which could be described using a curvilinear relationship, but expanded upon these findings by identifying a consistent point of inflection at 0.5m/s. The inverse relationship of the temporal parameters to speed was greater when walking slower than 0.5m/s, resulting in a point of inflection. Increased double support and stance-times (i.e. longer floor contact) resulted in longer stride and step-times. Consistent stride-parameter deviations for very slow walking speeds may indicate a change in gait strategy favouring floor contact time that developers of powered orthoses should take into consideration.

Some parameters may not have a linear relationship with slow walking speeds. This may be due to deviation from typical swing limb passive pendulum-like behaviour. Within normal walking speeds, passive swing limb movement promotes energy conservation (Holt, Jeng, Ratcliffe, & Hamill, 1995; Shemmell et al., 2007) and a linear relationship with stride-length and step-frequency occurs. At very slow walking speeds, passive control strategies may not allow forward progression due to increased postural control requirements and active swing limb acceleration to complete a shortened swing-phase (Otter et al., 2004). Prolonged double-support-time (Bauby & Kuo, 2000; Murray et al., 1984) and shortened swing-phase improve dynamic balance but force a non-linear break from passive pendulum-like behaviour. This is supported by our results with stride-time, step-time, and double-support-time showing an inflection point at 0.5m/s.

Changes in gait strategy have been observed among people with neurological injury and for simple sagittal gait models (Fukunaga et al., 2001; Jonsdottir et al., 2009). Maximal walking speeds of 0.5 m/s have been observed among persons with spinal cord injury as a consequence of reaching their maximum stride-length but not being able to increase stride frequency (Pepin et al., 2003). This strategy is similar to those with hemiplegic stroke who increase stride frequency instead of stride-length when asked to walk above their comfortable walking pace (Jonsdottir et al., 2009). Reduced or lack of ankle plantarflexion function (Fukunaga et al., 2001) greatly reduces the ability to generate the propelling force needed to increase stride frequency (Perry & Burnfield, 2010). Efforts to define gait without an active ankle at different walking speeds, using sagittal plane models with circular feet, have effectively represented gait kinematics up to 0.4 m/s. Faster speeds were modeled as well but with shorter steps and increasing cadence (Martin & Schmiedeler, 2014). The inability of this sagittal model to match human gait at faster speeds was the result of energy loss at the ankle, and this energy loss increased with increasing step-length. This may be the case with current robotic exoskeletons without actuated ankles, where they reach a functional limit for walking speed and safe stride-length, and a mechanical limit for stride frequency. Current exoskeleton designs without actuated ankles may need to increase stride frequency capabilities to enable walking speeds above 0.4m/s.

A limitation of this protocol is the use of a treadmill for walking evaluation. Treadmill overground comparison studies both at comfortable (Gates et al., 2012; Parvataneni, Ploeg, Olney, & Brouwer, 2009) and very slow walking speeds (Carpinella, Crenna, Rabuffetti, & Ferrarin, 2009; Stoquart et al., 2008) have yet to come to a consensus as to how overground differs from treadmill walking. A study by Gates et al., (2012) found that treadmill use in the CAREN virtual environment is similar enough to overground, when walking at a fixed leg-length normalized speed, but authors should be cautious when comparing step-time results from treadmill studies to overground walking (Gates, Darter, Dingwell, & Wilken, 2012).

This study evaluated an able-bodied cohort thus the generalizability of this study to pathological gait populations has yet to be determined. As well, the preliminary evaluation of these equations involved applying them to the same population that was used to generate the equations, which may bias the results. While this evaluation provides preliminary information on equation use, re-testing with a new sample of able-bodied and gait pathology participants is needed to verify the ecological validity of our outcomes.

3.6 Conclusion

This research showed that stride-parameters for walking speeds between 0.2 and 0.8 m/s can be modelled for use in gait assessment and lower extremity powered exoskeleton control. However, a non-linear inflection point at 0.5 m/s must be considered for stride-time, step-time, stance-time, and double-support-time. This inflection point suggested a change in gait strategy between very slow walking speeds, favouring even greater floor contact time. The relationships and equations defined in this research can be used to include this strategy in the development of biomimetic powered orthoses. This analysis, focusing on very slow walking speeds, helps provide a more complete characterisation of stride-parameters at very slow clinically relevant speeds. This research provides a valuable comparison-base for understanding pathological gait, with slow walking stride-parameters taken into consideration. The primary goal of this research was to provide lower extremity powered orthosis developers a tool to properly scale temporal-spatial stride-parameters for device trajectory development. In this regard, quadratic models may be more robust for step-length, stride-length, and stride frequency, previously considered as linear for model simplicity. A consistent inflection at 0.5 m/s should be considered in trajectory development to improve device floor contact time and device-user stability.

Chapter 4. Lower Limb Sagittal Kinematic and Kinetic Modeling of Very Slow Walking for Gait Trajectory Scaling

The contents of this chapter were published in PloS One:

Smith, A. J., Lemaire, E. D., & Nantel, J. (2018). Lower limb sagittal kinematic and kinetic modeling of very slow walking for gait trajectory scaling. PloS One, 13(9), e0203934.

4.1 Abstract

Lower extremity powered exoskeletons (LEPE) are an emerging technology that assists people with lower-limb paralysis. LEPE for people with complete spinal cord injury walk at very slow speeds, below 0.5m/s. For the able-bodied population, very slow walking uses different neuromuscular, locomotor, postural, and dynamic balance control. Speed dependent kinetic and kinematic regression equations in the literature could be used for very slow walking LEPE trajectory scaling; however, kinematic and kinetic information at walking speeds below 0.5 m/s is lacking. Scaling LEPE trajectories using current reference equations may be inaccurate because these equations were produced from faster than real-world LEPE walking speeds. An improved understanding of how able-bodied people biomechanically adapt to very slow walking will provide LEPE developers with more accurate models to predict and scale LEPE gait trajectories. Full body motion capture data were collected from 30 healthy adults while walking on an instrumented self-paced treadmill, within a CAREN-Extended virtual reality environment. Kinematic and kinetic data were collected for 0.2 m/s - 0.8 m/s, and self-selected walking speed. Thirty-three common sagittal kinematic and kinetic gait parameters were identified from motion capture data and inverse dynamics. Gait parameter relationships to walking speed, cadence, and stride-length were determined with linear and quadratic (second and third order) regression. For parameters with a non-linear relationship with speed, cadence, or stride-length, linear regressions were used to determine if a consistent inflection occurred for faster and slower walking speeds. Group mean equations were applied to each participant's data to determine the best performing equations for calculating important peak sagittal kinematic and kinetic gait parameters. Quadratic models based on walking speed had the strongest correlations with sagittal kinematic and kinetic

gait parameters, with kinetic parameters having the better results. The lack of a consistent inflection point indicated that the kinematic and kinetic gait strategies did not change at very slow gait speeds. This research showed stronger associations with speed and gait parameters then previous studies, and provided more accurate regression equations for gait parameters at very slow walking speeds that can be used for LEPE joint trajectory development.

4.2 Introduction

Motor adaptation to different gait speeds are relevant to lower extremity powered exoskeletons (LEPE) since predefined gait control strategies are typically used for persons with complete paraplegia (Yan, Cempini, Oddo, & Vitiello, 2015). Consistent with patients receiving neurological rehabilitation (Nymark et al., 2005), persons using a LEPE walk at speeds between 0.1m/s and 0.55 m/s (Aach et al., 2014; Arazpour et al., 2013, 2012; Benson et al., 2016; Farris et al., 2014; Fineberg et al., 2013; Kressler et al., 2014; Neuhaus, 2011; Ohta et al., 2007; Tanabe, Hirano, et al., 2013; Zeilig et al., 2012), with an average speed of 0.26 m/s (Louie et al., 2015). However, LEPE predefined joint trajectories are typically developed from able-bodied individuals walking within a normal range of walking speeds. Since walking slowly is considered to be more complex (Schablowski-Trautmann & Gerner, 2006) and uses different locomotor and postural control strategies (Holden et al., 1997; Nymark et al., 2005; Otter et al., 2004), LEPE may be improved with predefined joint trajectories based on speed-appropriate slow gait biomechanics.

Despite a wealth of biomechanics literature on a range of gait speeds (Borghese et al., 1996; Bovi et al., 2011; Han & Wang, 2011; Hanlon & Anderson, 2006; Lelas et al., 2003; Li et al., 2005; Murray et al., 1984; Nymark et al., 2005; Tommy Oberg & Karsznia, 1994; Schwartz et al., 2008; Stoquart et al., 2008), the slowest walking speed in studies that predicted kinematic and kinetic parameters was 0.5 m/s, and averaged greater than 0.9 m/s. From some of these works, kinematic peak sagittal parameters were found to be positively correlated with gait speed, but that R^2 from simple linear (R^2<0.60) and quadratic (R^2<0.45) regressions were weak (Hanlon & Anderson, 2006; Lelas et al., 2003). As well, kinematics were significantly less accurate when calculated from regression equations produced from gait speeds outside those being modeled (Hanlon & Anderson, 2006). Contrary to kinematics, gait kinetics have shown strong relationships with gait speed (Kirtley et al., 1985; Tommy Oberg & Karsznia, 1994), with R^2 greater than 0.90 for knee flexion (Kirtley et al., 1985) and extension (Lelas et al., 2003) moments. However, if regression equations are inaccurate at walking speeds outside the range they were produced from, even highly correlated kinetic equations may be inaccurate at very slow walking speeds.

The reasons for kinematics having lower correlations than kinetics may be gait speed variability and experimental methods (Ardestani et al., 2016; Astephen Wilson, 2012). An inherent problem with interpreting biomechanical results is that gait variable differences can often be partially or entirely explained by speed (Astephen Wilson, 2012). One method for controlling speed mediated effects on gait is the use of an instrumented treadmill to reduce outcome measure variability when researching task specific biomechanics (Andriacchi et al., 1977; Kirtley et al., 1985). However, treadmills that dictate constant walking speeds by reducing variability compared to overground walking (Riley et al., 2007) may not reflect the joint's natural mechanical environment (Astephen Wilson, 2012). However, this methodology would be sufficient for modeling kinematic and kinetic speed dependent changes in gait for LEPE development because a LEPE also imposes a consistent and less variable walking pattern. Recently, we assessed extremely slow walking speeds of able-bodied adults to determine if changes in strategy were required at LEPE walking speeds (Smith & Lemaire, 2018). A consistent inflection point at 0.5 m/s was found for step-time, stance-time, and double-support-time, suggesting a change in strategy at very slow speeds that favours increased ground contact time. The effect of these slow walking speeds on common sagittal plane kinematic and kinetic parameters has yet to be determined.

The primary goal of this research was to produce a set of reference equations derived from very slow gait speeds to improve modelling accuracy of peak sagittal gait parameters for gait trajectory scaling and LEPE development. This research included very slow walking speeds that are common for exoskeleton users. Since gait speed is the product of cadence and stride-length, we examined these three stride parameters for their relationship with sagittal kinematic and kinetic gait parameters. The research outcomes determined which stride parameter had the best relationships between very slow walking and peak sagittal kinetics and kinematics. Based on previous literature, we hypothesized that kinetics would have stronger associations with temporal-spatial parameters. From our previous research on stride parameters (Smith & Lemaire, 2018), we hypothesised that a change in gait strategy would occur at 0.5m/s, indicated by an inflection point for parameters with non-linear relationships with speed, cadence, or stride-length. An improved understanding of gait kinematics and kinetics at speeds achievable by exoskeleton device users, by identifying how able-bodied people biomechanically adapt to very slow gait speeds, will provide LEPE developers with better models for predicting and scaling exoskeleton gait trajectories.

4.3 Methods

4.3.1 Participants

Thirty able-bodied (AB) volunteers were recruited from staff, students, and volunteers at The Ottawa Hospital Rehabilitation Centre and University of Ottawa (15 males, 15 females; mass=75.8±13.2 kg, height=1.73±0.12 m; age=30±10 years). To be enrolled in the study participants did not have health issues that would affect walking on a treadmill. Prior to testing, volunteers were notified of potential risks of participating in this research and signed an informed consent form. This study, including consent forms, was approved by both the Ottawa Health Science Network and the University of Ottawa Research Ethics Boards.

4.3.2 Equipment

The CAREN-Extended virtual environment (Motekforce Link, Amsterdam, NL) was used for the movement activities and data collection. This system included 3D motion capture (Vicon, Oxford, UK), six degree of freedom (6-DOF) moving platform with an embedded dual-track treadmill (Bertec Corp. Columbus, OH) with force plates under each track sampled at 1000 Hz, 180° screen for 3D virtual world projection. Full body kinematics were tracked at 100 Hz, using a 6-DOF, 57-markerset (Wilken et al., 2012).

4.3.3 Procedure

Participant's height, weight, and leg dominance were collected. Height and weight were used to scale the biomechanical model to each participant for three dimensional motion analysis. Leg dominance was determined by the participants answer to "what leg would you use to kick a ball as far as possible". Participants were given time to acclimate to the seven slow walking speeds (0.2-0.8 m/s, incremented by 0.1) and to self-pace treadmill walking. Participants walked 40 meters at each walking speed (total 320 m), through a virtual park scene that provided realistic optic flow. At least 10 successful left and right strides of level walking were collected for each speed, where the participant cleanly contacted the two force plates with their right and left feet. Walking speeds were randomised to avoid learning bias.

4.3.4 Data analysis

Three-dimensional marker data were filtered with a 4^{th} order, low pass Butterworth filter (10Hz). A 13-segment model was defined using Visual3D (C-Motion) scaled to the participant's height and weight. Ground reaction force data were filtered with a zero lag Butterworth filter with a cut off frequency of 20 Hz. Matlab software (2016a, Mathworks, Matwick, MA) was used to identify 33 common peak sagittal kinematic and kinetic parameters (Table 4-1). Repeated measures analysis of variance (ANOVA) was performed to determine if leg dominance had an effect on very slow sagittal gait kinematics and kinetics, with a $p < 0.05$ considered to be statistically significant.

Group means and standard deviations for each parameter were calculated at each speed. Linear and quadratic (second and third order) regressions were calculated to determine group mean equations for each of 33 sagittal gait parameters and 3 stride parameters (speed, cadence, stride-length). Pearson correlations were applied to determine the strength of association between each stride parameter and mean peak sagittal gait parameters. Coefficient of determination (R^2) greater than 0.90 were considered strong, 70-89 moderate, 40-69 weak, and <39 poor.

For parameters with R^2<0.9, linear regressions between each sagittal gait parameter and speed, cadence, or stride-length were used to determine if a consistent inflection point occurred for faster and slower walking speeds. For each parameter, linear regressions were performed for the following six gait speed sets (m/s): SP, 0.8, 0.7; SP, 0.8, 0.7, 0.6; SP, 0.8, 0.7, 0.6, 0.5; SP, 0.8, 0.7, 0.6, 0.5, 0.4; SP, 0.8, 0.7, 0.6, 0.5, 0.4, 0.3; SP, 0.8, 0.7, 0.6, 0.5, 0.4, 0.3, 0.2. If the R^2 from a parameter's speed sets dropped and remained below 0.90 for subsequent sets, a non-linear change was identified. An inflection point was identified if a non-linear change occurred consistently at the same speed for greater than 50% of participants.

The group mean equations were applied to each participant's data to assess how well the equations represented the participant's peak sagittal kinematics and kinetics. The best performing equations (i.e. individual R^2) fit the largest number of participants with a R^2 greater than 0.90 and had the highest average R^2. If R^2 were equally as high for the same number of study participants, the simpler equation was chosen.

For parameters with R^2<0.9, linear regressions between each sagittal gait parameter and speed, cadence, or stride-length were used to determine if a consistent inflection point occurred for faster and slower walking speeds. For each parameter, linear regressions were performed for the following six gait speed sets (m/s): SP, 0.8, 0.7; SP, 0.8, 0.7, 0.6; SP, 0.8, 0.7, 0.6, 0.5; SP, 0.8, 0.7, 0.6, 0.5, 0.4; SP, 0.8, 0.7, 0.6, 0.5, 0.4, 0.3; SP, 0.8, 0.7, 0.6, 0.5, 0.4, 0.3, 0.2. If the R^2 from a parameter's speed sets dropped and remained below 0.90 for subsequent sets, a non-linear change was identified. An inflection point was identified if a non-linear change occurred consistently at the same speed for greater than 50% of participants.

Table 4-1: Peak sagittal kinematic and kinetic gait parameters.

Header	Parameter	Description
AAx1	Ankle Angle	Plantarflexion during early stance
AAx2	Ankle Angle	Dorsiflexion during stance
AAx3	Ankle Angle	Plantarflexion during swing
AAx4	Ankle Angle	Dorsiflexion during swing
AAxRG	Ankle Angle	Ankle range
KAx1	Knee Angle	Knee flexion at initial contact
KAx2	Knee Angle	Knee flexion during early stance
KAx3	Knee Angle	Knee extension during stance
KAx4	Knee Angle	Knee flexion during swing
KAxRG	Knee Angle	Knee range
HAx1	Hip Angle	Hip flexion during early stance
HAx2	Hip Angle	Hip extension during mid to late stance
HAx3	Hip Angle	Hip flexion during swing
HAxRG	Hip Angle	Hip range
AMx1	Ankle Mom	Dorsiflexor moment during early stance
AMx2	Ankle Mom	Plantarflexor moment during stance
KMx1	Knee Mom	Knee flexor moment just after initial contact
KMx2	Knee Mom	Knee extensor moment during early stance
KMx3	Knee Mom	Knee flexor moment during mid- late stance
KMx4	Knee Mom	Knee extensor moment during late stance
HMx1	Hip Mom	Hip extensor moment during stance
HMx2	Hip Mom	Hip flexor moment during stance
HMx3	Hip Mom	Hip extensor moment during swing
APx1	Ankle Power	Ankle power absorption during initial loading
APx2	Ankle Power	Ankle power absorption during mid-late stance
APx3	Ankle Power	Ankle power gen during stance
KPx1	Knee Power	1st generation power during early stance
KPx2	Knee Power	1st absorption power during early stance
KPx3	Knee Power	2nd generation power after loading response
KPx4	Knee Power	2nd absorption power during late stance
HPx1	Hip Power	Hip generation power during early stance
HPx2	Hip Power	Hip absorption power during late stance
HPx3	Hip Power	Hip generation power during late stance

The group mean equations were applied to each participant's data to assess how well the equations represented the participant's peak sagittal kinematics and kinetics. The best performing equations (i.e. individual R^2) fit the largest number of participants with a R^2 greater than 0.90 and had the highest average R^2. If R^2 were equally as high for the same number of study participants, the simpler equation was chosen.

To determine the difference between regression equations calculated outside the speed range of exoskeleton gait and our regression equations that were within the range, the predicted range between sagittal kinematics and kinetic parameters at 0.2m/s and 0.8m/s were computed using the best performing equations from Table 4-2 and 24 corresponding regression equations published by Lelas et al., (2013). The difference in the predicted range and difference as a percentage of the maximal range were compared between the two studies.

4.4 Results

At each speed interval, an average of 24 ± 8 steps were analyzed. Thirty-three common sagittal parameters were evaluated at the ankle, knee, and hip from the last 10 successful steps (Table 4-1). Peaks included 14 kinematic measures (joint angles, ranges) and 19 kinetic measures (joint moments, powers). No significant differences were observed between dominant and non-dominant limbs, therefore only the dominant limb was used for analysis.

From Pearson correlations of group mean data, gait speed had stronger correlations than stride-length and cadence for 18 of 33 parameters (KAx2, KAx4, HAx2, HAx3, KMx1, KMx2, KMx3, HMx1, HMx2, HMx3, APx1, APx3, KPx1, KPx3, KPx4, HPx1, HPx2, HPx3). Stride-length had the strongest association with five parameters (AAx3, AAxRG, AMx1, AMx2, KMx4), and cadence only two parameters (KAxRG, APx2). Hip flexion during early stance (HAx1) and hip range of motion (HAxRG) were associated equally with gait speed and stride-length. For all 33 parameters, R^2 were highest using second order quadratic equations. No consistent point of inflection was identified for any sagittal gait parameter.

From Pearson correlations of group mean regression equations fit to individual participant data, the same 12 sagittal gait parameters (AMx2, HMx1, APx1, KPx1, KPx2, KPx4, HPx2, HAxRG, HMx2, HMx3, APx3, HPx3) had strong associations with cadence, gait speed, and stride-length. Gait speed had the strongest associations, thus only results for speed were reported in Table 4-2. Equations for cadence and stride-length can be found in supporting information (Table 4-4 and Table 4-5). Of the 12 strongly correlated parameters for gait speed, all but one (HAxRG) were a kinetic parameter and most were best fit using a second order quadratic (AMx2, HMx1, APx1, KPx1, KPx2, KPx4, HPx2). Linear equations strongly predicted HAxRG, HMx2, HMx3, and APx3 while third order quadratic formulas strongly fit the kinetic parameter HPx3.

Parameters with moderate R^2 ($0.7<R^2<0.9$) that fit at least 50% of participants with individual $R^2 > 0.90$ were: KAxRG, HAx1, and HAx2 (kinematic parameters) and AMx1, KMx2, APx2, KPx3, and HPx1 (kinetic parameters). Moderate R^2 that fit less than 50% of participants were AAx3, AAxRG, KAx2, KAx4, HAx3 (kinematic parameters) and KMx1 and KMx4 (kinetic parameters). Weak and poor R^2 were found for kinematic parameters AAx1, AAx2, AAx4, KAx1, KAx3 and kinetic parameter KMx3.

Table 4-2: Maximum sagittal plane kinematics and kinetics parameter regression equations. Best performing equations are bolded. *Variables where more than 50% of samples had a $R^2 > 0.9$ gait speed (s).

Parameter	Peak	Linear Equation	R^2	Quadratic Equation 2nd Order	R^2	Quadratic Equation 3rd Order	R^2
Ankle Angle	**AAx1**	**$y = -0.69s - 7.45$**	0.38	$y = 5.45s^2 - 9.13s - 4.97$	0.30	$y = -8.47s^3 + 24.47s^2 - 20.93s - 2.99$	0.30
	AAx2	$y = 1.24s + 11.79$	0.32	**$y = -6.47s^2 + 11.25s + 8.84$**	0.57	$y = 1.46s^3 - 9.74s^2 + 13.28s + 8.5$	0.57
	AAx3	$y = -12.16s - 3.14$	0.76	$y = 0.08s^2 - 12.28s - 3.1$	0.76	**$y = 3.2s^3 - 7.11s^2 - 7.82s - 3.85$**	0.76
	AAx4	$y = -2.49s + 4.67$	0.46	**$y = 7.44s^2 - 14.01s + 8.07$**	0.56	$y = 6.03s^3 - 6.1s^2 - 5.61s + 6.66$	0.57
	AAxRG	$y = 9.63s + 19.57$	0.72	**$y = -4.25s^2 + 16.21s + 17.63$**	0.73	$y = 3.66s^3 - 12.47s^2 + 21.31s + 16.77$	0.73
Knee Angle	KAx1	$y = -1.07s + 2.08$	0.35	**$y = 10.19s^2 - 16.84s + 6.73$**	0.39	$y = -12.77s^3 + 38.87s^2 - 34.64s + 9.71$	0.41
	KAx2	$y = 10.21s + 1.63$	0.68	**$y = 9.91s^2 - 5.13s + 6.15$**	0.72	$y = -22.79s^3 + 61.07s^2 - 36.88s + 11.46$	0.72
	KAx3	$y = 2.89s - 1.02$	0.51	$y = 0.38s^2 + 2.3s - 0.85$	0.51	**$y = -3.4s^3 + 8.01s^2 - 2.43s - 0.05$**	0.52
	KAx4	$y = 13.37s + 47.39$	0.77	**$y = -11.77s^2 + 31.59s + 42.02$**	0.84	$y = -4.54s^3 - 1.57s^2 + 25.26s + 43.08$	0.84
	KAxRG	$y = 14.88s + 49.25$	0.76	**$y = -16.35s^2 + 40.19s + 41.8$***	0.88	$y = -5.85s^3 - 3.22s^2 + 32.04s + 43.16$	0.88
Hip Angle	HAx1	$y = 6.97s + 12.52$	0.81	**$y = -0.62s^2 + 7.92s + 12.24$***	0.81	$y = 2.13s^3 - 5.4s^2 + 10.89s + 11.75$	0.81
	HAx2	**$y = -7.46s - 7.17$***	0.85	$y = -2.14s^2 - 4.14s - 8.14$	0.85	$y = -1.58s^3 + 1.4s^2 - 6.34s - 7.78$	0.85
	HAx3	**$y = 6.03s + 15.94$**	0.75	$y = -3.01s^2 + 10.69s + 14.57$	0.74	$y = -5.97s^3 + 10.39s^2 + 2.37s + 15.96$	0.74
	HAxRG	**$y = 13.51s + 23.22$***	0.92	$y = -0.79s^2 + 14.74s + 22.85$	0.92	$y = -4.09s^3 + 8.39s^2 + 9.04s + 23.81$	0.92
Ankle Moment	AMx1	$y = -0.16s - 0.01$	0.89	**$y = -0.01s^2 - 0.14s - 0.02$***	0.89	$y = -0.01s^3 + 0.01s^2 - 0.15s - 0.01$	0.89
	AMx2	$y = 0.71s + 0.60$	0.93	**$y = -0.22s^2 + 1.04s + 0.5$***	0.95	$y = -0.03s^3 - 0.14s^2 + 1s + 0.51$	0.95
Knee Moment	KMx1	**$y = -0.17s - 0.06$**	0.78	$y = 0.02s^2 - 0.21s - 0.05$	0.78	$y = 0.09s^3 - 0.17s^2 - 0.09s - 0.07$	0.78
	KMx2	$y = 0.54s - 0.13$	0.84	**$y = 0.35s^2 + 0s + 0.03$***	0.89	$y = -0.32s^3 + 1.07s^2 - 0.45s + 0.11$	0.89
	KMx3	$y = -0.12s - 0.20$	0.53	**$y = -0.07s^2 + 0s - 0.23$**	0.55	$y = -0.12s^3 + 0.19s^2 - 0.17s - 0.2$	0.55
	KMx4	$y = 0.10s + 0.04$	0.72	**$y = 0.03s^2 + 0.06s + 0.05$**	0.73	$y = -0.1s^3 + 0.25s^2 - 0.08s + 0.08$	0.73
Hip Moment	HMx1	$y = 0.59s + 0.01$	0.92	**$y = 0.24s^2 + 0.22s + 0.11$***	0.94	$y = -0.15s^3 + 0.57s^2 + 0.02s + 0.15$	0.94
	HMx2	**$y = -0.53s - 0.07$***	0.95	$y = -0.14s^2 - 0.31s - 0.14$	0.96	$y = -0.02s^3 - 0.09s^2 - 0.34s - 0.13$	0.96
	HMx3	**$y = 0.31s - 0.03$***	0.93	$y = 0.07s^2 + 0.19s + 0.01$	0.93	$y = -0.17s^3 + 0.46s^2 - 0.05s + 0.05$	0.93
Ankle Power	APx1	$y = -0.45s + 0.11$	0.90	**$y = -0.31s^2 + 0.02s - 0.03$***	0.96	$y = -0.21s^3 + 0.16s^2 - 0.27s + 0.01$	0.96
	APx2	$y = -0.62s - 0.19$	0.71	$y = 0.79s^2 - 1.84s + 0.17$	0.88	**$y = 0.82s^3 - 1.06s^2 - 0.69s - 0.02$***	0.89
	APx3	**$y = 3.23s - 0.69$***	0.96	$y = 1.12s^2 + 1.49s - 0.17$	0.98	$y = -1.91s^3 + 5.41s^2 - 1.16s + 0.27$	0.98
Knee Power	KPx1	$y = 0.47s - 0.14$	0.85	**$y = 0.29s^2 + 0.02s - 0.01$***	0.89	$y = -0.38s^3 + 1.14s^2 - 0.51s + 0.08$	0.90
	KPx2	$y = -0.8s + 0.26$	0.81	**$y = -0.8s^2 + 0.44s - 0.11$***	0.93	$y = -0.07s^3 - 0.65s^2 + 0.34s - 0.09$	0.93
	KPx3	$y = 0.48s - 0.02$	0.87	$y = 0.12s^2 + 0.3s + 0.03$	0.87	**$y = 0.02s^3 + 0.08s^2 + 0.33s + 0.03$***	0.88
	KPx4	$y = -0.78s + 0.09$	0.92	**$y = -0.27s^2 - 0.37s - 0.04$***	0.93	$y = 0.2s^3 - 0.71s^2 - 0.09s - 0.08$	0.93
Hip Power	HPx1	$y = 0.58s - 0.06$	0.84	**$y = 0.14s^2 + 0.36s + 0$***	0.84	$y = 0.05s^3 + 0.04s^2 + 0.43s - 0.01$	0.84
	HPx2	$y = -0.47s + 0.09$	0.90	**$y = -0.34s^2 + 0.05s - 0.06$***	0.96	$y = -0.27s^3 + 0.26s^2 - 0.32s + 0$	0.96
	HPx3	$y = 0.74s - 0.08$	0.95	$y = 0.19s^2 + 0.44s + 0.01$	0.95	**$y = -0.25s^3 + 0.76s^2 + 0.09s + 0.07$***	0.96

Of 24 corresponding sagittal gait parameter regression equations reported by Lelas et al., (2003) (Table 4-3), 14 corresponded with the best performing equation types reported in Table 4-2. Excluding hip extension moment and hip power generation during loading response, gait parameters from Lelas (2003) equations were all overestimated. Predicted range of peak knee joint angles during stance and peak ankle plantarflexion angle differed by more than 5°, and by as much as 10.57°. Range of peak knee flexion moment during loading response and pre-swing, as well as peak ankle dorsiflexion moment predicted by Lelas (2003) were more the 62% greater than values predicted using our equations. Joint power was overestimated by at least 58.8% for hip power generation during pre-swing, knee absorption during loading response, and ankle peak absorption.

Table 4-3: Predicted range (0.2m/s to 0.8m/s) of sagittal kinematic and kinetic variables using the best equations from Table 4-2 and Lelas et al., (2003). Differences and differences as a percent of the maximum variable were between our study and Lelas et al (2003). Reg=Regression type, L=linear, Q2= second order quadratic, Q3= third order quadratic.

Peak Sagittal Gait Parameter	Units	Reg: Table 4-2		Lelas et al.		Difference	% of
		Range	Reg	Range	Reg		Max Range
Hip flexion	Degrees	4.38	(Q2)	4.43	(L)	0.05	1.1
Hip extension	Degrees	4.48	(L)	3.07	(L)	1.41	31.5
Knee extension at initial contact	Degrees	3.99	(Q2)	12.05	(Q2)	8.06	66.9
Knee flexion loading response	Degrees	2.89	(Q2)	13.46	(Q2)	10.57	78.6
Knee extension terminal stance	Degrees	1.63	(Q3)	9.96	(Q2)	8.33	83.6
Knee flexion swing	Degrees	11.89	(Q2)	7.04	(Q2)	4.85	40.8
Ankle plantarflexion loading response	Degrees	0.41	(L)	1.06	(L)	0.64	60.8
Ankle dorsiflexion mid stance	Degrees	2.87	(Q2)	1.44	(L)	1.43	49.8
Ankle plantarflexion	Degrees	7.35	(Q3)	2.27	(L)	5.08	69.1
Ankle dorsiflexion swing	Degrees	3.94	(Q2)	3.95	(Q2)	0.01	0.3
Hip flexion moment	Nm	23.95	(L)	24.94	(Q2)	0.99	4.0
Hip extension moment	Nm	20.78	(Q2)	20.26	(Q2)	-0.52	-2.5
Knee flexion moment loading response	Nm	7.68	(L)	25.72	(L)	18.04	70.1
Knee extension moment terminal Stance	Nm	4.07	(Q2)	3.90	(L)	-0.17	-4.2
Knee flexion moment pre-swing	Nm	3.16	(Q2)	11.69	(L)	8.53	72.9
Ankle dorsiflexion moment	Nm	6.78	(Q2)	17.93	(L)	11.15	62.2
Hip power generation loading response	W	22.59	(Q2)	10.91	(Q2)	-11.68	-51.7
Hip power absorption	W	13.10	(Q2)	20.95	(Q2)	7.85	37.5
Hip power generation pre-swing	W	28.92	(Q3)	70.14	(Q2)	41.23	58.8
Knee power absorption loading response	W	16.26	(Q2)	97.42	(Q2)	81.15	83.3
Knee power generation mid-stance	W	19.28	(Q3)	19.87	(L)	0.59	3.0
Knee power absorption pre-swing	W	28.92	(Q2)	32.73	(Q2)	3.82	11.7
Ankle power absorption	W	47.95	(Q3)	125.48	(Q3)	77.53	61.8
Ankle power generation pre-swing	W	145.93	(L)	176.13	(L)	30.20	17.1

4.5 Discussion

The primary goal of this study was to provide LEPE developers with equations for modelling speed related changes in sagittal peak joint kinematics and kinetics. These peaks could then be used to more appropriately scale predefined LEPE joint trajectories. Appropriately scaled trajectories may enhance LEPE function, making it easier for users to complete steps successfully (Neuhaus, 2011), enhancing mobility, balance, cadence, and walking speed of people with complete lower limb paralysis. This study compiled a comprehensive reference data set of 33 peak sagittal kinematic and kinetic parameters at very slow gait speeds that have previously received little attention in the literature.

The strongest regression equations were between peak kinetics and gait speed. When fit to participant data, these equations produced R^2 much higher than previously reported. For example, hip extension moment was reported to have a second order quadratic relationship with gait speed, with correlation coefficients and R^2 ranging between 0.72 and 0.89 (Crowninshield, Johnston, Andrews, & Brand, 1978; Kirtley et al., 1985; Lelas et al., 2003). We found that peak hip extension moments in early stance and late swing were best fit using second order quadratic and linear regressions, with both higher regression R^2 (0.94 and 0.93) and individually fitted coefficients (87% and 90%). The strength of correlations in this study may be due to our use of an instrumented treadmill which may reduce outcome measure variability (Astephen Wilson, 2012; Hak, Houdijk, Beek, & Dieën, 2013; Hanlon & Anderson, 2006).

The main limitation to this study was how to control walking speeds. A treadmill was used rather than vague instructions (e.g. “walk fast”, “walk slow”) that can result in an unbalanced dataset where a participant may not walk at a given speed for an equal number of strides (Schwartz et al., 2008). Treadmill studies offer the ability to collect numerous consecutive strides with greater reproducibility and reduce stride-length variability (Stoquart et al., 2008). The number of consecutive strides and reduced gait variability associated with fixed-speed treadmill use may explain why our regression values were greater than those previously reported; however, treadmill use may have influenced gait parameters (Bertram & Ruina, 2001) by shortening stride-length and cadence, increasing knee extension and forward trunk lean through stance, and increasing hip and knee flexion through swing (Arsenault et al., 1986; Murray, Spurr, Sepic, Gardner, & Mollinger, 1985). If data from these studies are used for clinical decision making on overground walking, the potential for less variability in the treadmill data should be considered. However, since LEPE impose consistent and less variable walking patterns, treadmill gait is appropriate for developing joint trajectories for powered exoskeleton devices. LEPE stride parameter variability can occur due to early foot strikes and varying step initiation timing, which are independent of preset joint trajectories. Therefore, research on short step correction control is also needed for safe and efficient device use.

Like our results and previous studies (Kirtley et al., 1985; Lelas et al., 2003; Tommy Oberg & Karsznia, 1994), sagittal kinematic and kinetic parameters correlated with speed, but kinematic parameters had poorer correlations. However, regression types were not always consistent with our results. Of 24 regression equations for peak sagittal kinematics, reported by Lelas (2004) (Table 4-3), only 14 were consistent with regression equations types in our research. As well, the range of calculated peak kinematics and kinetics between 0.2 m/s and 0.8 m/s differed between our results and Lelas (2004). Lelas (2004) produced regression equation at 0.5m/s, which was nearly twice the average LEPE user walking speed. Kinematic and kinetic regression equations from similar studies can be inaccurate at speeds achievable by a LEPE user (Hanlon & Anderson, 2006).

Though kinematic parameters had lower correlations, speed associations in this study were much stronger than correlation results in the literature. Lelas (2004) reported a poor linear relationship (R^2 = 0.14) for gait speed and peak hip extension (HAx2) during stance. Our results produced an average R^2 of 0.85. As well, knee flexion during loading response (KAx2) and swing (KAx4) had weak relationships with speed (R^2 = 0.60 and 0.43, respectively) in the Lelas (2004) study. Our results supported this quadratic relationship with speed but with moderate R^2 of 0.72 for KAx2 and 0.84 for KAx4. Kinematic parameters had low R^2, likely due to the many degrees of freedom available to the lower limb when adapting to various very slow gait speeds (Bernshteĭn, 1967; Winter, 1992). Therefore gait trajectory choices will differ across people and walking scenarios.

Lower kinematic correlations (i.e. below 0.9) are supported by studies investigating how able-bodied persons adapt to LEPE assisted gait (Gordon & Ferris, 2007; Kao & Ferris, 2009; Pei-Chun Kao, Lewis, & Ferris, 2010a, 2010b; Lewis & Ferris, 2011). With LEPE assistance, total ankle and hip moment (muscle plus exoskeleton) were almost identical to passive walking, with both walking scenarios producing large differences in joint angles and EMG patterns between LEPE assisted and control steps. Joint kinematic patterns may be less important to nervous system planning, with the lower limb adapting by prioritising kinetic optimisation (Sabes, Jordan, & Wolpert, 1998), unlike the upper-limb prioritises kinematic control during reaching (Krakauer, Ghilardi, & Ghez, 1999; Levin, Wenderoth, Steyvers, & Swinnen, 2003; Scheidt, Reinkensmeyer, Conditt, Rymer, & Mussa-Ivaldi, 2000; Wolpert, Ghahramani, & Jordan, 1995). Altering musculoskeletal mechanics by applying assistive forces results in variable kinematics and invariant moments of the lower limb, advancing our understanding of how the lower limb optimises motor adaptation. Kinetic parameters could also be used to predict exoskeleton mechanical output during different tasks, aiding robotic exoskeleton design.

4.6 Conclusion

The goal of this research was to provide better equations for LEPE developers to determine appropriate peak sagittal kinematics and kinetics for joint trajectory development. Quadratic models based on walking speed had the strongest correlations with most peak sagittal kinematic and kinetic gait parameters, with kinetic parameters having the better results. This research showed that peak sagittal kinematic and kinetic gait parameters, between 0.2 and 0.8 m/s, had a strong non-linear association with speed. The lack of a consistent inflection point indicated that the gait kinematic and kinetic strategy did not change at very slow gait speeds. Inconsistent inflection points may demonstrate how individuals adapt to slow speeds differently. While these equations should be tested on a separate dataset, within the same gait speed range, equations produced in this research showed stronger associations with speed then previous studies. The regression equations defined in this research should provide better results when modeling LEPE joint trajectories at very slow walking speeds.

Chapter 5. Estimating exoskeleton-human dynamics of persons with spinal cord injury walking with the assistance of a lower extremity powered exoskeleton prototype

5.1 Abstract

Most lower extremity powered exoskeletons (LEPE) allow persons with spinal cord injury (SCI) to stand and walk with crutch support. An appropriate modelling framework may provide a means to better understand LEPE and human dynamics when defining more natural motion and forces for LEPE control. A LEPE-human model was constructed from the ARKE exoskeleton (Bionik Labs) and a full body musculoskeletal model (Anybody). Simulations were driven by 3D motion data from five persons with SCI, trained to walk with ARKE. LEPE-human model output included SCI user temporal-spatial parameters, kinematics, kinetics, and reaction forces at thigh and shank straps. Restricted dorsiflexion ROM, large device anterior tilt, incomplete knee extension, and uncontrolled centre of pressure (COP) forward progression lifted the heel during stance. This triggered LEPE position control architecture to terminate each step before trajectory tracking at the knee and hip was complete. Incomplete trajectory tracking reduced hip extension and increased knee flexion through stance, increasing knee and hip support moments and thigh and shank strap reaction forces. LEPE knee joint flexion at step termination shortened participant limb-length geometrically, further shortening step-length, and LEPE walking speed. Step completion, knee extension, and support moments would be improved by allowing 20 degrees of dorsiflexion. Incorporating an ankle foot orthosis could improve ankle range of motion, COP control, and upright posture, thereby reducing loads on crutches and joints while increasing step-length, and walking speed. LEPE-human modeling could provide biomechanical data needed when designing intelligent and effective LEPE control.

5.2 Background

Assistive exoskeletons are autonomous devices that enable persons with lower limb weakness or paralysis to perform activities of daily living; including, walking, stairs, sitting, and standing (Viteckova et al., 2013). Control strategies for assistive lower extremity powered exoskeletons (LEPE) generally fit into two categories, position and adaptive control (Chen et al., 2016). Position control is the most common LEPE control strategy (Yan et al., 2015), where joints precisely track predefined trajectories without considering LEPE-human interaction forces. Target trajectories settings can be adjusted to user ability and device posture and feedback loops between joint position sensors and the LEPE controller can minimise deviations away from the target trajectory. Although position control exoskeletons allow individuals with complete SCI to regain independence and offers health benefits (Ditor et al., 2005; Giangregorio et al., 2005; Hicks & Ginis, 2008; Noreau, Proulx, Gagnon, Drolet, & Laramée, 2000; Ragnarsson, 2008). Position control may harm motor recovery of people with incomplete SCI since passively following imposed trajectories (slacking) can reduce effort and hinder motor learning (Crespo & Reinkensmeyer, 2008; Emken, Benitez, Sideris, et al., 2007). Adaptive control operates under the principle of assist-as-needed, where actuators at LEPE joints vary assistance according to user needs, thereby preventing slacking (Marchal-Crespo & Reinkensmeyer, 2009). Adaptive control considers both force and position, increasing or decreasing LEPE assistance to allow users to follow a desired trajectory (Banala, Kim, Agrawal, & Scholz, 2009), or correct deviations away from a target trajectory or force (Hussain, Xie, & Jamwal, 2013; Rajasekaran et al., 2018).

Regardless of strategy, LEPE control requires biomechanical data to provide comfortable and stable performance. These essential data include kinematic data (device posture, joint angles) and kinetic data (external forces, joint torque, interaction forces between the device and user). The choice of reference biomechanical data dictates LEPE behaviour and, if inappropriate, may impose unnatural gait patterns and assistance on users.

For LEPE control, trajectories and LEPE- human interaction forces can be obtained from able-bodied people walking with a LEPE in a passive mode (Banala, Agrawal, & Scholz, 2007; Banala et al., 2009; Emken et al., 2008; Hussain et al., 2013; Rajasekaran et al., 2018). However, able-bodied LEPE-human interaction forces can be significantly lower than users with SCI (Tamez-Duque et al., 2015). LEPE actuator impedance (i.e., residual stiffness) can as well influence able-bodied kinematics, making trajectories from passive-mode LEPE walking unnatural (Emken et al., 2008; Koopman et al., 2014). Unnatural trajectories can increase LEPE-human interaction joint torques (Asín-Prieto et al., 2015) and impose both unnatural gait patterns and assistance on users. Speed-based trajectory reconstruction from regression equations, generated from able-bodied persons walking without a LEPE (Koopman et al., 2014), can improve LEPE-human interaction and may lead to more natural gait patterns compared to pre-recorded kinematic references (Asín-Prieto et al., 2015). However, crutches are typically not used when generating able-bodied LEPE trajectories, thereby making both posture and loading patterns different from SCI users. A modelling framework based on SCI user data and speed appropriate gait parameters could provide better human-machine dynamics when developing the LEPE control architecture.

Musculoskeletal modeling can calculate underlying forces and moments and, when combined with CAD modeling software, enable human-machine interaction analysis. LEPE-human models have been created to output joint torques and joint angles (Yang Li, Guan, Tong, & Xu, 2015; Shi et al., 2008), and evaluate control algorithms (Pan, Gao, Miao, & Cao, 2015). However, the simple human models in these studies were incapable of analyzing human musculoskeletal systems. Robust human musculoskeletal models have been combined with LEPE CAD models (Ferrati et al., 2013; Pan et al., 2015; Shourijeh et al., 2017) but, due to the lack of appropriate biomechanical data, no model has simulated LEPE use with real LEPE user kinematic data. Deriving required biomechanical data for defining LEPE motion and assistance from LEPE users with a LEPE-human model may be more appropriate and provide more comfortable and stable assistance.

The purpose of this study was to investigate LEPE-human dynamics for people with complete SCI. By using SCI biomechanics to drive a LEPE-human model, the human dynamics output better reflects device use in practice. In addition to adding to the knowledge-base on LEPE-human biomechanics, this research presents a modeling framework that could be used to calculated relevant LEPE-human kinematics and kinetics to improve device control and design.

5.3 Methods

5.3.1 Participants

A convenience sample recruited five persons with complete SCI (Table 5-1) from The Ottawa Hospital Rehabilitation Centre and Spinal Cord Injury Ontario. Participants could stand unassisted within a standing frame for 60 seconds, had sufficient upper-body strength to use crutches, and fit the LEPE. This study was approved by The Ottawa Hospital Research Ethics Board and all participants provided informed consent.

5.3.2 Instrumentation

The ARKE (Bionik Laboratories Inc., Toronto, ON, CAN) LEPE has 6 degrees of freedom (DOF), non-backdrivable actuators at the hip and knee, computerised tablet, and two forearm crutches. Sensors determined activity changes-of-state (e.g., initiating a step by leaning forward and to the right) and tablet input changed device mode (walking, stop walking, standing, sitting) and customised reference trajectories to participant needs. Walking, sitting, and standing movements were position controlled based on predefined trajectories.

Table 5-1: Participant demographics. Standard deviation (SD)

Participant	Sex	ASIA Score	Injury Level	Age [years]	Height [cm]	Weight [kg]
N01	M	A	T6	41	180.0	77.0
N02	M	A	T12	30	175.3	72.7
N03	M	A	T3	24	193.0	73.4
N04	M	A	T6	49	172.0	70.5
N05	F	A	T12	46	175.0	79.1
Mean (SD)				39.5 (10.7)	176.8 (8.3)	74.8 (3.5)

Biomechanical data were collected during independent overground walking along an eight-metre path, using participants preferred reference trajectory settings. 3D motion data were sampled at 100 Hz using a 10-camera motion capture system (Vicon, Oxford, UK). A custom 6 DOF full body marker set tracked the exoskeleton, user, and crutches (Figure 5-1). The marker set placed markers directly on the LEPE lower limb; thus, ankle, knee, and hip kinematics reflected the ARKE. The upper-limb, torso, and crutch kinematics were driven by markers placed on these segments and reflect the user. Ground reaction forces (GRF) were measured at 1000 Hz using two force plates embedded in the floor (Bertec, Columbus, OH; Advance Medical Technology Inc., Watertown, MA). Crutches, instrumented with strain gauges in a full Wheatstone bridge, collected axial forces at 50 Hz. Crutch data were interpolated to 100Hz using a fourth order spline curve. Each participant completed five walking trials.

5.3.3 LEPE-Human model

A model was developed and validated (Fournier, Lemaire, Smith, & Doumit, 2018) to combine the ARKE exoskeleton and AnyBody Modelling System (AMS) (AnyBody Technology) (“anybodytech.com: Frontpage,” n.d.). This model integrated the Anybody GaitFullBody model (37 segments, 69 DOF) with a Solidworks (Dassault Systèmes SolidWorks Corporation) CAD assembly of ARKE (Figure 5-1). The ARKE model weighed 33.6kg, consisted of 13 segments, with 5 DOF (3 at the hip, 1 at the knees, 1 at the ankles). Two additional DOF (frontal and transverse) were added to the exoskeleton hip to allow LEPE deformation (bending and twisting).

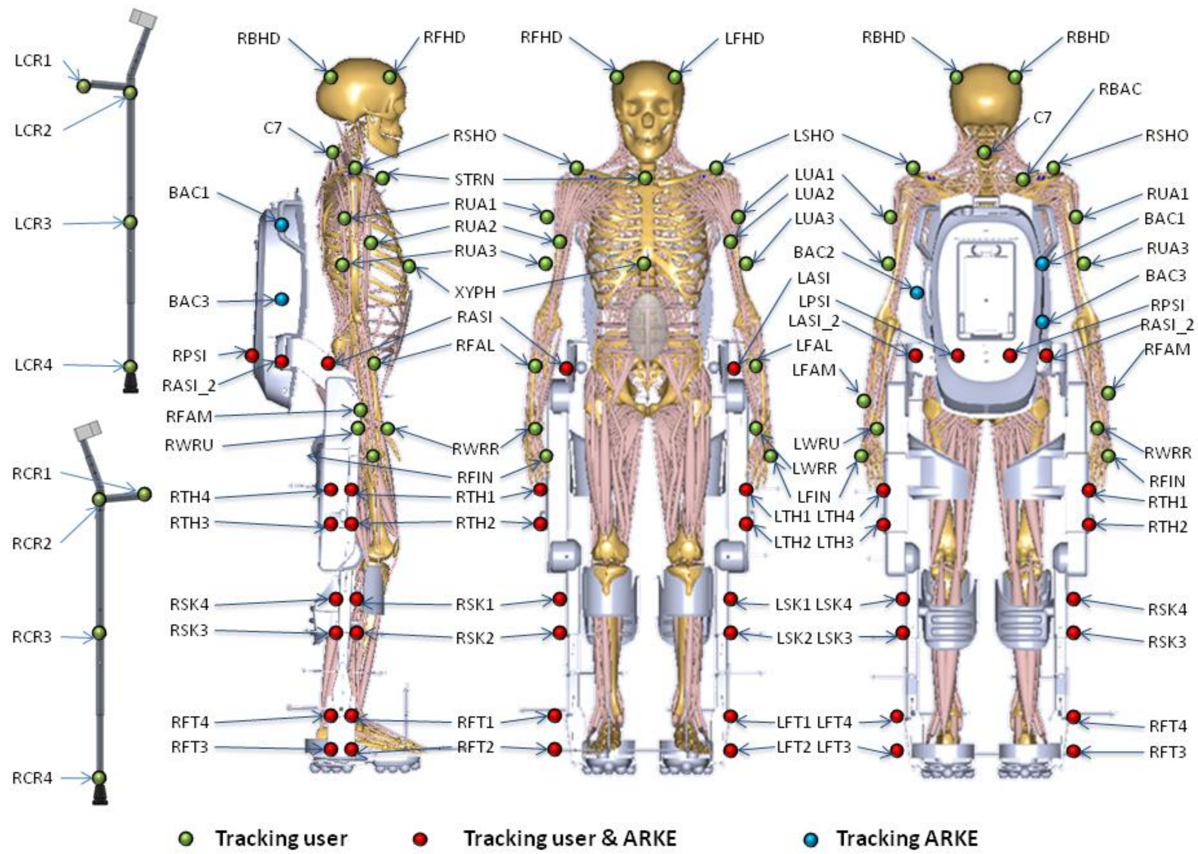

Figure 5-1: Custom 6-DOF full body marker set relative placement with visualization AMS GaitFullBody, crutches, and the ARKE CAD assemblies file.

5.3.4 LEPE-human Interaction

It was assumed that GFB and ARKE CAD model were aligned at the ankle and hips which were kinematically constrained in all 6 DOF. Constrains were also used at the knee in only the anterior posterior axis. “Soft” constraints were used at the knee and hip to allow for some relative motion and prevent the model from being kinematically over-constrained. Interaction forces were applied in all DOF at the foot. At the pelvis, thigh, and shank, interaction forces were applied only in the anterior-posterior and mediolateral axes. Axial loading was assumed to be minimal and was left unconstrained (i.e., no friction). Interaction forces between the crutch handle and hand were applied in all DOF. Normal forces were applied between the crutch cuff and GFB model forearm. 3D marker data and external forces from force plates and crutches were input for the LEPE-human model. The AMS solved inverse dynamic equations to determine net reaction forces at the joints and strap constraints.

5.3.5 Data Analysis

Foot on and foot off where determined using GRF data, calculated at the first frame the vertical GRF exceeded or dropped below 20 N respectively. Force plate data were low-pass filtered using a second-order zero phase dual pass Butterworth filter with 15 Hz cut off frequency. Custom Matlab software (2016a, Mathworks, Matwick, MA) was used to calculate stride-time, step-time, stance-time, swing-time, double-support-time (DST), stride-length, and step-length. Matlab software was used to identify common peak sagittal kinematic and kinetic parameters as well as point interaction forces at thigh and strap constraints (contact forces). Mediolateral, and anterior-posterior contact forces (N/kg) at the thigh and shank straps were used to determine loading periods (i.e., zero crossing between medial and lateral or between anterior and posterior). Impulses were calculated using trapezoid numerical interpolation, with total impulse being all positive or all negative impulses for the stride. Average and maximum pressure at thigh and shank straps where estimated from contact forces by dividing average and peak force by shank and thigh medial, lateral, anterior, and poster strap areas. Crutch percent error was determined by comparing GRF vectors to axial forces recorded by instrumented crutches.

To evaluate kinematic and kinetic requirements for biomimetic slow walking using a LEPE and to provide insight into device function and how speed appropriate model-based gait patterns could improve LEPE performance, ARKE pre-defined kinematic and kinetic peak parameters use were compared to gait parameters generated from slow walking specific regression equations (SWR) (Smith, Fournier, Lemaire, & Nantel, 2018; Smith & Lemaire, 2018). ARKE speed settings on the tablet (ARKE-speed) were also compared with measured speeds.

5.4 Results

5.4.1 Stride Parameters

All participants adopted a reciprocal gait pattern during exoskeleton training. Walking speed averaged 0.14 m/s ± 0.01, ranging between 0.11 m/s and 0.18 m/s, and was 0.21 m/s below ARKE-speed (0.35 m/s). Stride-time duration (4.81 s ± 0.35) was nearly 2 seconds longer than SWR (3.02 s ± 0.10). Participant stance period was between 73% and 82% of the stride cycle, with a double-support-time (1.03 ± 0.09 s) similar to SWR (1.25 ± 0.15 s). Average swing-time (1.00 ± 0.09 s) was nearly twice SWR (0.58 ± 0.00). Steps were often short (89.6±6.3% of total number of steps), which were handled well by the ARKE control system. Stride and step-lengths (Table 5-2) were similar between dominant and non-dominant limbs, and were consistent with

SWR able-bodied stride-lengths at matched walking speeds. Minimum foot clearance was 0.05 cm, averaging 0.07 ± 0.02 m, and average step width was 0.36 ± 0.01 m.

Table 5-2: Measured and slow-walking-regression (SWR) stride parameters (average and standard deviation) at a matched walking speed 0.14 m/s.

Stride parameters	Measured	SWR
Stride-time (s)	4.81 (0.35)	3.02 (0.10)
Step-time (s)	2.24 (0.22)	1.49 (0.05)
Stance-time (s)	3.82 (0.59)	2.70 (0.20)
Swing-time (s)	1.00 (0.09)	0.58 (0.00)
Double-support-time (s)	1.25 (0.15)	1.03 (0.09)
Stride-length (m)	0.59 (0.03)	0.57 (0.02)
Step-length (m)	0.29 (0.03)	0.29 (0.01)

5.4.2 Kinematic Parameters

Since the ARKE moves symmetrically, LEPE users walked symmetrically. Therefore, peak sagittal joint angles were only reported for the left leg (Table 5-3, Figure. 5-2). The ankle remained in dorsiflexion throughout stance. Maximum dorsiflexion during stance was 16.8° ± 2.4°, ranging from 13.8 ° to 18.9°, and SWR was 10.3° ± 0.2. Dorsiflexion during swing (11.1° ± 2.8) was nearly twice the SWR value (6.2° ± 0.3). Ankle range of motion (ROM) was 15.9° ± 2.5, smaller than SWR (17.9° ± 0.3).

Table 5-3: Slow-walking-regression (SWR) and measured peak sagittal joint angles (degrees). average (standard deviation)

Parameter	SWR	Measured
Plantarflexion during early stance	-7.6 (0.0)	0.9 (2.6)
Dorsiflexion during stance	10.3 (0.2)	16.8 (2.4)
Plantarflexion during swing	-5.1 (0.2)	2.5 (3.0)
Dorsiflexion during swing	6.2 (0.3)	11.1 (2.8)
Ankle range of motion	17.9 (0.3)	15.9 (2.5)
Knee flexion at initial contact	4.5 (0.5)	25.2 (7.1)
Knee flexion during stance	0.2 (0.0)	7.1 (5.2)
Knee flexion during swing	46.3 (0.6)	76.4 (2.8)
Knee range of motion	46.6 (0.7)	69.9 (3.4)
Hip flexion peak during early stance	13.4 (0.2)	33.2 (5.1)
Hip extension peak mid to late stance	-8.2 (0.2)	4.6 (4.6)
Hip flexion peak during swing	16.8 (0.1)	40.1 (3.2)
Hip range of motion	25.1 (0.3)	35.5 (2.0)

The knee remained flexed 25.2° ± 7.1 at initial contact, ranging between 15.6° to 35.5, compared to SWR of 4.5° ± 0.5. No loading phase was observed but the knee remained consistently flexed throughout stance (7.1° ± 5.2). Measured peak knee flexion during swing (76.4° ± 2.8) and knee ROM (69.9° ± 3.4) were much greater than SWR (46.3° ± 0.6 and 26.6° ±

0.7). Hip flexion in early stance (33.2° ± 5.1) and late swing (40.1° ± 3.2) were more than double the SWR results (13.4° ± 0.2 and 16.8° ± 0.1, respectively). The hip did not go into extension between terminal stance and pre-swing, remaining flexed. Even without hip extension, ROM was 10.5° greater than able-bodied SWR. ARKE adduction (2.07° ± 1.0) and abduction (-1.59° ± 0.6) were small. Device torso anterior tilt was similar between participants (min: 13.3° ± 1.3, max: 22.7° ± 1.4). Participant anterior trunk angles were greater than device torso anterior angles (min: 17.8° ± 1.3°; max: 28.6° ± 2.0).

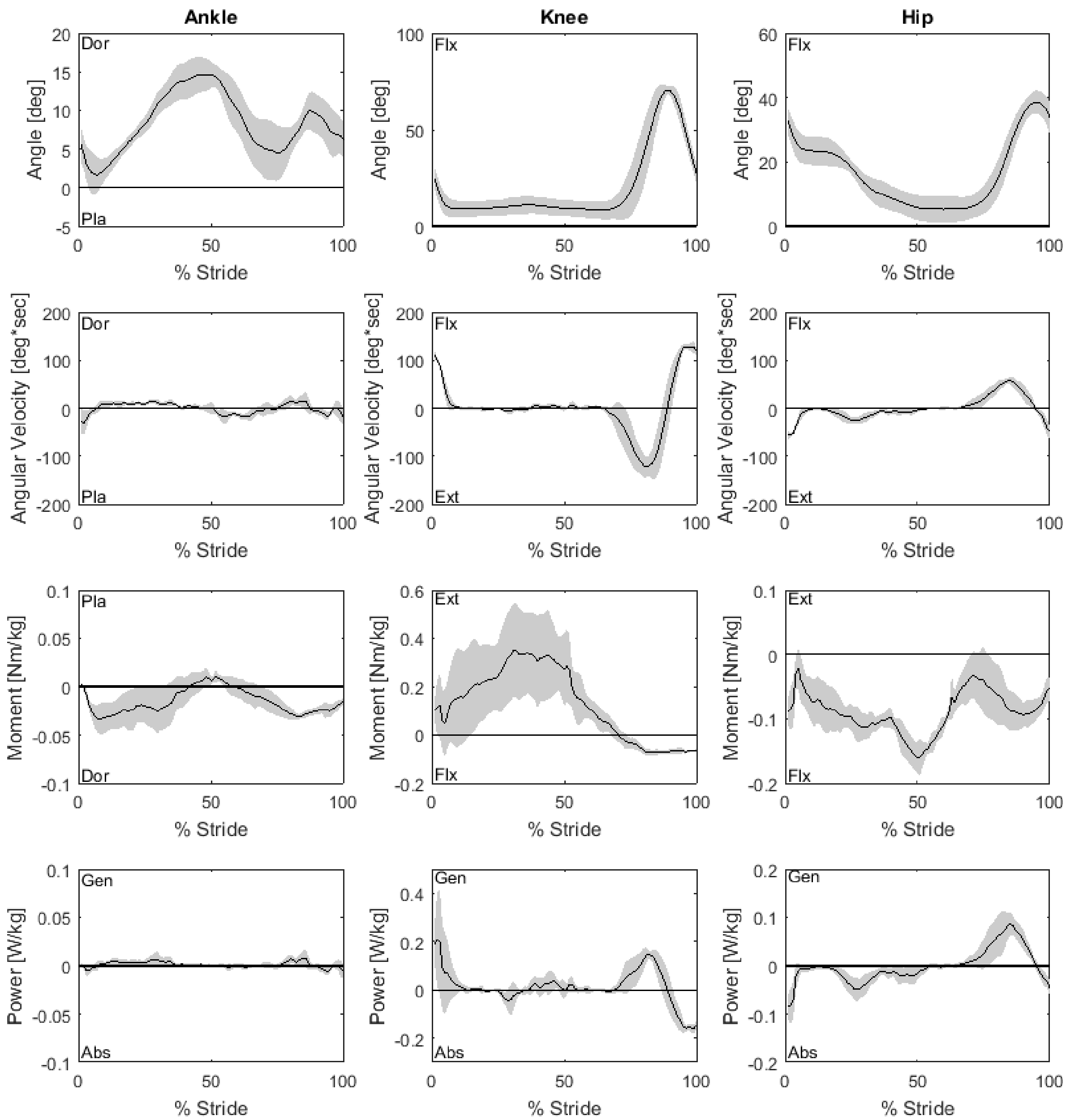

Figure 5-2**:** Participant with SCI average joint angle, angular velocity, moment, and power for the ankle (column 1), knee (column 2), and hip (column 3) walking overground with LEPE assistance. Shaded areas identify standard deviation.

5.4.3 Kinetic Parameters

Average crutch percent error was 4.1% ± 3.1%. Crutch support kept the centre of pressure (COP) under the ankle joint from initial contact until contralateral heel contact (Figure 5-3), resulting in low amplitude plantar flexion moments for the first 50% of ground contact. The COP moved forward after contralateral heel contact at the end of terminal stance. Lack of an ankle joint actuator resulted in a near zero plantar flexion moment at push-off (0.02 Nm/kg ± 0.01) compared to SWR (0.65 Nm/kg ± 0.02). Joint powers were also small (Table 5-4).

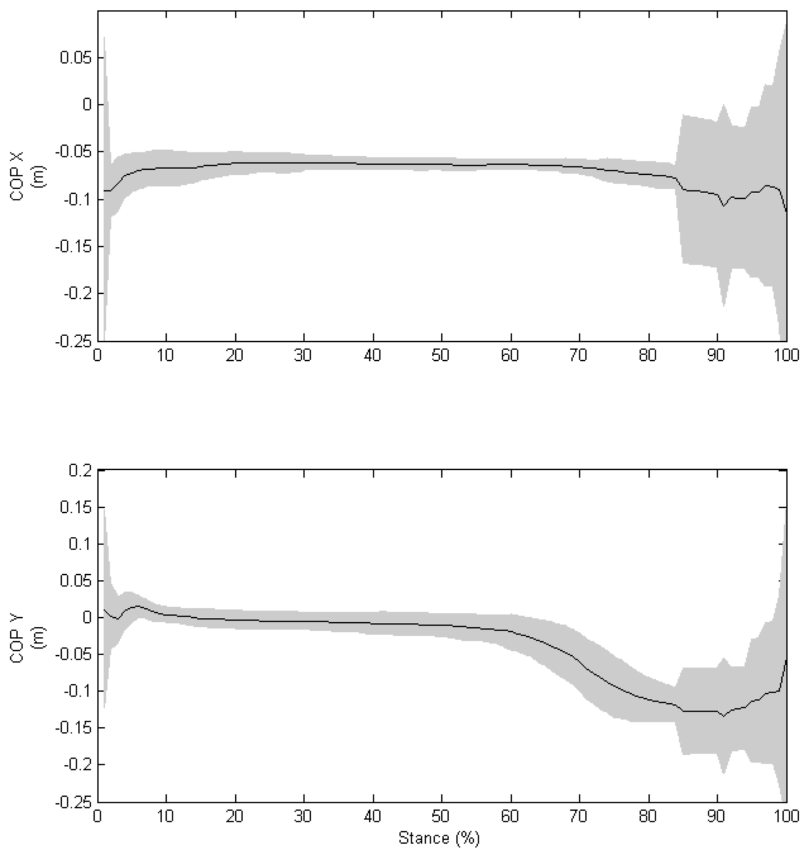

Figure 5-3: Average and standard deviation for centre of pressure trajectory over stance for all participants.

With the knee flexed through stance, eccentric extension moments were required to prevent limb collapse (Table 5-4). At initial contact, greater knee flexion and a posterior GRF vector created an extension moment (0.17 Nm/kg ± 0.11), contrary to the small SWR flexor moment (-0.08 Nm/kg ± 0.00) to prevent knee collapse. The knee rapidly extended 20° during loading response, resulting in a power generation spike (0.31 W/kg ± 0.19). Decreased knee flexion reduced the knee extension moment (0.02 N/kg ± 0.13), as the GRF vector passed closer to knee joint during loading, to near the SWR value (0.04 Nm/kg ± 0.00). As participants leaned forward onto their support-limb to initiate contralateral swing, crutch control kept the GRF vector vertical and through the ankle. At contralateral foot off, knee moment (0.50 Nm/kg ± 0.16) peaked as participants rolled onto the support limb, with the GRF vector pointing vertically behind the knee joint. Knee extensor moments remained high through mid to late stance. Without ARKE powered ankle push-off, a concentric knee flexor moment (-0.09 N/kg ± 0.02) was generated to flex the knee and lift the foot off the ground. Through stance and swing, ARKE torso angle was greater than 13.6° ± 1.3 anterior tilt. This posture resulted in near zero hip extension moments during stance and swing, with a larger than predicted hip flexor moment at the end of terminal stance into pre-swing (Table 5-4).

Table 5-4 Slow-walking-regression (SWR) and measured peak sagittal joint actuator moments and powers, average (standard deviation).

Parameter	**Units**	**SWR**	**Measured**
Dorsiflexor moment during early stance	Nm/kg	-0.04 (0.00)	-0.05 (0.02)
Plantarflexor moment during stance	Nm/kg	0.65 (0.02)	0.02 (0.01)
Knee moment just after initial contact	Nm/kg	-0.08 (0.00)	0.17 (0.11)
Knee moment during early stance	Nm/kg	0.04 (0.00)	0.02 (0.13)
Knee moment during mid- late stance	Nm/kg	-0.23 (0.00)	0.50 (0.16)
Knee moment during late stance	Nm/kg	0.06 (0.00)	-0.09 (0.02)
Hip extensor moment during stance	Nm/kg	0.15 (0.01)	0.00 (0.03)
Hip flexor moment during stance	Nm/kg	-0.15 (0.01)	-0.21 (0.03)
Hip extensor moment during swing	Nm/kg	0.01 (0.01)	0.01 (0.04)
Ankle power absorption during initial loading	W/kg	-0.03 (0.00)	-0.01 (0.01)
Ankle power absorption during mid-late stance	W/kg	-0.27 (0.04)	-0.01 (0.00)
Ankle power during late stance	W/kg	-0.22 (0.08)	0.02 (0.01)
1st generation power during early stance	W/kg	0.00 (0.00)	0.31 (0.19)
1st absorption power during early stance	W/kg	-0.06 (0.01)	-0.13 (0.04)
2nd generation power after loading response	W/kg	0.08 (0.01)	0.22 (0.03)
2nd absorption power during late stance	W/kg	-0.1 (0.01)	-0.20 (0.03)
Hip generation power during early stance	W/kg	0.05 (0.01)	0.02 (0.01)
Hip absorption power during late stance	W/kg	-0.06 (0.00)	-0.08 (0.01)
Hip generation power during late stance	W/kg	0.10 (0.01)	0.11 (0.02)

5.4.4 Strap Contact Forces

Maximum contact force (1.20 N/kg ± 0.43) and impulse (17.2 Ns/kg ± 6 5.89) were greatest on the anterior shank strap (Table 5-5). Peak anterior strap forces (0.82 N/kg ± 0.40) and impulses (11.69 N/kg ± 5.96) during mid to late stance were larger than peak force (-0.79 N/kg ± 0.40) and impulse (-9.91 N/kg ± 6.87) (Figure 5-4). The smaller lateral shank strap area (123.19 cm^2) resulted in average (1.41 kPa ± 0.82) and peak (4.49 kPa ± 2.31) contact pressures double those at the larger (243.14 cm^2) anterior shank strap (Average: 0.70 N ± 0.33; max: 2.36 ± 1.16).

Table 5-5 Maximum contact forces (N/kg), impulses (Ns/kg), and average and maximum pressures (kPa) at the shank and thigh straps. %GC = percent gait cycle.

Segment	% GC	Side	Force	Impulse	Average Pressure	Maximum Pressure
Shank	0-26	Lateral	-0.32 (0.04)	-1.23 (1.03)	-0.39 (0.36)	-1.79 (0.10)
	26-68	Lateral	-0.79 (0.40)	-9.91 (6.87)	-1.41 (0.82)	-4.49 (2.31)
	25112	Lateral	-0.25 (0.06)	-3.66 (0.91)	-0.71 (0.07)	-1.42 (0.28)
	Total	Lateral	-0.85 (0.41)	-15.36 (4.3)	-1.11 (1.17)	-4.6 (0.21)
	Total	Medial	0.22 (0.06)	0.54 (0.66)	0.31 (0.34)	0.77 (0.05)
	0-21	Posterior	-0.75 (0.06)	-2.96 (2.03)	-0.48 (0.18)	-2.20 (0.15)
	21-75	Anterior	0.82 (0.40)	11.69 (5.96)	0.70 (0.33)	2.36 (1.16)
	75-100	Anterior	0.38 (0.12)	5.11 (1.94)	0.62 (0.39)	1.06 (0.25)
	Total	Posterior	-0.75 (0.08)	-3.44 (0.49)	-0.41 (0.43)	-2.20 (0.15)
	Total	Anterior	1.20 (0.43)	17.26 (5.89)	0.80 (0.67)	2.44 (1.01)
Thigh	0-53	Lateral	-0.43 (0.05)	-11.49 (3.62)	0.71 (0.23)	1.21 (0.17)
	53-100	Medial	0.53 (0.12)	13.88 (0.94)	1.02 (0.06)	1.73 (0.25)
	0-26	Posterior	-0.94 (0.07)	-7.24 (2.81)	1.02 (0.40)	2.92 (0.23)
	26-55	Anterior	0.58 (0.22)	7.07 (3.79)	0.74 (0.35)	1.62 (0.62)
	55-80	Posterior	-0.33 (0.14)	-4.09 (2.20)	0.54 (0.26)	1.00 (0.40)
	80-100	Anterior	0.21 (0.31)	3.79 (1.04)	0.56 (0.15)	0.57 (0.89)
	Total	Posterior	-0.94 (0.07)	-11.33 (3.91)	-0.08 (0.06)	-2.92 (0.23)
	Total	Anterior	0.73 (0.34)	10.86 (1.08)	0.07 (0.05)	2.06 (1.00)

Medial and lateral thigh contact force loading periods, maximum forces, impulses, average pressures, and maximum pressures were similar. The lateral thigh strap was loaded for the first half of the gait-cycle, with forces peaking during single-leg-support. Contact forces switched to the medial thigh at 53 % GC, peaking just after contralateral heel contact. Maximum posterior thigh force peaked during the first 26% of GC. Maximum anterior forces were slightly smaller, peaking during mid-stance into pre-swing (26-55 % GC). Hip mediolateral pressures at the larger thigh straps were lower than those at the shank. The maximum and peak contact pressures at the thigh were both 2.92 kPa ± 0.23 posteriorly, during loading phase (0-26 % GC).

Total impulse was greatest at the anterior and lateral shank strap, during early-stance into mid-swing (Table 5-5). Mediolateral shank strap impulse was almost entirely lateral (lateral: -15.36 Ns ± 4.30; medial 0.54 Ns ± 0.66), and greatest during mid-stance into pre-swing (26-68 % GC). Anterior-posterior shank impulse was mainly anterior (anterior: 17.26 Ns/kg ± 5.89; posterior: -3.44 Ns/kg ± 0.49), and greatest following the loading phase to terminal stance (21-75 % GC). For the thigh, total impulse was slightly larger on the medial straps (13.88 Ns ± 0.94) through the last half of the gait-cycle (53-100 % GC). Impulse was similar anteriorly and posteriorly.

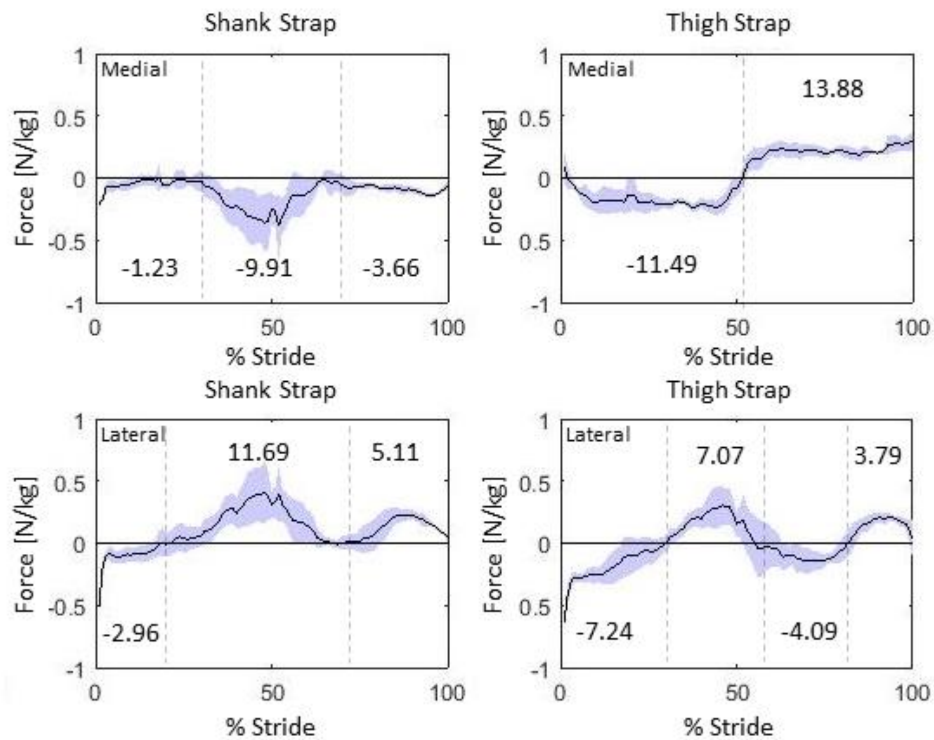

Figure 5-4: Contact forces [N/kg] at ARKE thigh and shank straps. Vertical dashed lines (--) indicate transitions between negative and positive impulse (N·s).

5.5 Discussion

This research investigated LEPE-human dynamics for people with complete SCI. The five participants successfully walked with ARKE after 19, half-hour training sessions. The LEPE-human model enabled comparison of SCI user dynamics with relevant speed-matched able-bodied gait parameters. Restricted ARKE dorsiflexion and uncontrolled centre of pressure forward progression promoted early stance phase termination, partial steps, and slow LEPE walking speeds. Dorsiflexion angle and support moments were amplified by large device anterior tilt and knee flexion through stance. These aspects are important to control approaches and should be considered when designing LEPE.

Walking speed set on the ARKE averaged 0.35 m/s ± 0.05 across participants; however, speeds achieved by SCI participants were less than half, averaging 0.14 m/s ± 0.01. Walking speed was slowed by short steps (i.e., incomplete hip and knee joint trajectories due to early heel-on or heel-off) and pauses when initiating successive steps. Shortened step-lengths are consistent with slow walking speeds (Smith & Lemaire, 2018). LEPE trajectories, design, and controls that adapt well to user walking speed should enable more step trajectories to be completed. However, control methods, such as those used in ARKE, need to accommodate for short steps since this can be anticipated in everyday use.

Partial stepping may have been due to early step termination. Restricted ankle dorsiflexion ROM (Max = 15°) caused the shank to hit the dorsiflexion hard stop, creating a plantar flexion moment, and lifted the heel. Heel lift triggered the ARKE heel switch and terminated swing phase on the contralateral limb. With crutch support, 13.3° ± 1.3 of anterior tilt provided a large base of support, but maintained ankle dorsiflexion near its hard stop. Anterior tilt was consistent with SCI ReWalk users; however, dorsiflexion was allowed to exceeded 15° (Talaty et al., 2013). Using a similar model driven by able-bodied kinematics at very slow walking speeds (0.2 m/s to 0.8 m/s), dorsiflexion exceeded 15° due to the increased anterior tilt required to accommodate ARKE inertial properties (Fournier, 2018). Allowing 20° of dorsiflexion may prevent early heel raise, however for safety and user confidence, dorsiflexion dampening may be required between 15 and 20 degrees to control forward body rotation over the foot. This accommodation may only be safe or benefit users with full ankle ROM. Contractures limiting passive ROM at the ankle, knee and hip were reported as the leading reason for person not qualifying for LEPE feasibility studies (Gagnon et al., 2018; Kozlowski, Bryce, & Dijkers, 2015). Therefor this accommodation may be unsafe for many users with musculoskeletal impairments limiting ankle ROM.

Knee joint flexion through stance, due to early foot-on, geometrically increased the dorsiflexion angle. Foot clearance was achieved because the ARKE partial step algorithm increased hip and knee ROM, lifting the foot higher to accommodate a shortened support limb. This successfully enabled participants to walk while varying step-length, but may have perpetuated early foot-on by increasing ROM and swing-time. Kinematic accommodations have a large impact on gait parameter settings. Increasing ROM to accommodate toe clearance affects step frequency. To accommodate increases in ROM and maintain step-time, the LEPE would have to proportionally increase joint angular velocity, which may be unsafe due to increased swing limb inertia (Swift, 2011). Incorporating step-length reduction or increasing swing-limb angular velocity into step controls would reduce swing-time, knee flexion during stance (i.e., since the step would be completed), and improve stability due to shorter single-limb-support-time. To accommodate inertial changes, LEPE-human models could be used to research system dynamics using different swing limb frequencies, crutch strategies, and device designs to determine an optimal and safe control strategy.

Device posture contributed to greater joint loads than SWR. Knee flexion and device anterior tilt required constant support moments at the knee, hips, and arms to prevent LEPE collapse (Figure 5-3). ARKE's non-backdrivable joint actuators provided strong resistance torques without requiring a power source (Controzzi, Bassi Luciani, & Montagnani, 2017). However, backdrivability would be advantageous for people who do not required full LEPE assistance (Claros et al., 2016; Huo et al., 2016). Backdrivable motors would have consequences for supporting the postures reported in this research, requiring active resistance to support large and constant knee and hip sagittal support moments. Device posture should be considered when designing LEPE position and force reference trajectories.

Large anterior tilt was supported by crutches and the user upper-limb. Crutch support also controlled COP progression ahead of the ankle joint. Like persons with gastrocnemius weakness who change their gait strategy to avoid COP progression ahead of the ankle joint, crutch use kept the COP underneath the ankle joint, minimising external dorsiflexion moments (Lehmann, Condon, de Lateur, & Smith, 1985; Perry, Mulroy, & Renwick, 1993). This strategy improved stability but kept the GRF vector far behind LEPE actuators, creating large knee and hip joint support moments. The COP only progressed forward after contralateral heel-contact (Fig 4).

Strap pressure allowance metrics reported a threshold between 5.3 and 6.7 kPa before skin oxygenation is impaired (Cho et al., 2012). The greatest average (1.41 kPa ± 0.82) and maximum (4.49 kPa ± 2.31) pressures on the lateral shank were within acceptable contact pressure ranges. Contact forces and impulses were highest at the anterior and lateral shank from mid to late stance as participants leaned on their support limb to allow contralateral limb swing. During this period, the support limb was bent at the knee which loaded the anterior and lateral shank cuff stance. Though forces were higher on the anterior shank strap, surface are of the later shank cuff were smaller, resulting in pressures twice that experienced on the lateral shank (Table 5-5). Tissue damage is proportional to muscle and fat tissue (Makhsous et al., 2007), and most vulnerable at boney regions like the front of the tibia (Dudek, Marks, Marshall, & Chardon, 2005). Since participants with SCI have less protective tissue due to atrophy, they are at a greater risk of tissue injury. Since the anterior shank had the highest and most prolonged loading periods, increasing the padding area at these locations may prevent tissue damage.

This study was not without limitations. Actuator impedance or friction, muscle spasticity, and poor LEPE-human joint alignment could have resulted in under or overestimated joint torques and contact pressures. In addition, pressures were estimated from simulated point forces spread equally across the strap surfaces, in the absence of sheer or frictional forces. The LEPE-human model could be improved by using dynamic constraints similar to Cho et al., (Cho et al., 2012) to model straps, and statically optimised contact pressure to be as low as possible (van den Bogert & Su, 2008). Future studies should validate pressures and joint torques from LEPE-human models in-vivo, utilising sensor systems within actuators and strap locations during device use.

5.6 Conclusion

This research combined an "exoskeleton mechanical model" with a "musculoskeletal model" to characterise LEPE-human dynamics. Step completion, knee extension, and support moments would be improved if device posture were more upright. Incorporating an "ankle foot orthosis type design" could improve COP control, and upright posture could be improved using a trunk orthosis, thereby reducing loads on crutches and joints while increasing stance limb-length, step-length, and walking speed. Strap contact pressures would benefit from improved device posture, but these calculated pressures were small enough to allow adequate circulation. The LEPE-human model facilitated informed design recommendations for improving LEPE device function and could be used to design a device with minimal impact on COM position. This study shows the potential of LEPE-human modeling in the exoskeleton iterative design process. Our LEPE-human model provides exoskeleton developers with relevant LEPE-human dynamics data and could advance LEPE control approaches.

Chapter 6. Upper-extremity joint loads of persons with spinal cord injury walking with a lower extremity powered exoskeleton and forearm crutches

The contents of this chapter were submitted to the Journal of Biomechanics:

Smith, A. J., Fournier, B.N., Nantel, J., & Lemaire, E. D. (2019). Upper-extremity joint loads of persons with spinal cord injury walking with a lower extremity powered exoskeleton and forearm crutches. Journal of Biomechanics. Under review.

6.1 Abstract

Lower extremity powered exoskeletons (LEPE) with crutch support can provide upright mobility to persons with complete spinal cord injury (SCI); however, crutch use for balance and weight transfer may increase upper-extremity (UE) joint loads and injury risk. Current biomechanical models are insufficient to estimate a SCI person's UE forces during LEPE-assisted gait. This research presented the first LEPE-human musculoskeletal model to estimate UE biomechanics, driven by 3D motion data of persons with complete SCI walking with LEPE and crutch assistance. Forearm crutches instrumented with strain gages, force plates, and a 3D motion capture system were used to collect kinematic and kinetic data from five persons with complete SCI while walking with the ARKE exoskeleton. Model output estimated participant UE kinematics, kinetics, and crutch forces. Compared to inverse dynamic biomechanical crutch model studies of persons with incomplete SCI, LEPE users walked with more anterior trunk tilt and twice the shoulder flexion angle. Anterior tilt increased forces and moments at the crutch, shoulder, and elbow. Crutch floor contact periods were 30-40% longer, resulting in UE joint impulses 5 to 12 times greater than previously reported. Reducing UE load is important to reduce ambulatory assistive device overuse injuries. Incorporating a variable assist ankle joint or more experience with LEPE walking may reduce UE joint loads and minimise injury risk. Study outcomes provide a quantitative understanding of UE dynamics during LEPE walking that can be used to improve device training, rehabilitation, and device design.

6.2 Introduction

Mobility is a primary concern for persons with spinal cord injury (SCI) (Simpson, Eng, Hsieh, Wolfe, & Spinal Cord Injury Rehabilitation Evidence Scire Research Team, 2012). New lower extremity powered exoskeletons (LEPE) can provide upright mobility for many people with complete or incomplete SCI (iSCI), with most LEPE requiring forearm crutches for balance and weight transfer. For lower limb orthosis users, crutches or canes increase the base of support, improving balance control and independence by providing lateral, anterior, and posterior stability (Bateni & Maki, 2005; Lapointe et al., 2001). The axial force placed on forearm crutches by persons with iSCI can reach 50% body weight (Melis, Torres-Moreno, Barbeau, & Lemaire, 1999). This load is supported by the upper-extremities, in particular the glenohumeral (GH) joint that is not well adapted to bear weight.

High UE joint loads among persons with SCI during transfers (D. Gagnon, Nadeau, Noreau, Dehail, & Gravel, 2008; D. Gagnon, Nadeau, Noreau, Dehail, & Piotte, 2008; Pentland & Twomey, 1994), wheelchair propulsion (Kulig et al., 2001, 1998; Mulroy, Farrokhi, Newsam, & Perry, 2004), and crutch use (Bateni & Maki, 2005; Ulkar, Yavuzer, Guner, & Ergin, 2003) have been linked to shoulder pain (Gellman, Sie, & Waters, 1988; Requejo et al., 2005; Sie, Waters, Adkins, & Gellman, 1992) and UE pathologies; including, shoulder impingement syndrome, destructive shoulder arthroplasty, degenerative arthritis, and carpal tunnel syndrome (Boninger et al., 2002; Lal, 1998). Research using three dimensional (3D) motion capture and instrumented crutches have been conducted to prevent or minimise UE injury from crutch use (Perez-Rizo et al., 2017; Requejo et al., 2005; Slavens, Bhagchandani, Wang, Smith, & Harris, 2011; Slavens, Sturm, & Harris, 2010). Of these studies, most have limited sample sizes, investigated populations without complete paralysis or SCI, and used simplified inverse dynamic models. Furthermore force transferred to the UE is inversely proportional to lower limb strength (Gellman et al., 1988) and differs depending on the support aid (Haubert et al., 2006; Melis et al., 1999; Waters, Yakura, Adkins, & Barnes, 1989), crutch gait pattern (Perez-Rizo et al., 2017), and pathology (Slavens et al., 2011). Thus, UE loads from previous studies with SCI participants may not apply to LEPE-assisted gait.

At the shoulder, three bones form the GH joint and participate in arm movement, making scapula movement difficult to track with skin markers. Despite efforts to standardise UE biomechanical modelling (Wu et al., 2005), tracking difficulty has contributed to wide variations in shoulder, elbow, and wrist forces reported across different UE models as they do not adequately represent bone and muscle geometry, essential to modeling and the calculation of shoulder forces (Konop et al., 2009; Perez-Rizo et al., 2017; Requejo et al., 2005; Slavens et al., 2011; Slavens, Sturm, & Harris, 2008; Slavens et al., 2010; Slavens, Sturm, Wang, & Harris, 2006).

Inverse dynamic musculoskeletal models incorporate bones, ligaments, and muscles, and use 3D motion and external force data to calculate segment and joint kinematics and kinetics, muscle activations, and internal contact forces. The Delft Shoulder and Elbow Model (DSEM) (van der Helm, 1997), SIMM model (Holzbaur, Murray, & Delp, 2005), Newcastle model (Charlton & Johnson, 2006), and AnyBody Modeling System (AMS) (Damsgaard, Rasmussen, Christensen, Surma, & de Zee, 2006) are examples of UE musculoskeletal models. Both DSEM and AMS were validated against in-vivo shoulder force data (Bergmann et al., 2007). The AMS shoulder model had excellent joint force vector direction but overestimated maximum joint force by 27%, compared to experimental results (Rasmussen, Zee, Tørholm, & Damsgaard, 2007). These results improved after model customisation by deactivating the supraspinatus to simulate the participant's muscles dysfunction, thereby reducing muscle force overestimation during static shoulder abduction to less than 2% (Nolte, Augat, & Rasmussen, 2008).

Understanding shoulder forces during LEPE-assisted gait would provide insight into UE injury risk and mechanisms of potential shoulder injury. When walking with forearm crutches, forces at the shoulder are less than those during transfers (D. Gagnon, Nadeau, Noreau, Dehail, & Piotte, 2008), and have been found to be comparable (Haubert et al., 2006) or higher than wheelchair propulsion (Kulig et al., 1998; Slavens, Sturm, Bajournaite, & Harris, 2009) depending on the gait and crutch pattern. Previous studies have reported swing through gait patterns; where patients move their crutches together, swinging their legs forward like a pendulum, to have larger loads at the shoulder (Slavens et al., 2008) then both wheelchair propulsion and reciprocal gait with crutches (Slavens et al., 2009). In our previous research (Smith et al., 2019), persons with complete SCI relied heavily on their crutches for support and control when walking with a LEPE. LEPE-assisted gait patterns could produce shoulder forces greater than forces during wheelchair propulsion or during more strenuous swing through gait. Unfortunately, LEPE-human models in the literature have not incorporated crutch assistance. To understand UE forces during LEPE-assisted gait, a comprehensive LEPE-human model including crutches must be used, driven by real 3D motion data from a LEPE user with SCI.

This study created and evaluated a 3D LEPE-human model with forearm crutches and UE. The hypothesis was that shoulder and elbow forces during LEPE walking would be greater than the literature on reciprocal crutch gait with iSCI participants. This model will allow researchers and design engineers to evaluate lower and UE forces, including loads from different crutch support techniques, when designing exoskeleton devices, or exploring how a device functions with varying muscle contributions simulating pathology.

6.3 Methods

6.3.1 Participants

Five volunteers (4 men, 1 woman) with complete SCI were recruited from The Ottawa Hospital Rehabilitation Centre (TOHRC) and Spinal Cord Injury Ontario. Participants provided written consent to participate in the study. The study and consent form received approval from the Ottawa Health Science Network and the University of Ottawa Research Ethics Boards. Average participant age was 38.0 ± 10.7. All participants had motor complete thoracic SCI between T3 and T12. Participants were assessed by a physiatrist and physiotherapist to ensure that they could stand for 60 s within a standing frame and had sufficient upper-body strength to operate the LEPE (ARKE, Bionik Labs Inc. Toronto, Canada) with forearm crutches. Participants were screened for past neurological injuries other than complete SCI, along with any cognitive, psychological, or physical comorbidity that may have interfered with the study protocol. Hip width, thigh-length, and shank-length were measured to setup the ARKE for each participant.

6.3.2 Model Description

A biomimetic model (Figure 6-1) driven by 3D motion data of participants walking with ARKE was built using the AnyBody Modeling System (AnyBody Technology, Alborg Denmark). This model included crutches and the ARKE LEPE. Segment 3D motion data and external contact forces were input for the AMS software, which calculated inverse dynamics to determine muscle and joint forces. To solve for the redundancy of muscle recruitment problem (Damsgaard et al., 2006), a muscle recruitment optimisation algorithm determined muscle force. the AMS muscle recruitment optimization algorithm was implemented to determine muscle forces (Equation 6.1),

$$G = \sum_i \left(\frac{f_i}{N_i}\right)^p \qquad (6.1)$$

where *G* is the function to minimize, *i* the muscle identifier, *f* is the muscle force, *N* is the maximum muscle force and *p* is an exponent value (default, *p*= 3). Muscle strengths were optimized to be as small as possible.

The GaitFullBody (GFB) model was used (Damsgaard et al., 2006; Lemieux, Nuño, Hagemeister, & Tétreault, 2012), with the shoulder model based on the Dutch Shoulder Group data and modeling assumptions (van der Helm, 1994; van der Helm, 1997). The shoulder model simulates 118 muscles on each side with 3 DOF at the shoulder, 1 at the elbow, and two at the wrist. The skeleton was scaled anthropometrically from each participant's limb parameters.

6.3.3 SCI LEPE-human model

For a complete description of the SCI LEPE-human model please see (Fournier et al., 2018). A SolidWorks (Dassault Systemes SolidWorks Corporation) ARKE model was provided by Bionik Laboratories Inc. The ARKE model mass was 33.6 kg and all 13 segments and their inertial properties were accurately represented. Constraints were set between LEPE and GFB model segments, with feet and pelvis constraints in all 6 DOF (i.e. to align the hip joint centres) and knee constraints in the anterior posterior axis. Interaction forces were applied in all DOF at the foot but only in the anterior-posterior and mediolateral axes at the pelvis, thigh, and shank. Axial loading was assumed to be minimal and was left unconstrained (i.e. no friction).

Forearm crutches were modeled in SolidWorks and imported into AMS, including all inertial properties. The instrumented crutch's axial load data were applied to the end of their respective crutch model in the axial direction. Normal forces were applied between the modelled crutch cuff and GFB forearm. Interaction forces between the modelled crutch handle and hand were applied in all DOF. Maximum linear force was set to 50N and maximum moment to 50 Nm. Maximal vertical strength, within the local vertical crutch axis, was set to 500 N.

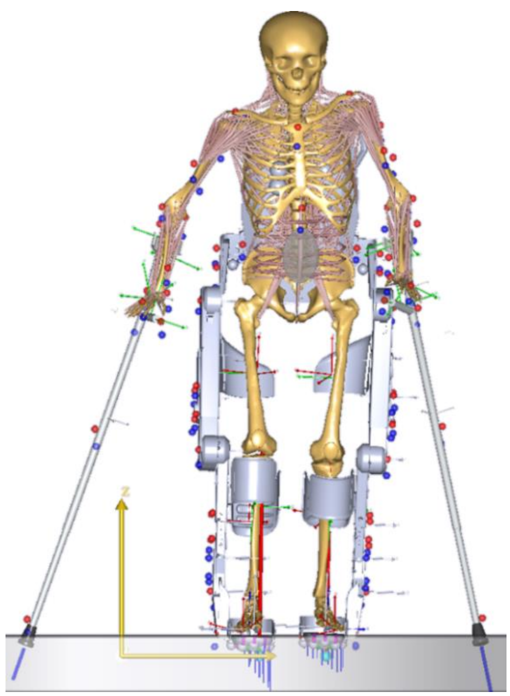

Figure 6-1: SCI LEPE-human model and motion capture markers.

3D motion data were collected during independent overground walking along an eight-metre space using the participant's preferred ARKE walking settings. Kinematic data were sampled at 100 Hz using a 9-camera Vicon 3D motion capture system (Vicon, Oxford, UK). A custom 6 DOF full body marker set tracked the LEPE, person, and crutches (Figure 6-2). Markers on the LEPE were used to calculate LEPE lower limb motion and human- LEPE model constraints. UE, torso, and crutch kinematics were calculated from markers on the human UE , torso, and crutch. Two force plates (Bertec, Columbus, OH; Advance Medical Technology Inc. Watertown, MA) measured ground reaction forces at 1000 Hz. Crutches, instrumented with strain gauges in a full Wheatstone bridge, collected axial forces at 50 Hz. Crutch data were interpolated to 100Hz using a fourth order spline curve. Each participant completed five walking trials. Walking trials were considered complete if the participant cleanly struck the force plates with their right and left feet.

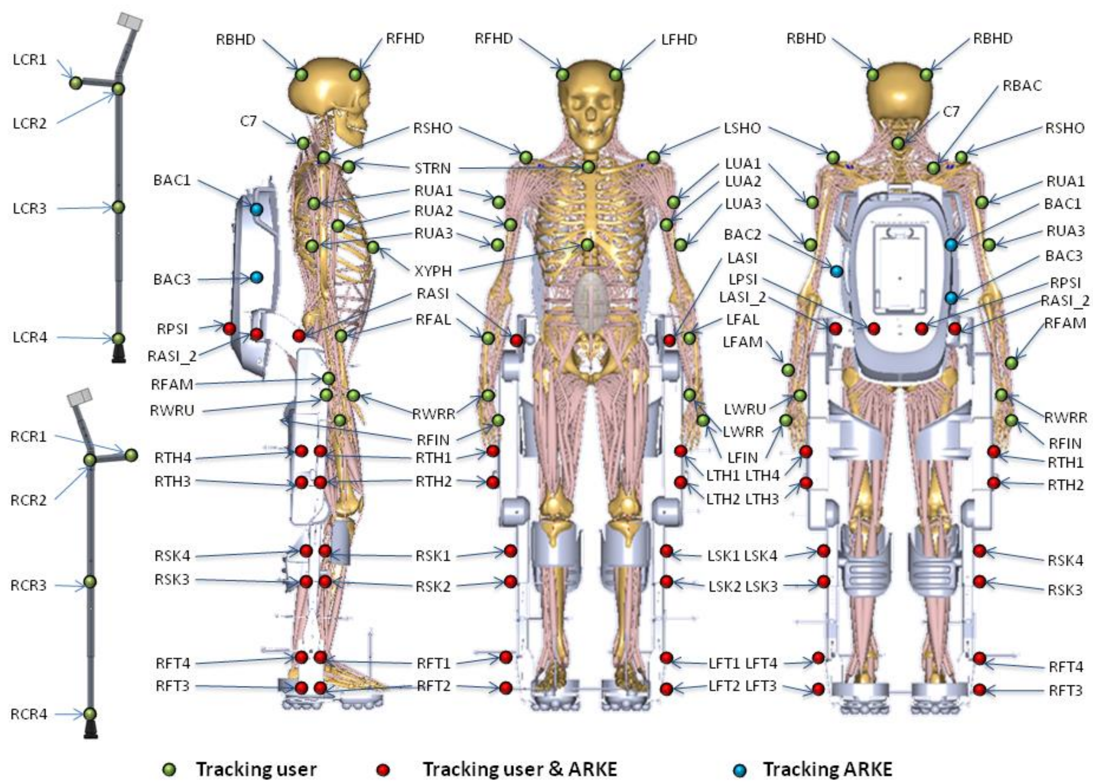

Figure 6-2: Customized six degree of freedom marker set.

The LEPE-human model outputted shoulder and elbow kinematics and joint moments, as well as superior-inferior, anterior-posterior, and mediolateral forces. All variables were normalised to 100% of the gait cycle (GC). Forces and moments were normalised to the person's weight (kg). Impulse was not normalised. Shoulder and elbow peak kinematic and kinetic values were extracted and impulses were calculated using custom Matlab software. Descriptive statistics were calculated and compared to the literature; including, mean and standard deviation of joint trajectories, moments, and forces. Crutch percent error were determined at the beginning of every trial by comparing GRF vectors to axial forces recorded by instrumented crutches.

6.4 Results

6.4.1 Crutch support periods

All participants adopted a reciprocal gait pattern (Figure 6-3) to walk with LEPE assistance, at an average speed of 0.14 m/s ± 0.1. At left-foot-ground-contact (LFON), the left support limb and the right crutch were in contact with the ground. Left-crutch-off (LCOFF) occurred at 4% GC and remained off the ground until left-crutch-on (LCON) at 14% GC. The right crutch remained in contact with the ground until right-crutch-off (RCOFF) at 52% GC, remaining off the ground until right-crutch-on (RCOFF) at 64% GC. Total ground contact was 87% for right and 90% for left crutches. All periods had at least three-points of contact with the ground. Crutch and foot contact events divided the GC into four crutch phases: left-crutch-repositioning (LCR) between LFON and LCON (0% to14% GC); left-crutch-loading (LCL) between LCON and right-foot-on (RFON) (14% to 50% GC); right-crutch-repositioning (RCR) between RFON and RCON (50% to 64% GC); right-crutch-loading (RCL) between RCON and second LFON (64% to 100% GC).

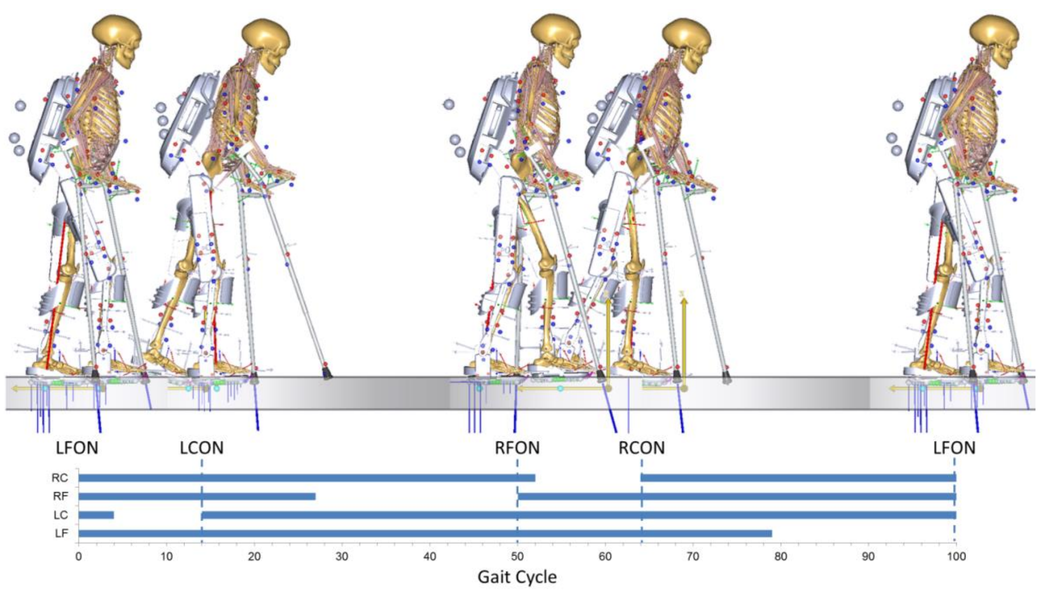

Figure 6-3: Crutch phases, with bars indicating ground contact for right crutch (RC), right foot (RF), left crutch (LC), and left foot (LF). Vertical dashed lines indicate left-crutch-on (LCON), right-foot-on (RFON), right-crutch-on (RCON), and left-foot-on (LFON).

6.4.2 Kinematics

Right (37.6° ± 4.6) and left (33.2° ± 3.5) shoulder abduction peaked during crutch repositioning, never abducting below 20.5° ± 5.1 for right and 12.9° ± 2.4 for left (Table 6-1,

Figure 6-4). The support phase began with the support limb shoulder flexed 5.6° ± 5.21. Shoulder flexion increased at LCOFF, peaking at 33.2° ± 4.8 during early LCL (18% GC), extending to 5.4° ± 5.5 of flexion in early RCL (70 % GC). The right shoulder just reached extension during LCL, peaking at -0.8° ± 4.5 just after RFON (52% GC) and peaked in flexion (28.7° ± 4.3) during early RCL (67% GC). The left shoulder was internally rotated through stance, peaking at 26.1° ± 6.9 in early LCL (24% GC), rotating externally to -6.4° ± 6.9 during RCL (72% GC). The right crutch mirrored this but was phase shifted, rotating externally to -6.4° ± 7.3 during RCL (72% GC) and internally rotating during LCL to 27.4° ± 8.4. The elbows remained flexed at a minimum of 21.8° ± 3.5 (right) and 15.8° ± 3.1 (left). Elbow flexion peaked at the end of crutch repositioning (right = 40.4° ± 3.9, left = 39.7° ± 4.3).

Table 6-1: Peak shoulder and elbow angles (°). Mean, standard deviation (SD), and timing within the gait cycle (%GC). *Az* (+, internal rotation), *Ax* (+, flexion), and *Ay* (+, abduction).

Shoulder	**Right**			**Left**		
	Mean	**SD**	**%GC**	**Mean**	**SD**	**%GC**
Az Max	37.6	4.6	55	33.2	3.5	11
Az Min	20.5	5.1	89	12.9	2.4	57
Ax Max	28.7	4.3	67	33.2	4.8	18
Ax Min	-0.8	4.5	52	5.4	5.5	70
Ay Max	27.4	8.4	79	26.1	6.9	24
Ay Min	-1.1	4.9	26	-6.4	7.3	72
Elbow						
Ax Max	39.7	4.3	66	40.4	3.9	14
Ax Min	21.8	3.5	56	15.8	3.1	54

6.4.3 Crutch forces

Crutch forces (Table 6-2) were applied at the hand and forearm cuff. Average crutch percent error was 4.1% ± 3.1%. Left crutch forces were higher in compression (*Fz*) and progression (*Fy*). Axial crutch loads peaked midway through the GC at 3.25 N/kg ± 0.43 (right) and 4.00 N/kg ± 0.76 (left). Inferior *Fz* peak crutch forces at right (-3.07 N/kg ± 0.37) and left (-3.81 N/kg ± 0.68) hands were slightly less than axial crutch loads. *Fy* forces were highest when acting posteriorly on the cuff (right 0.31 N/kg ± 0.08; left 0.41 N/kg ± 0.08) and hand (right 0.31 N/kg ± 0.07; left 0.39 N/kg ± 0.07). *Fx* forces were similar and relatively low.

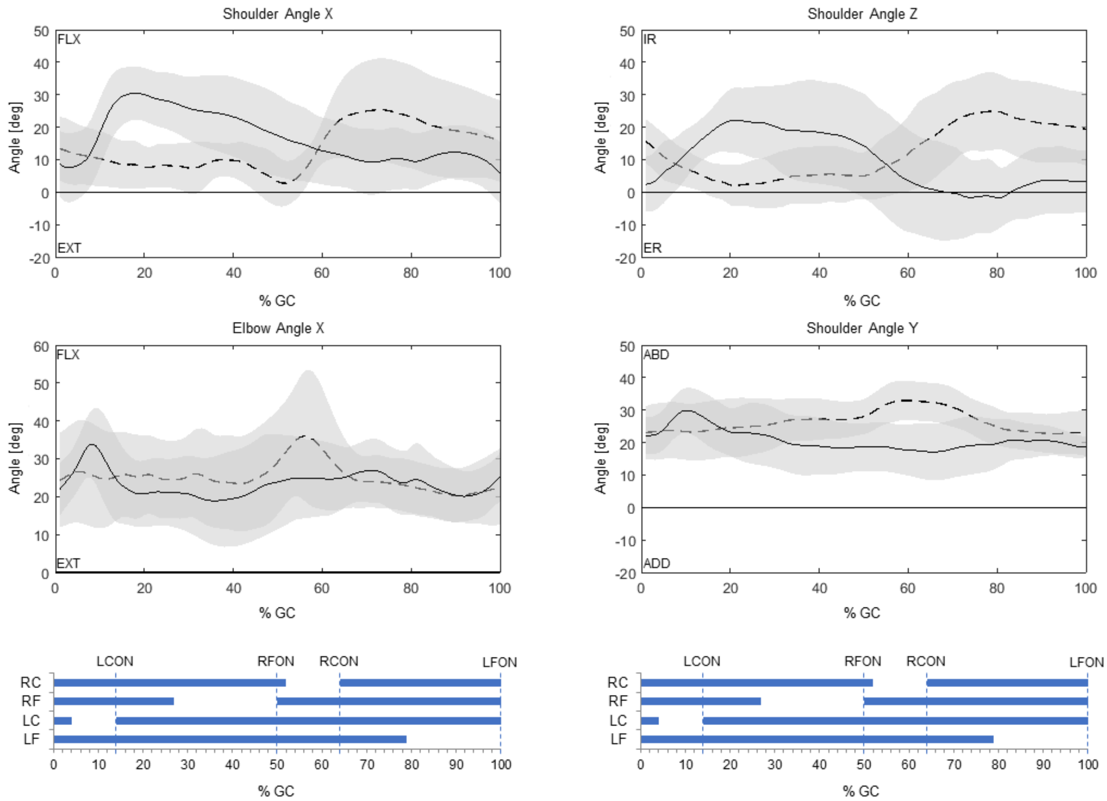

Figure 6-4: Grand ensemble for UE kinematics for the right (- -) and left (–) arms (grey represents standard deviation). Bars indicate crutch phases: right crutch (RC), right foot (RF), left crutch (LC), left foot (LF), left-crutch-on (LCON), right-foot-on (RFON), right-crutch-on (RCON), left-foot-on (LFON).

Table 6-2: Peak crutch forces (N/kg) normalised to participant mass (kg). Mean, standard deviation (SD), and timing within the gait cycle (%GC). *Fa* axial crutch force, *Fz* superior (+) inferior (-), *Fx* medial (+) lateral (-), and *Fy* anterior (+) posterior (-).

	Right			**Left**		
Crutch	**Mean**	**SD**	**%GC**	**Mean**	**SD**	**%GC**
Fa Max	3.25	0.38	46	4.00	0.76	56
Cuff						
Fx Min	-0.15	0.06	57	-0.17	0.04	58
Fx Max	0.09	0.02	43	0.08	0.07	25
Fy Min	-0.31	0.08	49	-0.41	0.08	59
Hand						
Fy Min	-0.31	0.07	51	-0.39	0.07	63
Fy Max	0.04	0.02	47	0.06	0.03	31
Fx Min	-0.13	0.02	46	-0.08	0.07	24
Fx Max	0.14	0.06	57	0.20	0.04	58
Fz Max	0.13	0.02	46	0.13	0.02	28
Fz Min	-3.07	0.37	46	-3.81	0.68	58

6.4.4 Joint force, impulse, and moment

Right and left shoulder superior (*Fz*) peak forces were similar (right = 1.57 N/kg ± 0.28; left = 1.71 N/kg ± 0.44), both occurring during swing and RCL (Table 6-3, Figure 5). Superior forces at right (5.24 N/kg ± 1.12) and left (5.36 N/kg ± 1.08) elbows were similar, and greater than the shoulder and hand. The left superior peak elbow force occurred at LCOFF; however, the right peak occurred during RCL (73% GC), just before foot-off (79% GC). Medially directed forces on the shoulder were greater on the right (0.94 N/kg ± 0.21) than the left (-0.75 N/kg ± 0.14) and occurred during contralateral crutch loading periods (right 25% GC; left 74% GC). The greatest posteriorly directed force (*Fy*) on the shoulder joint occurred on the left (-1.32 N/kg ± 0.35), just after RCR (66% GC). At the elbow, medial forces were greater on the right (1.26 N/kg ± 0.21) during LCL (45% GC) than the left during RCL (81% GC). Right peak posterior forces were lower (-0.90 N/kg ± 0.26) and occurred during RCL (78% GC). Peak posterior loads at the elbow were again greater than the shoulder, and greater on the left (-4.01 N/kg ± 1.12) than the right (-3.02 N/kg ± 0.92). The right and left peak posterior loads occurred during contralateral crutch loading periods.

Table 6-3: Peak joint kinetic forces (N/kg) and moments (Nm/kg) normalised to participant mass (kg). Mean, standard deviation (SD), and timing within the gait cycle (%GC). Forces: *Fz* superior (+) inferior (-), *Fx* medial (+) lateral (-),*Fy* anterior (+) posterior (-). Moments: *Mz* internal rotation (+) external rotation (-), *Mx* flexion (+) extension (-), *My* adduction (+) abduction (-).

	Shoulder						**Elbow**					
	Right			**Left**			**Right**			**Left**		
	Mean	**SD**	**%GC**	**Mean**	**SD**	**%GC**	**Mean**	**SD**	**%GC**	**Mean**	**SD**	**%GC**
***Fz* Max**	1.57	0.28	88	1.71	0.44	82	5.24	1.12	73	5.36	1.08	4
***Fx* Max**	0.94	0.21	25	0.75	0.14	74	1.26	0.21	45	1.40	0.37	81
***Fy* Min**	-0.90	0.26	78	-1.32	0.38	69	-3.02	0.92	40	-4.01	1.12	66
***Mz* Max**	0.03	0.02	70	0.08	0.04	36	0.04	0.01	41	0.03	0.01	6
***Mz* Min**	-0.04	0.02	22	-0.07	0.03	58	-0.01	0.00	0	-0.02	0.01	19
***Mx* Max**	0.14	0.06	26	0.19	0.09	68	0.08	0.01	48	0.09	0.03	18
***Mx* Min**	-0.08	0.03	69	-0.10	0.04	19	-0.09	0.02	31	-0.13	0.03	66
***My* Max**	0.16	0.05	34	0.15	0.04	16	0.08	0.02	36	0.07	0.02	2
***My* Min**	-0.07	0.05	75	-0.14	0.06	48	-0.02	0.01	62	-0.03	0.02	21

Peak transverse internal rotation moment at the shoulder occurred during crutch loading and was greater on the left than the right (Table 6-3, Figure 6-5.). Peak external moments were greater on the left, during opposite limb crutch loading. At the elbows, peak internal and external moments were similarly low, all occurring during LCR or LCL. At the shoulder, peak sagittal flexion moments were larger on the left and occurred during contralateral crutch loading. Peak extension moments were slightly larger on the left and occurred during early crutch loading. Flexion moments at the elbows were similar, occurring at terminal stance just before RCOFF and early LCL. Extension moments were greater on the left and occurred during contralateral crutch loading. Peak frontal abduction moments at the left and right shoulders were similar, both occurring during LCL. Left shoulder peak adduction moments were greater, occurring just before RCR at the end of terminal stance (50% GC), with right shoulder moments half of the left and occurring during RCL. Peak abduction and adduction angles at the elbows were similarly small.

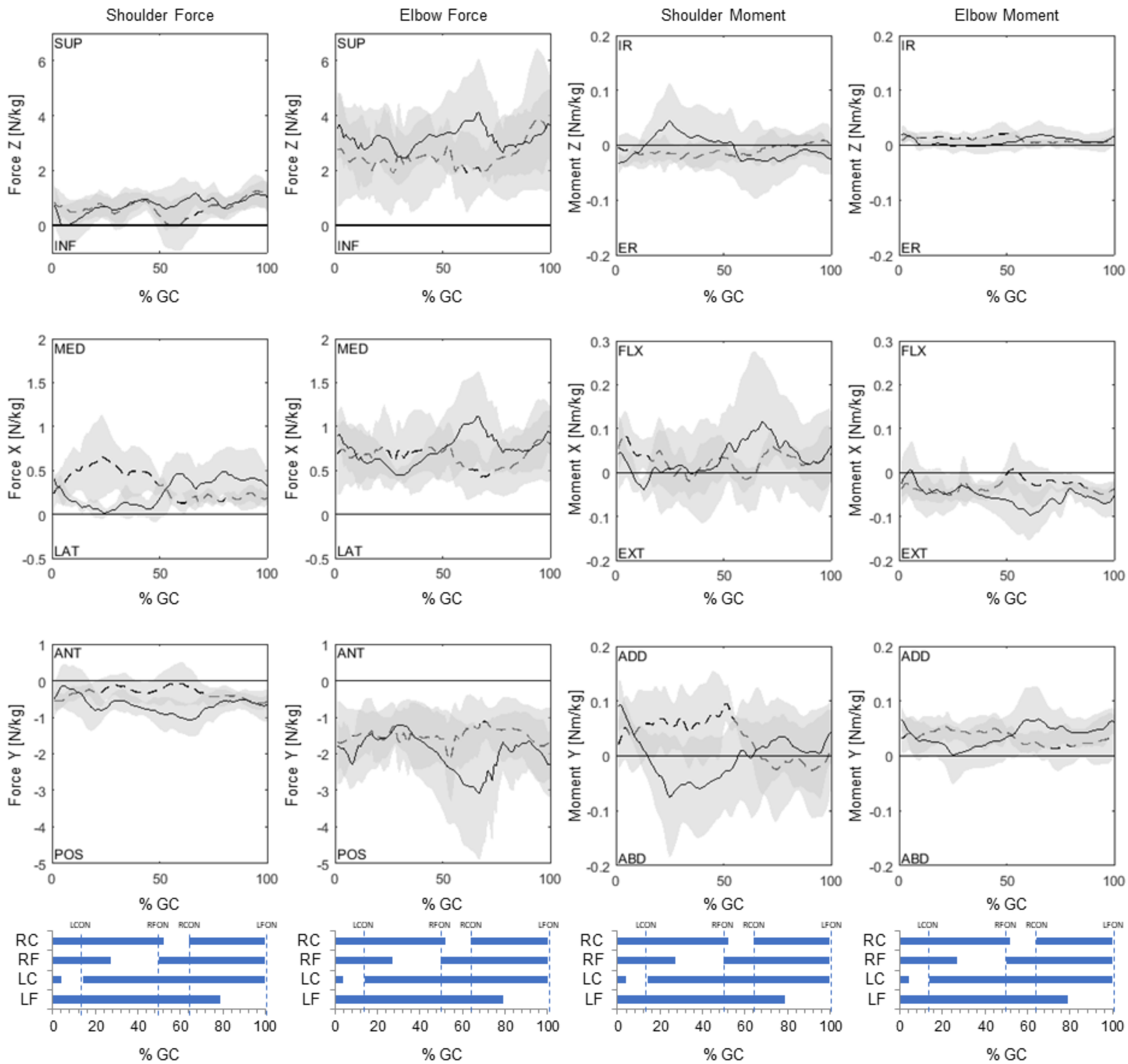

Figure 6-5: Grand ensemble for UE kinetics for the right (- -) and left (–) arms (grey represents standard deviation). The bars at the bottom indicate ground contact periods for the right crutch (RC), right foot (RF), left crutch (LC), and left foot (LF). Vertical dashed lines indicate left-crutch-on (LCON), right-foot-on (RFON), right-crutch-on (RCON), and left-foot-on (LFON). Forces: *Fz* superior (SUP,+) inferior (INF, -), *Fx* medial (MED,+) lateral (LAT,-), and *Fy* anterior (ANT,+) posterior (POS,-). Moments: *Mz* internal rotation (IR,+) external rotation (ER,-), *Mx* flexion (FLX,+), extension (EXT -), and *My* adduction (ADD, +) abduction (ABD, -).

Weight bearing impulse (Table 6-4) was largest on the superior shoulder and elbow joints, and similar between UE. Posterior impulse was the next largest on the posterior shoulder and elbow; however, posterior impulse was greater on the left shoulder and elbow, compared to the right. Medial impulse was the smallest, and similar between limbs. Impulse was greater at the elbow compared to the shoulder.

Table 6-4: Joint impulse (N·s) when the crutch was in contact with the ground. Median, min, max and standard deviation (SD) over the gait cycle. *Fz* superior (+) inferior (-), *Fx* medial (+) lateral (-), and *Fy* anterior (+) posterior (-).

	Right					**Left**				
Shoulder	**Median**	**Min**	**Max**	**Mean**	**SD**	**Median**	**Min**	**Max**	**Mean**	**SD**
F*z* Superior	5367.38	4235.78	6903.16	5585.08	1022.84	6168.14	4320.59	7380.13	5939.25	1138.28
F*x* Medial	2418.58	2067.23	3285.36	2571.36	487.74	1989.73	1268.59	2979.96	2100.34	624.25
F*y* Posterior	-2777.50	-3600.70	-1915.76	-2821.93	664.46	-5163.25	-6792.04	-3917.31	-5201.55	996.23

	Right					**Left**				
Elbow	**Median**	**Min**	**Max**	**Mean**	**SD**	**Median**	**Min**	**Max**	**Mean**	**SD**
F*z* Superior	18880.72	15548.90	23825.91	19184.35	2920.41	23926.13	19881.97	27269.51	23692.96	2776.85
F*x* Medial	5031.87	4124.66	6017.97	4996.39	688.44	5621.86	4673.26	6174.38	5513.71	566.75
F*y* Posterior	-11524.15	-13719.26	-8808.57	-11366.58	1831.61	-15005.32	-17157.15	-11553.77	-14609.53	2181.76

6.5 Discussion

The UE are essential for LEPE balancing and important for weight transfer between limbs, especially during the learning phase. The LEPE-human model in this research used kinematic and kinetic data from persons with SCI walking with the ARKE exoskeleton, including instrumented crutches, to enable relevant examination of shoulder and elbow joint forces and moments during locomotion. This modelling approach provided useful information on how and when shoulder and elbow loading occurred, which can be used for designing exoskeleton devices or exploring how a device functions with varying muscle contributions from simulated pathology.

Results from five persons with complete SCI walking with the ARKE LEPE confirmed our hypothesis that shoulder and elbow forces would be greater than published shoulder and elbow forces of persons with iSCI walking with forearm crutches. This was likely due to kinematic and crutch strategy differences, as well as physical capacity differences between populations with complete and incomplete SCI. UE axial forces were greater, occurred earlier, and lasted longer than previous studies. LEPE users must establish stability sooner than other crutch-assisted walking tasks. This strategy has been observed at slower speeds (Slavens et al., 2008) where increased floor contact periods are important (Smidt & Mommens, 1980; Smith & Lemaire, 2018).

Compared to published literature, the forearm crutches were angled more forward, with shoulder flexion exceeding 33°. Persons with iSCI walk with less than 18° shoulder flexion (Perez-Rizo et al., 2017; Requejo et al., 2005). As well, participants in this study averaged more than 17.8° forward trunk tilt, peaking at 28.6°, compared to ambulatory persons with SCI who walk with a more neutral or extended trunk (Melis et al., 1999). Forward and lateral leaning is required to initiate a step, which is a common strategy with commercial LEPE. With experience, people may reduce forward trunk tilt for step initiation.

Forward leaning places greater reliance on forearm crutches, leading to crutch forces two and a half times greater than previous studies. Total crutch contact periods for the right and left crutches were 90% of GC, 30%-40% longer than previous studies (Requejo et al., 2005; Slavens et al., 2011). Greater crutch contact periods and forces produced between 5 and 12 times higher joint impulses than iSCI walking with crutch assistance (Haubert et al., 2006). Increased crutch load may cause UE joint and muscle pain, fatigue, and increase energy cost of walking (Lal, 1998; Talaty et al., 2013).

Crutch support also controls COP progression when using an exoskeleton (Smith et al., 2019), in the absence of an actuated ankle. Upright posture, could be improved using additional or modified strapping, or by incorporating a thoracolumbosacral orthosis (TLSO). Recent use of a TLSO significantly improved trunk extension and walking speed of persons with SCI walking with the advanced reciprocating gait orthosis (ARGO) (Arazpour, Gharib, et al., 2015; Arazpour et al., 2016). Step-frequency, step-length, distance walked and the physical cost index of walking with ARGO were also improved, though not significantly. Upright posture, COP control, joint stability, joint loading, heel rise, stride-length, energy demand, and gait speed could be improved by incorporating an ankle foot orthosis (AFO) into LEPE design (Bregman, Harlaar, Meskers, & de Groot, 2012; Mooney & Herr, 2016; J. Perry & Clark, 1997; J. Perry, Fontaine, & Mulroy, 1995; Ploeger, Bus, Brehm, & Nollet, 2014). This is supported by research showing that joint requirements for biomimetic slow walking using a LEPE could be improved with a variable assist ankle (Fournier, 2018).

Compared to reciprocal gait of persons with iSCI, greater superior, posterior, and medial forces were observed and are injury risk mechanisms for the shoulder and elbow (Perez-Rizo et al., 2017; Slavens et al., 2008). Posterior forces were even greater than forces during more strenuous swing through gait, which may present an increased injury risk. Gagnon et al., 2008 also found high superiorly (2.91 N/kg) and posteriorly (–3.14 N/kg) directed joint forces during split pivot transfers from a wheelchair (D. Gagnon, Nadeau, Noreau, Dehail, & Gravel, 2008; D. Gagnon, Nadeau, Noreau, Dehail, & Piotte, 2008). Though pivot transfer forces are twice the forces observed in this study, repetitive shoulder loading may fatigue and elevate the risk of LEPE users' developing an impingement, capsule instability, or joint degeneration. Shoulder resultant forces during manual wheelchair propulsion, determined using a similar musculoskeletal model, exceeded 300 N, depending on wheelchair axial position (Dubowsky, Rasmussen, Sisto, & Langrana, 2008). These wheelchair propulsion forces were twice the forces in this study, suggesting that LEPE crutch assisted ambulation may have less risk of overuse shoulder injury than wheelchair use. This is in contrast to previous studies where resultant wheelchair propulsion shoulder forces were less than forearm crutches (Haubert et al., 2006; Kulig et al., 2001, 1998). This discrepancy may be due to previous crutch and wheelchair models not adequately representing essential bone and muscle geometry when calculating forces.

Joint moments in this study were also greater than published data on forearm crutch assisted gait. Like previous studies, shoulder and elbow moments were predominantly in flexion and internal rotation. Unlike previous papers that showed predominant adduction moments (Perez-Rizo et al., 2017; Requejo et al., 2005) or abduction moments (Opila, Nicol, & Paul, 1987), abduction moments in this study occurred as weight transferred onto the support limb, to prevent shoulder adduction. The contralateral UE adduction moment resisted abduction and controlled mediolateral movements.

Results across all five participants had large variability. This is likely due to level of injury and how quickly a user adapts to LEPE assistance, and its effect on model output. Variability could be reduced by evaluating a larger sample of community ambulatory LEPE users who have more LEPE walking experience. However, results from the five novice LEPE users are useful when assessing the movement requirements and risk of injury during LEPE rehabilitation. Reducing shoulder load is important to reduce ambulatory assistive device overuse injuries, muscle pain, fatigue, and energy cost of walking. Higher forces particularly at the shoulder compared to persons with iSCI walking with forearm crutches, highlight that LEPE users with more sever neurological injuries rely heavily on support aids to remain up right. This observation supports the need for developing pre-training rehabilitation program (Gagnon et al., 2018), that incorporates strength training for persons with SCI to ensure UE joints are strong enough to initiate LEPE training.

Chapter 7. General discussion

To provide a biomimetic basis for LEPE controls, this thesis explored how able-bodied adults walked at gait speeds between 0.2 m/s and self-paced. Characterising gait parameters at very slow and natural walking speeds enabled the development of reference equations for stride, kinematic, and kinetic parameters. These equations are useful for LEPE designers since they are comprehensive, easy to apply, and remove the need for multiple speed-specific walking trajectories in the control system. As well, this research presented a full body model of persons with SCI using the ARKE LEPE. To determine human-machine interactions, this research incorporated all external contact forces and inertial properties of the ARKE and user, and was driven using real LEPE SCI user kinematics. Together, this research provided a modeling framework for measuring and tuning LEPE-human dynamics that could be used to advance LEPE design and control.

All the objectives for this thesis were met:

7.1 Objective 1: Define how able-bodied persons walk at very slow speeds, consistent with device use.

Consistent with the literature and our hypothesis, stride-parameters changed with different walking speeds. However, speed relationships that were previously considered linear for step-length, stride-length, and stride-frequency were stronger when calculated using non-linear models. Non-linear relationships with speed were also found for stride-time, step-time, stance-time, and DST, with a consistent inflection point at 0.5 m/s. This suggests that able-bodied persons switch walking strategy at very slow speeds to increase floor contact time rather than modifying foot displacement. Considering that slower walking speeds with shorter step-lengths, faster step-times, and longer DST have been characterised as cautious and safe; changes in gait strategy that increase ground contact time may be more indicative of a safe stepping strategy, and thereby may improve dynamic stability during LEPE walking.

Since speed is the product of step-frequency and stride-length, this research also examined relationships between these parameters and sagittal kinematics and kinetics. It was hypothesised that a change in gait strategy would occur at 0.5 m/s for kinematic and kinetic parameters, with non-linear relationships with speed, cadence, or stride-length. Based on previous regression analyses of walking speeds effect on gait, it was hypothesised that kinetics would correlate more strongly with stride-parameters. Non-linear, quadratic models showed the strongest correlations with walking speed. Despite the strong non-linear relationships, no consistent inflection point was found, indicating that kinematic and kinetic strategies did not change consistently at very slow speeds. Confirming our hypothesis, kinetic gait parameters were more strongly correlated with stride parameters; however, many kinematic gait parameter relationships with speed were strong, R^2 averaging 0.85. Since regression equations from this research were derived from speed appropriate data, these equations should be more appropriate for LEPE users.

There is recent and rapidly growing interest in the clinical and technological utility of speed dependent gait parameters that define how able-bodied persons walk at very slow speeds (objective 1). Since *"Temporal-spatial gait parameter models of very slow walking"* was published (March 2018), the article has been cited to explain speed effects on gait parameters during lower limb orthoses use (Farah, Baddour, & Lemaire, 2019), virtual-reality rehabilitation (Szczesna, Blaszczyszyn, Pawlyta, & Michalczuk, 2018), and clinical decision making (Conradsson & Halvarsson, 2019; Steinberg, Nemet, Pantanowitz, & Eliakim, 2018; Turcato et al., 2018). In support of the existence of a distinct slow walking gait strategy at walking speeds below 0.5 m/s, Smith & Lemaire, (2018) has been well cited to explain distinct, speed related changes in limb coordination (Little, McGuirk, & Patten, 2019) and improved LEPE walking speed (Ramanujam et al., 2018).

Within a year, including the publication of chapters three and four, seven articles have been published that modeled temporal-spatial (Fang et al., 2019; Smith & Lemaire, 2018), and kinematic (Stansfield, Hawkins, Adams, & Bhatt, 2018; Stansfield, Hawkins, Adams, & Church, 2018), and or kinetic (Fukuchi & Duarte, 2019; Smith, Lemaire, & Nantel, 2018) gait parameters using regression modeling techniques over a "wider" range of walking speeds. Prior to this influx of articles, the last article to publish SWR equations was in 2014 (Koopman et al., 2014), and prior to that in 2003 (Lelas et al., 2003). Despite this interest and the proposed use of published models for robotic-assisted therapy, recently published models (excluding Smith & Lemaire, 2018 and Smith, Lemaire, & Nantel, 2019) failed to include walking speeds below 0.4 m/s. Therefore, the utility of these models is limited for estimating step parameters, angular trajectories, and force inputs for LEPE control. With the emergence of new regression models developed with a wider range of walking speeds, research into the validity of published regression models are needed.

Validation analyses require comprehensive biomechanical data sets be made publicly available to enable comparisons of estimated gait parameters that are less biased. These datasets must include both raw and processed kinematics, kinetics, and temporal gait data, from overground and treadmill walking trials, at a wide range of gait speeds. In this regard, the acceptance of data sharing and replication studies were recently advocated (Ferber, Osis, Hicks, & Delp, 2016; Knudson, 2017) to "improve the validity of inferences from data in biomechanics research". Fukuchi et al., (2018), in support of this proposed action, recently made public a dataset of three-dimensional overground and treadmill walking kinematics and kinetics of 24 young (27.6±4.4 years) and 18 older adults (62.7±8.0 years), at a range of gait speeds (Fukuchi, Fukuchi, & Duarte, 2018). Results from validation studies would provide support for individual models, or help to combine multiple regression models to create a more comprehensive tool, if found to be valid. However, even Fukuchi et al., (2018) recently published dataset did not included walking trials at LEPE appropriate speeds below 0.4 m/s.

7.2 Objective 2: Develop and apply a comprehensive LEPE-human spinal cord injured (SCI) musculoskeletal model to solve human-machine interactions based on real LEPE user biomechanics.

The model presented in this research addressed previous limitations and contributed many firsts to biomechanical research; including, being driven by kinematics and kinetics of SCI LEPE users, model crutch kinematics and kinetics, and incorporate all external forces acting on the user when determining LEPE-human interaction forces. LEPE-human model output provided user joint kinetics and strap contact forces between the device and user. These data provided needed information to calculate forces between the device and participant and net joint moments during device use.

SWR-based gait parameters provided a biomimetic reference to compare ARKE predefined LEPE reference trajectories and resultant net joint moments. Net joint moments and contact forces were strongly influenced by device posture, which differed greatly from calculated able-bodied kinematics. This is consistent with studies that have successfully implemented SWR models for the rehabilitation exoskeleton LOPES (Kooij, Veneman, & Ekkelenkamp, 2006) and LEPE H2 prototype (Bortole & Pons, 2013). Able-bodied LEPE assisted gait was more natural when LEPE controllers used reference trajectories generated using SWR (Tufekciler, van Asseldonk, & van der Kooij, 2011) compared to able-bodied LEPE assisted gait using predefined LEPE reference trajectories (Asín-Prieto et al., 2015). SWR trajectory generation reduced impedance magnitude and variability compared to predefined reference trajectories were used for control. The authors proposed that reduced LEPE-human impedance would improve LEPE performance and make it easier for new users to learn how to walk with H2 assistance (Asín-Prieto et al., 2015). Successful implementation of regression models into the main controller of LOPES and the H2 LEPE support the utility of SWR equations for LEPE control, and their use in a novel adaptive control system to provide reference patterns that dynamical change to alter walking speeds are currently underway.

To dynamically generate trajectories for LEPE control, machine learning techniques have been applied to obtain prediction algorithms that automatically estimate temporal gait parameters and construct angular trajectories (Martinez, Kuzmicheva, Ristić-Durrant, & Graeser, 2017; Liu , Wu, Wang, & Chen, 2017). Described as a “highly flexible” nonlinear regression models, neural network’s strong non-linear mapping capability have made them a powerful tool for generating reference trajectories for LEPE control. However, similar to gait parameter regression models (Lelas et al., 2003), angular trajectories generated by artificial neural networks have resulted in poor kinematic predictability (Martinez et al., 2017). As well, training data for these neural networks must reflect the real work application. For example, Luu , et al. (2014) reported gait patterns at 0.25 m/s using a neural network regression model trained using walking trial data at speeds between 0.55 m/s and1.3 m/s (Luu, Low, Qu, Lim, & Hoon, 2014). Neural network estimated hip ROM was 10 degrees greater than results from SWR equations (Fluit et al., 2014; Smith & Lemaire, 2018; Smith et al., 2018) and clinical gait analysis at match walking speeds (Nymark et al., 2005). Estimated stride-time (57.2 s) was more similar to a walking speed of 1.5 m/s. Neural networks had difficulty estimating common kinematic parameters (peaks) at very slow speeds when input values (speed, step-frequency, and stride-length) were small (Martinez, Kuzmicheva, & Gräser, 2016). Further research into the use of neural networks are required to avoid generating “strange behaviors” and to investigate slow walking strategies at very slow walking speeds that are appropriate for LEPE use.

Research in this thesis showed the potential of combining musculoskeletal and CAD models to determine human-machine interactions for improve LEPE control. LOPES, H1 and H2 LEPE used adaptive control based on SWR and estimated feedforward predicted joint torques needed to follow desired angles, velocities, and accelerations. Adaptive controllers model LEPE-human interaction using equations of motion (Equation 2.1). The modelling framework presented in this research could improve LEPE design efficiency, safety, and provide a means to better understand human-machine interaction when developing LEPE control architecture. Recently, we successfully validated our LEPE-human model using AMS ground reaction force prediction against real force plate data, presented in this thesis (Fournier et al., 2018) with both real SCI LEPE users and able-bodied slow walking kinematics. The biomimetic model could be used to simulate LEPE-human interaction with minimal crutch use and estimate impedance thresholds and joint torques for LEPE adaptive control.

This research presented the first LEPE-human musculoskeletal model to estimate upper-extremity biomechanics, driven by 3D motion data of persons with complete SCI walking with LEPE and crutch assistance. Participants relied heavily on their crutches for support and control when walking with ARKE. It was hypothesized that shoulder and elbow forces during LEPE walking would be greater than the literature on reciprocal crutch gait with incomplete SCI participants. Consistent with our hypothesis, greater superior, posterior, and medial joint forces were observed. Posterior forces were even greater than those observed during more strenuous swing through gait. Higher forces present an increased injury risk to LEPE users. Repetitive shoulder loading may fatigue and elevate the risk of LEPE users developing an impingement, capsule instability, or joint degeneration. Joint moments were two and a half times greater than published data on forearm crutch assisted gait. Joint impulses were between five and 12 times greater than incomplete SCI walking with crutch assistance. However, modelled wheelchair propulsion forces in the literature were twice those estimated during LEPE use. Considering kinematics of four-point crutch gait, forearm crutches and the torso in this thesis were angled more forward. Total crutch contact periods for the right and left crutches were 30%-40% longer than previous studies.

This research, for the first time, provided a quantitative understanding of upper-extremity human dynamics during LEPE walking. The outcomes support the need for pre-training rehabilitation for potential LEPE users (Gagnon et al., 2018). Improving upright posture is critical for reducing loads transmitted to the upper-extremity via forearm crutches observed in this study (Arazpour, Gharib, et al., 2015; Arazpour et al., 2016). The LEPE-human SCI model could be customised to investigate different LEPE configurations, perhaps incorporating a TCLO to improve trunk extension, by calculating upper-extremity joint loads. Varying levels of injury could be simulated using the LEPE-human SCI model, by customising muscle involvement to the participant’s injury.

7.3 LEPE design recommendations

Characterising LEPE-human model output lead to informed design recommendations to be made for improving LEPE function. Improving upright posture and step completion are critical for improving LEPE walking speed and step completion, reducing LEPE-human interaction forces and efficient device use.

Upright posture may be improved using a thoracolumbosacral orthosis or by improving shoulder and chest strapping. Reducing trunk flexion may increase step completion, step-length, and walking speed, while also reducing upper and lower limb loading, increasing walking distance and reducing physiological cost of LEPE use.

Increasing maximum dorsiflexion to 20° may prevent early heel raise, while allowing participants to maintain a large base of support. However, contractures limiting ROM at the ankle, knee, and hip joints are common among persons with SCI. Contracture(s) prevented the majority of patients screened by physiotherapists in this and previous feasibility studies from participating (Gagnon et al., 2018; Kozlowski et al., 2015). For safety and user confidence, dorsiflexion dampening may be required to control "forward fall" body rotation over the foot. Incorporating step-length reduction and increased swing-limb angular velocity in a "partial step correction algorithm" would reduce swing-time, knee flexion during stance, and dorsiflexion, thereby improving stability and step completion.

Upright posture, COP control, joint stability, joint loading, heel rise, stride-length, energy demand, and gait speed could be improved by incorporating an ankle foot orthosis (AFO) into LEPE design. Our group recently showed that mechanical joint requirements for biomimetic slow walking with ARKE could be met at the ankle using a passive phase and speed dependent variably stiff ankle, utilising quadratic elastic spring elements (Fournier, 2018). A LEPE ankle of this design could improve step completion and overall device function. Since the lateral and anterior shank had the greatest and most prolonged loading periods, increasing the padding area at these locations may be advised, even though pressures during this research were below the threshold for tissue damage.

Reducing upper and lower limb load is important to reduce ambulatory assistive device overuse injuries, muscle pain, fatigue, and energy cost of walking. Higher forces particularly at the shoulder compared to persons with iSCI walking with forearm crutches, highlight that LEPE users with more sever neurological injuries rely heavily on support aids to remain up right. This observation in addition to high incidences of skin aberrations, fractures to the talus (Benson et al., 2016) and calcaneus (Gagnon et al., 2018), prevalence of (spasticity) and contracture, risk of falls, general soreness, and fatigue supports the need for developing pre-training rehabilitation program (Gagnon et al., 2018), to ensure patients and potential users are fit enough to initiate LEPE training.

7.4 Future Work

This research contributed to knowledge on stride parameters, kinematics, and kinetics during very slow walking; musculoskeletal-LEPE modeling, and human dynamics during LEPE operation. This research also led to new questions and areas of inquiry:

1. Mounting evidence suggests that gait parameter change at slow walking speeds below 0.5 m/s, representing distinct gait strategies. Further research into this phenomenon is required to determine if these changes represent a gait strategy unique to very slow speeds.
2. With growing interest and the emergence of new regression models developed from data sets with a wide range of walking speeds, research into the validity of published regression models are needed. These regression models should be evaluated using separate data set. Results from these studies would provide support for individual models, or help to combine multiple regression models to create a more comprehensive tool.
3. Kinematic regression models typically have low correlations to speed. This could be due to intrinsic variability or gait parameter variability between people. Evidence suggests that experimentally controlling walking speed using an instrumented treadmill may improve gait parameter relationships with speed, but at the sacrifice of model ecological validity. Though many studies have evaluated human gait parameter differences between overground and treadmill walking, the external validity of treadmill gait parameter data continues to be debated. Therefore, regression models developed on both treadmills and overground data should be cross-validated.
4. Data gather for this study were from 15 health men and 15 health women. Significant kinematic differences have been reported between men and women, and small difference with increasing age. In general, women exhibit greater pelvic tilt, pelvic obliquity (side up), hip flexion and extension, and knee flexion (Stansfield, Hawkins, Adams, & Bhatt, 2018; Stansfield, Hawkins, Adams, & Church, 2018). Older adults conversely exhibit minor reductions in hip and knee ROM (Kerrigan et al., 1998; Tommy Oberg & Karsznia, 1994). Research is needed to determine if the current regression models are appropriate for an aging population, or for both men and women.
5. The use of regression modeling for determining appropriate LEPE trajectories is an area of growing interest. Control architectures that require force input could use regression position and force model data to develop an adaptive control strategy. With regression equations from

this research, desired angular trajectories and forces could be reconstructed and tested on an existing LEPE or model that utilizes adaptive control.

6. Recently we validated our LEPE-human model using predicted and real ground reaction force data (Fournier et al., 2018). The validated biomimetic model incorporates all inertial properties of the ARKE device into inverse dynamic calculations. This model could be used to determine desired LEPE joint interaction forces and moments with minimal crutch use. Models using these data would more accurately estimate LEPE interaction forces and moments, may be more appropriate in determining force thresholds for adaptive control strategies, and allow the designer to vary human moment generation capacity.
7. The biomimetic approach assumes that healthy slow walking is optimal for LEPE use; however, altered system inertia from the added LEPE weight may alter appropriate gait dynamics. Advancement of LEPE and user ability will enable persons with lower limb paralysis or weakness to walk faster, which may substantially alter LEPE-human gait dynamics. To accommodate increased walking speeds, LEPE-human models could be used to research system dynamics using different swing limb frequencies, crutch strategies, and devices to determine an optimal control strategy.
8. Generic musculoskeletal models can be customized with subject-specific information. Testing the sensitivity of the output variables (i.e. kinematics, kinetics, contact forces) to changes in levels of paralysis is of crucial importance when evaluating the feasibility of new control strategies or mechanical designs. This could include for different pathologies or level of injuries. For example, including lower limb muscles when simulating paraplegia would as well more accurately simulate impedance of lower limb joint and soft tissues.

References

Aach, M., Cruciger, O., Sczesny-Kaiser, M., Höffken, O., Meindl, R. C., Tegenthoff, M., … Schildhauer, T. A. (2014). Voluntary driven exoskeleton as a new tool for rehabilitation in chronic spinal cord injury: a pilot study. *The Spine Journal: Official Journal of the North American Spine Society*, *14*(12), 2847–2853. https://doi.org/10.1016/j.spinee.2014.03.042

Agarwal, P., Kuo, P. H., Neptune, R. R., & Deshpande, A. D. (2013). A novel framework for virtual prototyping of rehabilitation exoskeletons. *2013 IEEE 13th International Conference on Rehabilitation Robotics (ICORR)*, 1–6. https://doi.org/10.1109/ICORR.2013.6650382

Agarwal, P., Narayanan, M. S., Lee, L.-F., Mendel, F., & Krovi, V. N. (2010). *Simulation-based design of exoskeletons using musculoskeletal analysis*. 1357–1364. https://doi.org/10.1115/DETC2010-28572

Alton, F., Baldey, L., Caplan, S., & Morrissey, M. C. (1998). A kinematic comparison of overground and treadmill walking. *Clinical Biomechanics*, *13*(6), 434–440. https://doi.org/10.1016/S0268-0033(98)00012-6

Andriacchi, T. P., Ogle, J. A., & Galante, J. O. (1977). Walking speed as a basis for normal and abnormal gait measurements. *Journal of Biomechanics*, *10*(4), 261–268. https://doi.org/10.1016/0021-9290(77)90049-5

anybodytech.com: Frontpage. (n.d.). Retrieved March 19, 2017, from https://www.anybodytech.com/

Aoyagi, D., Ichinose, W. E., Harkema, S. J., Reinkensmeyer, D. J., & Bobrow, J. E. (2007). A robot and control algorithm that can synchronously assist in naturalistic motion during body-weight-supported gait training following neurologic injury. *IEEE Transactions on Neural Systems and Rehabilitation Engineering*, *15*(3), 387–400.

Arazpour, M., Bani, M. A., Kashani, R. V., Ghomshe, F. T., Mousavi, M. E., & Hutchins, S. W. (2013). Effect of powered gait orthosis on walking in individuals with paraplegia. *Prosthetics and Orthotics International*, *37*(4), 261–267. https://doi.org/10.1177/0309364612463164

Arazpour, M., Chitsazan, A., Hutchins, S. W., Mousavi, M. E., Takamjani, E. E., Ghomshe, F. T., … Bani, M. A. (2012). Evaluation of a novel powered gait orthosis for walking by a spinal cord injury patient. *Prosthetics and Orthotics International*, *36*(2), 239–246. https://doi.org/10.1177/0309364611435690

Arazpour, M., Gharib, M., Hutchins, S. W., Bani, M. A., Curran, S., Mousavi, M. E., & Saberi, H. (2015). The influence of trunk extension in using advanced reciprocating gait orthosis on walking in spinal cord injury patients: A pilot study. *Prosthetics and Orthotics International*, *39*(4), 286–292. https://doi.org/10.1177/0309364614531010

Arazpour, M., Hutchins, S. W., & Bani, M. A. (2015). The efficacy of powered orthoses on walking in persons with paraplegia. *Prosthetics and Orthotics International*, *39*(2), 90–99. https://doi.org/10.1177/0309364613520031

Arazpour, M., Samadian, M., Bahramizadeh, M., Ahmadi Bani, M., Gharib, M., Hosseini, S. A., … Mardani, M. A. (2016). The effect of trunk extension on physiological cost index in spinal cord injury patients when using the advanced reciprocating gait orthosis: A pilot study. *Prosthetics and Orthotics International*, *40*(6), 696–702. https://doi.org/10.1177/0309364615592700

Ardestani, M. M., Ferrigno, C., Moazen, M., & Wimmer, M. A. (2016). From normal to fast walking: Impact of cadence and stride length on lower extremity joint moments. *Gait & Posture*, *46*, 118–125. https://doi.org/10.1016/j.gaitpost.2016.02.005

Arsenault, A. B., Winter, D. A., & Marteniuk, R. G. (1986). Treadmill versus walkway locomotion in humans: an EMG study. *Ergonomics*, *29*(5), 665–676. https://doi.org/10.1080/00140138608968301

Asín-Prieto, G., Shimoda, S., González, J., Pons, J. L., del-Ama, A. J., Gil-Agudo, Á., & Moreno, J. C. (2015). Testing the Generation of Speed-Dependent Gait Trajectories to Control a 6DoF Overground Exoskeleton. In H. Liu, N. Kubota, X. Zhu, R. Dillmann, & D. Zhou (Eds.), *Intelligent Robotics and Applications* (pp. 495–501). Springer International Publishing.

Astephen Wilson, J. L. (2012). Challenges in dealing with walking speed in knee osteoarthritis gait analyses. *Clinical Biomechanics*, *27*(3), 210–212. https://doi.org/10.1016/j.clinbiomech.2011.09.009

Banala, S. K., Agrawal, S. K., & Scholz, J. P. (2007). Active Leg Exoskeleton (ALEX) for Gait Rehabilitation of Motor-Impaired Patients. *2007 IEEE 10th International Conference on Rehabilitation Robotics*, 401–407. https://doi.org/10.1109/ICORR.2007.4428456

Banala, S. K., Kim, S. H., Agrawal, S. K., & Scholz, J. P. (2009). Robot Assisted Gait Training With Active Leg Exoskeleton (ALEX). *IEEE Transactions on Neural Systems and Rehabilitation Engineering*, *17*(1), 2–8. https://doi.org/10.1109/TNSRE.2008.2008280

Bateni, H., & Maki, B. E. (2005). Assistive devices for balance and mobility: benefits, demands, and adverse consequences. *Archives of Physical Medicine and Rehabilitation*, *86*(1), 134–145.

Bauby, C. E., & Kuo, A. D. (2000). Active control of lateral balance in human walking. *Journal of Biomechanics*, *33*(11), 1433–1440.

Behrman, A. L., Bowden, M. G., & Nair, P. M. (2006). Neuroplasticity after spinal cord injury and training: an emerging paradigm shift in rehabilitation and walking recovery. *Physical Therapy*, *86*(10), 1406–1425. https://doi.org/10.2522/ptj.20050212

Benson, I., Hart, K., Tussler, D., & Middendorp, J. J. van. (2016). Lower-limb exoskeletons for individuals with chronic spinal cord injury: findings from a feasibility study. *Clinical Rehabilitation*, *30*(1), 73–84. https://doi.org/10.1177/0269215515575166

Bergmann, G., Graichen, F., Bender, A., Kääb, M., Rohlmann, A., & Westerhoff, P. (2007). In vivo glenohumeral contact forces--measurements in the first patient 7 months postoperatively. *Journal of Biomechanics*, *40*(10), 2139–2149. https://doi.org/10.1016/j.jbiomech.2006.10.037

Bernshteĭn, N. A. (1967). *The co-ordination and regulation of movements*. Retrieved from http://books.google.com/books?id=F9dqAAAAMAAJ

Bertram, J. E., & Ruina, A. (2001). Multiple walking speed-frequency relations are predicted by constrained optimization. *Journal of Theoretical Biology*, *209*(4), 445–453. https://doi.org/10.1006/jtbi.2001.2279

Birch, N., Graham, J., Priestley, T., Heywood, C., Sakel, M., Gall, A., … Signal, N. (2017). Results of the first interim analysis of the RAPPER II trial in patients with spinal cord injury: ambulation and functional exercise programs in the REX powered walking aid. *Journal of NeuroEngineering and Rehabilitation*, *14*(1), 60. https://doi.org/10.1186/s12984-017-0274-6

Blaya, J. A., & Herr, H. (2004). Adaptive control of a variable-impedance ankle-foot orthosis to assist drop-foot gait. *IEEE Transactions on Neural Systems and Rehabilitation Engineering*, *12*(1), 24–31. https://doi.org/10.1109/TNSRE.2003.823266

Boninger, M. L., Souza, A. L., Cooper, R. A., Fitzgerald, S. G., Koontz, A. M., & Fay, B. T. (2002). Propulsion patterns and pushrim biomechanics in manual wheelchair propulsion. *Archives of Physical Medicine and Rehabilitation*, *83*(5), 718–723.

Borghese, N. A., Bianchi, L., & Lacquaniti, F. (1996). Kinematic determinants of human locomotion. *The Journal of Physiology*, *494*(3), 863–879. https://doi.org/10.1113/jphysiol.1996.sp021539

Bortole, M., & Pons, J. L. (2013). Development of a exoskeleton for lower limb rehabilitation. *Biosystems and Biorobotics*, *1*, 85–90. https://doi.org/10.1007/978-3-642-34546-3_14

Bovi, G., Rabuffetti, M., Mazzoleni, P., & Ferrarin, M. (2011). A multiple-task gait analysis approach: Kinematic, kinetic and EMG reference data for healthy young and adult subjects. *Gait & Posture*, *33*(1), 6–13. https://doi.org/10.1016/j.gaitpost.2010.08.009

Bregman, D. J. J., Harlaar, J., Meskers, C. G. M., & de Groot, V. (2012). Spring-like Ankle Foot Orthoses reduce the energy cost of walking by taking over ankle work. *Gait & Posture*, *35*(1), 148–153. https://doi.org/10.1016/j.gaitpost.2011.08.026

Cao, H., Ling, Z., Zhu, J., Wang, Y., & Wang, W. (2009). Design frame of a leg exoskeleton for load-carrying augmentation. *2009 IEEE International Conference on Robotics and Biomimetics, ROBIO 2009*, 426–431. Retrieved from http://www.scopus.com/inward/record.url?eid=2-s2.0-77951447044&partnerID=40&md5=72f4f9260878c7e4bce4fc464558d75f

Carpinella, I., Crenna, P., Rabuffetti, M., & Ferrarin, M. (2009). Coordination between upper- and lower-limb movements is different during overground and treadmill walking. *European Journal of Applied Physiology*, *108*(1), 71–82. https://doi.org/10.1007/s00421-009-1168-5

Charlton, I. W., & Johnson, G. R. (2006). A model for the prediction of the forces at the glenohumeral joint. *Proceedings of the Institution of Mechanical Engineers. Part H, Journal of Engineering in Medicine*, *220*(8), 801–812. https://doi.org/10.1243/09544119JEIM147

Chen, B., Ma, H., Qin, L.-Y., Gao, F., Chan, K.-M., Law, S.-W., … Liao, W.-H. (2016). Recent developments and challenges of lower extremity exoskeletons. *Journal of Orthopaedic Translation*, *5*, 26–37. https://doi.org/10.1016/j.jot.2015.09.007

Cho, K., Kim, Y., Jung, M., & Lee, K. (2012). Analysis and evaluation of a combined human - exoskeleton model under two different constraints condition. *Proceedings of the International Summit on Human Simulation*, 1–10.

Claros, M. J., Soto, R., Gordillo, J. L., Pons, J. L., & Contreras-Vidal, J. L. (2016). Robotic assistance of human motion using active-backdrivability on a geared electromagnetic motor. *International Journal of Advanced Robotic Systems*, *13*(2). https://doi.org/10.5772/62331

Conradsson, D., & Halvarsson, A. (2019). The effects of dual-task balance training on gait in older women with osteoporosis: A randomized controlled trial. *Gait & Posture*, *68*, 562–568. https://doi.org/10.1016/j.gaitpost.2019.01.005

Controzzi, M., Bassi Luciani, L., & Montagnani, F. (2017). Unified approach to bi-directional non-back drivable roller clutch design. *Mechanism and Machine Theory*, *116*, 433–450. https://doi.org/10.1016/j.mechmachtheory.2017.06.010

Crenshaw, R. P., & Vistnes, L. M. (1989). A decade of pressure sore research: 1977-1987. *Journal of Rehabilitation Research and Development*, *26*(1), 63–74.

Crespo, L., & Reinkensmeyer, D. (2008). Haptic guidance can enhance motor learning of a steering task. *Journal of Motor Behavior*, *40*(6), 545–556. https://doi.org/10.3200/JMBR.40.6.545-557

Crowninshield, R. D., Johnston, R. C., Andrews, J. G., & Brand, R. A. (1978). A biomechanical investigation of the human hip. *Journal of Biomechanics*, *11*(1), 75–85. https://doi.org/10.1016/0021-9290(78)90045-3

Damsgaard, M., Rasmussen, J., Christensen, S. T., Surma, E., & de Zee, M. (2006). Analysis of musculoskeletal systems in the AnyBody Modeling System. *Simulation Modelling Practice and Theory*, *14*(8), 1100–1111. https://doi.org/10.1016/j.simpat.2006.09.001

Den Otter, A. R., Geurts, A. C. H., Mulder, T., & Duysens, J. (2007). Abnormalities in the temporal patterning of lower extremity muscle activity in hemiparetic gait. *Gait and Posture*, *25*(3), 342–352.

Ditor, D. S., MacDonald, M. J., Kamath, M. V., Bugaresti, J., Adams, M., McCartney, N., & Hicks, A. L. (2005). The effects of body-weight supported treadmill training on cardiovascular regulation in individuals with motor-complete SCI. *Spinal Cord*, *43*(11), 664–673.

Dobkin, B., Apple, D., Barbeau, H., Basso, M., Behrman, A., Deforge, D., … Scott, M. (2006). Weight-supported treadmill vs over-ground training for walking after acute incomplete SCI. *Neurology*, *66*(4), 484–492.

Du, H., Newton, P. J., Salamonson, Y., Carrieri-Kohlman, V. L., & Davidson, P. M. (2009). A review of the six-minute walk test: Its implication as a self-administered assessment tool. *European Journal of Cardiovascular Nursing*, *8*(1), 2–8. https://doi.org/10.1016/j.ejcnurse.2008.07.001

Dubowsky, S. R., Rasmussen, J., Sisto, S. A., & Langrana, N. A. (2008). Validation of a musculoskeletal model of wheelchair propulsion and its application to minimizing shoulder joint forces. *Journal of Biomechanics*, *41*(14), 2981–2988. https://doi.org/10.1016/j.jbiomech.2008.07.032

Dudek, N. L., Marks, M. B., Marshall, S. C., & Chardon, J. P. (2005). Dermatologic conditions associated with use of a lower-extremity prosthesis. *Archives of Physical Medicine and Rehabilitation*, *86*(4), 659–663. https://doi.org/10.1016/j.apmr.2004.09.003

Emken, J. L., Benitez, R., & Reinkensmeyer, D. J. (2007). Human-robot cooperative movement training: Learning a novel sensory motor transformation during walking with robotic assistance-as-needed. *Journal of NeuroEngineering and Rehabilitation*, *4*(1), 8. https://doi.org/10.1186/1743-0003-4-8

Emken, J. L., Benitez, R., Sideris, A., Bobrow, J. E., & Reinkensmeyer, D. J. (2007). Motor adaptation as a greedy optimization of error and effort. *Journal of Neurophysiology*, *97*(6), 3997–4006.

Emken, J. L., Harkema, S. J., Beres-Jones, J. A., Ferreira, C. K., & Reinkensmeyer, D. J. (2008). Feasibility of manual teach-and-replay and continuous impedance shaping for robotic locomotor training following spinal cord injury. *IEEE Transactions on Bio-Medical Engineering*, *55*(1), 322–334. https://doi.org/10.1109/TBME.2007.910683

Esquenazi, A., Talaty, M., Packel, A., & Saulino, M. (2012). The ReWalk powered exoskeleton to restore ambulatory function to Individuals with thoracic-level motor-complete spinal cord injury: *American Journal of Physical Medicine & Rehabilitation*, *91*(11), 911–921. https://doi.org/10.1097/PHM.0b013e318269d9a3

Fang, J., Mu, Z., Xu, Z., Xie, L., Yang, G.-Y., & Zhang, Q. (2019). Models for temporal-spatial parameters in walking with cadence ratio as the independent variable. *Medical & Biological Engineering & Computing*, *57*(4), 877–886. https://doi.org/10.1007/s11517-018-1919-8

Farah, J. D., Baddour, N., & Lemaire, E. D. (2019). Design, development, and evaluation of a local sensor-based gait phase recognition system using a logistic model decision tree for orthosis-control. *Journal of NeuroEngineering and Rehabilitation*, *16*. https://doi.org/10.1186/s12984-019-0486-z

Farris, R. J., Quintero, H. A., & Goldfarb, M. (2011). Preliminary evaluation of a powered lower limb orthosis to aid walking in paraplegic individuals. *IEEE Transactions on Neural Systems and Rehabilitation Engineering: A Publication of the IEEE Engineering in Medicine and Biology Society*, *19*(6), 652–659. https://doi.org/10.1109/TNSRE.2011.2163083

Farris, R. J., Quintero, H. A., Murray, S. A., Ha, K. H., Hartigan, C., & Goldfarb, M. (2014). A preliminary assessment of legged mobility provided by a lower limb exoskeleton for persons with paraplegia. *IEEE Transactions on Neural Systems and Rehabilitation Engineering : A Publication of the IEEE Engineering in Medicine and Biology Society*, *22*(3), 482. https://doi.org/10.1109/TNSRE.2013.2268320

Farris, R. J., Quintero, H. A., Withrow, T. J., & Goldfarb, M. (2009). Design of a joint-coupled orthosis for FES-aided gait. *2009 IEEE International Conference on Rehabilitation Robotics, ICORR 2009*, 246–252. https://doi.org/10.1109/ICORR.2009.5209623

Ferber, R., Osis, S. T., Hicks, J. L., & Delp, S. L. (2016). Gait biomechanics in the era of data science. *Journal of Biomechanics*, *49*(16), 3759–3761. https://doi.org/10.1016/j.jbiomech.2016.10.033

Ferrati, F., Bortoletto, R., & Pagello, E. (2013). Virtual modelling of a real exoskeleton constrained to a human musculoskeletal model. In N. F. Lepora, A. Mura, H. G. Krapp, P. F. M. J. Verschure, & T. J. Prescott (Eds.), *Biomimetic and Biohybrid Systems* (pp. 96–107). Retrieved from http://link.springer.com/chapter/10.1007/978-3-642-39802-5_9

Fineberg, D. B., Asselin, P., Harel, N. Y., Agranova-Breyter, I., Kornfeld, S. D., Bauman, W. A., & Spungen, A. M. (2013). Vertical ground reaction force-based analysis of powered exoskeleton-assisted walking in persons with motor-complete paraplegia. *The Journal of Spinal Cord Medicine*, *36*(4), 313–321. https://doi.org/10.1179/2045772313Y.0000000126

Flaspöler, E., Hauke, A., & Pappachan, P. (2010). *The human machine interface as an emerging risk.* Retrieved from http://dx.publications.europa.eu/10.2802/21813

Fluit, R., Andersen, M. S., Kolk, S., Verdonschot, N., & Koopman, H. F. J. M. (2014). Prediction of ground reaction forces and moments during various activities of daily living. *Journal of Biomechanics*, *47*(10), 2321–2329. https://doi.org/10.1016/j.jbiomech.2014.04.030

Focke Martinez, S., Kuzmicheva, O., Ristić-Durrant, D., & Graeser, A. (2017). Individualization of Gait Therapy Through Patient-Tailored Trajectory Generation. In J. Ibáñez, J. González-Vargas, J. M. Azorín, M. Akay, & J. L. Pons (Eds.), *Converging Clinical and Engineering Research on Neurorehabilitation II* (Vol. 15, pp. 1393–1397). https://doi.org/10.1007/978-3-319-46669-9_228

Fournier, B. (2018). *Model and Characterization of a Passive Biomimetic Ankle for Lower Extremity Powered Exoskeleton* (Thesis, Université d'Ottawa / University of Ottawa). http://dx.doi.org/10.20381/ruor-21642

Fournier, B. N., Lemaire, E. D., Smith, A. J. J., & Doumit, M. (2018). Modeling and Simulation of a Lower Extremity Powered Exoskeleton. *IEEE Transactions on Neural Systems and Rehabilitation Engineering*, *26*(8), 1596–1603. https://doi.org/10.1109/TNSRE.2018.2854605

Frenkel-Toledo, S., Giladi, N., Peretz, C., Herman, T., Gruendlinger, L., & Hausdorff, J. M. (2005). Effect of gait speed on gait rhythmicity in Parkinson's disease: variability of stride time and swing time respond differently. *Journal of NeuroEngineering and Rehabilitation*, *2*(1), 23. https://doi.org/10.1186/1743-0003-2-23

Fukuchi, C. A., & Duarte, M. (2019). A prediction method of speed-dependent walking patterns for healthy individuals. *Gait & Posture*, *68*, 280–284. https://doi.org/10.1016/j.gaitpost.2018.12.006

Fukuchi, C. A., Fukuchi, R. K., & Duarte, M. (2018). A public dataset of overground and treadmill walking kinematics and kinetics in healthy individuals. *PeerJ*, *6*, e4640. https://doi.org/10.7717/peerj.4640

Fukunaga, T., Kubo, K., Kawakami, Y., Fukashiro, S., Kanehisa, H., & Maganaris, C. N. (2001). In vivo behaviour of human muscle tendon during walking. *Proceedings: Biological Sciences*, *268*(1464), 229–233.

Gagnon, D. H., Escalona, M. J., Vermette, M., Carvalho, L. P., Karelis, A. D., Duclos, C., & Aubertin-Leheudre, M. (2018). Locomotor training using an overground robotic exoskeleton in long-term manual wheelchair users with a chronic spinal cord injury living in the community: Lessons learned from a feasibility study in terms of recruitment, attendance, learnability, performance and safety. *Journal of NeuroEngineering and Rehabilitation*, *15*(1), 12. https://doi.org/10.1186/s12984-018-0354-2

Gagnon, D., Nadeau, S., Noreau, L., Dehail, P., & Gravel, D. (2008). Quantification of reaction forces during sitting pivot transfers performed by individuals with spinal cord injury. *Journal of Rehabilitation Medicine*, *40*(6), 468–476. https://doi.org/10.2340/16501977-0192

Gagnon, D., Nadeau, S., Noreau, L., Dehail, P., & Piotte, F. (2008). Comparison of peak shoulder and elbow mechanical loads during weight-relief lifts and sitting pivot transfers among manual wheelchair users with spinal cord injury. *Journal of Rehabilitation Research and Development*, *45*(6), 863–873.

Gates, D., Darter, B., Dingwell, J., & Wilken, J. (2012). Comparison of walking overground and in a Computer Assisted Rehabilitation Environment (CAREN) in individuals with and without transtibial amputation. *Journal of Neuroengineering and Rehabilitation*, *9*, 81. https://doi.org/10.1186/1743-0003-9-81

Gates, D. H., Darter, B. J., Dingwell, J. B., & Wilken, J. M. (2012). Comparison of walking overground and in a Computer Assisted Rehabilitation Environment (CAREN) in individuals with and without transtibial amputation. *Journal of NeuroEngineering and Rehabilitation*, *9*(1), 81. https://doi.org/10.1186/1743-0003-9-81

Gates, D. H., Dingwell, J. B., Scott, S. J., Sinitski, E. H., & Wilken, J. M. (2012). Gait characteristics of individuals with transtibial amputations walking on a destabilizing rock surface. *Gait & Posture*, *36*(1), 33–39. https://doi.org/10.1016/j.gaitpost.2011.12.019

Gellman, H., Sie, I., & Waters, R. L. (1988). Late complications of the weight-bearing upper extremity in the paraplegic patient. *Clinical Orthopaedics and Related Research*, (233), 132–135.

Giangregorio, L. M., Hicks, A. L., Webber, C. E., Phillips, S. M., Craven, B. C., Bugaresti, J. M., & McCartney, N. (2005). Body weight supported treadmill training in acute spinal cord injury: impact on muscle and bone. *Spinal Cord*, *43*(11), 649–657.

Gordon, K. E., & Ferris, D. P. (2007). Learning to walk with a robotic ankle exoskeleton. *Journal of Biomechanics*, *40*(12), 2636–2644. https://doi.org/10.1016/j.jbiomech.2006.12.006

Grieve, D. W., & Gear, RuthJ. (1966). The relationships between length of stride, step frequency, time of swing and speed of walking for children and adults. *Ergonomics*, *9*(5), 379–399. https://doi.org/10.1080/00140136608964399

Griffin, R., Cobb, T., Craig, T., Daniel, M., Dijk, N. van, Gines, J., … Neuhaus, P. (2017). Stepping Forward with Exoskeletons: Team IHMC?s Design and Approach in the 2016 Cybathlon. *IEEE Robotics Automation Magazine*, *24*(4), 66–74. https://doi.org/10.1109/MRA.2017.2754284

Guan, X., Ji, L., Wang, R., & Huang, W. (2016). Optimization of an unpowered energy-stored exoskeleton for patients with spinal cord injury. *2016 38th Annual International Conference of the IEEE Engineering in Medicine and Biology Society (EMBC)*, 5030–5033. https://doi.org/10.1109/EMBC.2016.7591857

Hak, L., Houdijk, H., Beek, P. J., & Dieën, J. H. van. (2013). Steps to Take to Enhance Gait Stability: The Effect of Stride Frequency, Stride Length, and Walking Speed on Local Dynamic Stability and Margins of Stability. *PLOS ONE*, *8*(12), e82842. https://doi.org/10.1371/journal.pone.0082842

Han, Y., & Wang, X. (2011). The biomechanical study of lower limb during human walking. *Science China Technological Sciences*, *54*(4), 983–991. https://doi.org/10.1007/s11431-011-4318-z

Hanlon, M., & Anderson, R. (2006). Prediction methods to account for the effect of gait speed on lower limb angular kinematics. *Gait & Posture*, *24*(3), 280–287. https://doi.org/10.1016/j.gaitpost.2005.10.007

Harkema, S. J. (2001). Neural plasticity after human spinal cord injury: application of locomotor training to the rehabilitation of walking. *The Neuroscientist*, *7*(5), 455–468. https://doi.org/10.1177/107385840100700514

Harkema, S. J., Hillyer, J., Schmidt-Read, M., Ardolino, E., Sisto, S. A., & Behrman, A. L. (2012). Locomotor Training: As a treatment of spinal cord injury and in the progression of neurologic rehabilitation. *Archives of Physical Medicine and Rehabilitation*, *93*(9), 1588–1597. https://doi.org/10.1016/j.apmr.2012.04.032

Hartigan, C., Kandilakis, C., Dalley, S., Clausen, M., Wilson, E., Morrison, S., … Farris, R. (2015). Mobility Outcomes Following Five Training Sessions with a Powered Exoskeleton. *Topics in Spinal Cord Injury Rehabilitation*, *21*(2), 93–99. https://doi.org/10.1310/sci2102-93

Hassani, W., Mohammed, S., Rifaï, H., & Amirat, Y. (2014). Powered orthosis for lower limb movements assistance and rehabilitation. *Control Engineering Practice*, *26*, 245–253. https://doi.org/10.1016/j.conengprac.2014.02.002

Haubert, L. L., Gutierrez, D. D., Newsam, C. J., Gronley, J. K., Mulroy, S. J., & Perry, J. (2006). A comparison of shoulder joint forces during ambulation with crutches versus a walker in persons with incomplete spinal cord injury. *Archives of Physical Medicine and Rehabilitation*, *87*(1), 63–70. https://doi.org/10.1016/j.apmr.2005.07.311

He, H., & Kiguchi, K. (2008). A study on EMG-based control of exoskeleton robots for human lower-limb motion assist. *Proceedings of the IEEE/EMBS Region 8 International Conference on Information Technology Applications in Biomedicine, ITAB*, 292–295. Retrieved from http://www.scopus.com/inward/record.url?eid=2-s2.0-50049123327&partnerID=40&md5=29415ef8c355aee9611e61b1e2526ce8

Herr, H. (2009). Exoskeletons and orthoses: classification, design challenges and future directions. *Journal of NeuroEngineering and Rehabilitation*, *6*(1), 1. https://doi.org/10.1186/1743-0003-6-21

Hicks, A. L., & Ginis, K. A. M. (2008). Treadmill training after spinal cord injury: It’s not just about the walking. *Journal of Rehabilitation Research & Development*, *45*(2), 241–248.

Hof, A. L., Elzinga, H., Grimmius, W., & Halbertsma, J. P. K. (2002). Speed dependence of averaged EMG profiles in walking. *Gait & Posture*, *16*(1), 78–86.

Holden, J. P., Chou, G., & Stanhope, S. J. (1997). Changes in knee joint function over a wide range of walking speeds. *Clinical Biomechanics*, *12*(6), 375–382.

Holt, K. G., Jeng, S. F., Ratcliffe, R., & Hamill, J. (1995). Energetic Cost and Stability during Human Walking at the Preferred Stride Frequency. *Journal of Motor Behavior*, *27*(2), 164–178. https://doi.org/10.1080/00222895.1995.9941708

Holzbaur, K. R. S., Murray, W. M., & Delp, S. L. (2005). A model of the upper extremity for simulating musculoskeletal surgery and analyzing neuromuscular control. *Annals of Biomedical Engineering*, *33*(6), 829–840.

Huo, W., Mohammed, S., Moreno, J. C., & Amirat, Y. (2016). Lower Limb Wearable Robots for Assistance and Rehabilitation: A State of the Art. *IEEE Systems Journal*, *10*(3), 1068–1081. https://doi.org/10.1109/JSYST.2014.2351491

Hussain, S., Xie, S. Q., & Jamwal, P. K. (2013). Adaptive Impedance Control of a Robotic Orthosis for Gait Rehabilitation. *IEEE Transactions on Cybernetics*, *43*(3), 1025–1034. https://doi.org/10.1109/TSMCB.2012.2222374

Ibarra, J. C. P., Santos, W. M. dos, Krebs, H. I., & Siqueira, A. A. G. (2014). Adaptive impedance control for robot-aided rehabilitation of ankle movements. *5th IEEE RAS/EMBS International Conference on Biomedical Robotics and Biomechatronics*, 664–669. https://doi.org/10.1109/BIOROB.2014.6913854

Ivanenko, Y. P., Poppele, R. E., & Lacquaniti, F. (2004). Five basic muscle activation patterns account for muscle activity during human locomotion. *The Journal of Physiology*, *556*(1), 267–282. https://doi.org/10.1113/jphysiol.2003.057174

Johnson, W. B., Fatone, S., & Gard, S. A. (2009). Walking mechanics of persons who use reciprocating gait orthoses. *Journal of Rehabilitation Research & Development*, *46*(3), 435–446.

Jonsdottir, J., Recalcati, M., Rabuffetti, M., Casiraghi, A., Boccardi, S., & Ferrarin, M. (2009). Functional resources to increase gait speed in people with stroke: Strategies adopted compared to healthy controls. *Gait & Posture*, *29*(3), 355–359. https://doi.org/10.1016/j.gaitpost.2009.01.008

Jung, Y., Jung, M., Ryu, J., Yoon, S., Park, S.-K., & Koo, S. (2016). Dynamically adjustable foot-ground contact model to estimate ground reaction force during walking and running. *Gait & Posture*, *45*, 62–68. https://doi.org/10.1016/j.gaitpost.2016.01.005

Kaelin-Lane, A., Sawaki, L., & Cohen, L. G. (2005). Role of voluntary drive in encoding an elementary motor memory. *Journal of Neurophysiology*, *93*(2), 1099–1103.

Kagawa, T., & Uno, Y. (2009). Gait pattern generation for a power-assist device of paraplegic gait. *Proceedings - IEEE International Workshop on Robot and Human Interactive Communication*, 633–638. https://doi.org/10.1109/ROMAN.2009.5326348

Kahn, L. E., Lum, P. S., Rymer, W. Z., & Reinkensmeyer, D. J. (2006). Robot-assisted movement training for the stroke-impaired arm: Does it matter what the robot does? *Journal of Rehabilitation Research and Development*, *43*(5), 619–630.

Kang, S. J., Ryu, J. C., Moon, I. H., Kim, K. H., & Mun, M. S. (2007). *Walker gait analysis of powered gait orthosis for paraplegic*. *14*, 2889–2891. Retrieved from Scopus.

Kao, P. -C, & Ferris, D. P. (2009). Motor adaptation during dorsiflexion-assisted walking with a powered orthosis. *Gait and Posture*, *29*(2), 230–236.

Kao, Pei-Chun, Lewis, C. L., & Ferris, D. P. (2010a). Invariant ankle moment patterns when walking with and without a robotic ankle exoskeleton. *Journal of Biomechanics*, *43*(2), 203–209. https://doi.org/10.1016/j.jbiomech.2009.09.030

Kao, Pei-Chun, Lewis, C. L., & Ferris, D. P. (2010b). Joint kinetic response during unexpectedly reduced plantar flexor torque provided by a robotic ankle exoskeleton during walking. *Journal of Biomechanics*, *43*(7), 1401–1407. https://doi.org/10.1016/j.jbiomech.2009.12.024

Kerrigan, D. C., Todd, M. K., Della Croce, U., Lipsitz, L. A., & Collins, J. J. (1998). Biomechanical gait alterations independent of speed in the healthy elderly: Evidence for specific limiting impairments. *Archives of Physical Medicine and Rehabilitation*, *79*(3), 317–322. https://doi.org/10.1016/S0003-9993(98)90013-2

Kiguchi, K., & Imada, Y. (2009). EMG-based control for lower-limb power-assist exoskeletons. *2009 IEEE Workshop on Robotic Intelligence in Informationally Structured Space, RiiSS 2009 - Proceedings*, 19–24. Retrieved from http://www.scopus.com/inward/record.url?eid=2-s2.0-67650364776&partnerID=40&md5=78318d349537df4c2aceca9df09a2fed

Kirtley, C., Whittle, M. W., & Jefferson, R. J. (1985). Influence of walking speed on gait parameters. *Journal of Biomedical Engineering*, *7*(4), 282–288. https://doi.org/10.1016/0141-5425(85)90055-X

Knudson, D. (2017). Confidence crisis of results in biomechanics research. *Sports Biomechanics*, *16*(4), 425–433. https://doi.org/10.1080/14763141.2016.1246603

Kolakowsky-Hayner, S. A. (2013). Safety and feasibility of using the eksoTM bionic exoskeleton to aid ambulation after spinal cord injury. *Journal of Spine*. https://doi.org/10.4172/2165-7939.S4-003

Kong, K., Moon, H., Hwang, B., Jeon, D., & Tomizuka, M. (2009). Impedance compensation of SUBAR for back-drivable force-mode actuation. *IEEE Transactions on Robotics*, *25*(3), 512–521.

Kong, K., Moon, H., Jeon, D., & Tomizuka, M. (2010). Control of an exoskeleton for realization of aquatic therapy effects. *IEEE/ASME Transactions on Mechatronics*, *15*(2), 191–200.

Konop, K. A., Strifling, K. M. B., Wang, M., Cao, K., Schwab, J. P., Eastwood, D., … Harris, G. F. (2009). A biomechanical analysis of upper extremity kinetics in children with cerebral palsy using anterior and posterior walkers. *Gait and Posture*, *30*(3), 364–369. https://doi.org/10.1016/j.gaitpost.2009.06.012

Kooij, H. van der, Veneman, J., & Ekkelenkamp, R. (2006). Design of a compliantly actuated exo-skeleton for an impedance controlled gait trainer robot. *2006 International Conference of the IEEE Engineering in Medicine and Biology Society*, 189–193. https://doi.org/10.1109/IEMBS.2006.259397

Koopman, B., van Asseldonk, E. H. F., & van der Kooij, H. (2014). Speed-dependent reference joint trajectory generation for robotic gait support. *Journal of Biomechanics*, *47*(6), 1447–1458. https://doi.org/10.1016/j.jbiomech.2014.01.037

Kozlowski, A. J., Bryce, T. N., & Dijkers, M. P. (2015). Time and Effort Required by Persons with Spinal Cord Injury to Learn to Use a Powered Exoskeleton for Assisted Walking. *Topics in Spinal Cord Injury Rehabilitation*, *21*(2), 110–121. https://doi.org/10.1310/sci2102-110

Krakauer, J. W., Ghilardi, M.-F., & Ghez, C. (1999). Independent learning of internal models for kinematic and dynamic control of reaching. *Nature Neuroscience*, *2*(11), 1026.

Kressler, J., Thomas, C. K., Field-Fote, E. C., Sanchez, J., Widerström-Noga, E., Cilien, D. C., … Nash, M. S. (2014). Understanding therapeutic benefits of overground bionic ambulation: exploratory case series in persons with chronic, complete spinal cord injury. *Archives of Physical Medicine and Rehabilitation*, *95*(10), 1878-1887.e4. https://doi.org/10.1016/j.apmr.2014.04.026

Kubota, S., Nakata, Y., Eguchi, K., Kawamoto, H., Kamibayashi, K., Sakane, M., … Ochiai, N. (2013). Feasibility of rehabilitation training with a newly developed wearable robot for patients with limited mobility. *Archives of Physical Medicine and Rehabilitation*, *94*(6), 1080–1087. https://doi.org/10.1016/j.apmr.2012.12.020

Kulig, K., Newsam, C. J., Mulroy, S. J., Rao, S., Gronley, J. K., Bontrager, E. L., & Perry, J. (2001). The effect of level of spinal cord injury on shoulder joint kinetics during manual wheelchair propulsion. *Clinical Biomechanics (Bristol, Avon)*, *16*(9), 744–751.

Kulig, K., Rao, S. S., Mulroy, S. J., Newsam, C. J., Gronley, J. K., Bontrager, E. L., & Perry, J. (1998). Shoulder joint kinetics during the push phase of wheelchair propulsion. *Clinical Orthopaedics and Related Research*, (354), 132–143.

Kwa, H. K., Noorden, J. H., Missel, M., Craig, T., Pratt, J. E., & Neuhaus, P. D. (2009). Development of the IHMC Mobility Assist Exoskeleton. *IEEE International Conference on Robotics and Automation, 2009. ICRA '09*, 2556–2562. https://doi.org/10.1109/ROBOT.2009.5152394

Lal, S. (1998). Premature degenerative shoulder changes in spinal cord injury patients. *Spinal Cord*, *36*(3), 186–189.

Lapointe, R., Lajoie, Y., Serresse, O., & Barbeau, H. (2001). Functional community ambulation requirements in incomplete spinal cord injured subjects. *Spinal Cord*, *39*(6), 327–335. https://doi.org/10.1038/sj.sc.3101167

Lehmann, J. F., Condon, S. M., de Lateur, B. J., & Smith, J. C. (1985). Gait abnormalities in tibial nerve paralysis: a biomechanical study. *Archives of Physical Medicine and Rehabilitation*, *66*(2), 80–85.

Lelas, J. L., Merriman, G. J., Riley, P. O., & Kerrigan, D. C. (2003). Predicting peak kinematic and kinetic parameters from gait speed. *Gait & Posture*, *17*(2), 106–112. https://doi.org/10.1016/S0966-6362(02)00060-7

Lemaire, E. D., Smith, A. J., Herbert-Copley, A., & Sreenivasan, V. (2017). Lower extremity robotic exoskeleton training: Case studies for complete spinal cord injury walking. *NeuroRehabilitation*, *41*(1), 97–103. https://doi.org/10.3233/NRE-171461

Lemieux, P.-O., Nuño, N., Hagemeister, N., & Tétreault, P. (2012). Mechanical analysis of cuff tear arthropathy during multiplanar elevation with the AnyBody shoulder model. *Clinical Biomechanics (Bristol, Avon)*, *27*(8), 801–806. https://doi.org/10.1016/j.clinbiomech.2012.04.008

Levin, O., Wenderoth, N., Steyvers, M., & Swinnen, S. P. (2003). Directional invariance during loading-related modulations of muscle activity: evidence for motor equivalence. *Experimental Brain Research*, *148*(1), 62–76. https://doi.org/10.1007/s00221-002-1277-4

Lewis, C. L., & Ferris, D. P. (2011). Invariant hip moment pattern while walking with a robotic hip exoskeleton. *Journal of Biomechanics*, *44*(5), 789–793. https://doi.org/10.1016/j.jbiomech.2011.01.030

Li, L., Haddad, J. M., & Hamill, J. (2005). Stability and variability may respond differently to changes in walking speed. *Human Movement Science*, *24*(2), 257–267. https://doi.org/10.1016/j.humov.2005.03.003

Li, Yang, Guan, X., Tong, Y., & Xu, C. (2015). Design and Simulation Study of the Translational-knee Lower Extremity Exoskeleton. *Mechanics*, *21*(3), 207–213. https://doi.org/10.5755/j01.mech.21.3.8795

Li, Ying, Wang, X., Xu, P., Zheng, D., Liu, W., Wang, Y., & Qiao, H. (2013). SolidWorks/SimMechanics-Based Lower Extremity Exoskeleton Modeling Procedure for Rehabilitation. In M. Long (Ed.), *World Congress on Medical Physics and Biomedical Engineering May 26-31, 2012, Beijing, China* (pp. 2058–2061). Retrieved from http://link.springer.com/chapter/10.1007/978-3-642-29305-4_540

Liao, Y., Wang, C., Wu, X., Lu, F., Wang, P., & Cai, S. (2015). On the mechanical design and control of a self-adaptive exoskeleton chair. *2015 IEEE International Conference on Information and Automation*, 937–942. https://doi.org/10.1109/ICInfA.2015.7279421

Little, V. L., McGuirk, T. E., & Patten, C. (2019). Inter-joint and temporal coordination change in very slow walking. *BioRxiv*, 588095. https://doi.org/10.1101/588095

Liu, D.-X., Wu, X., Wang, C., & Chen, C. (2017). Gait trajectory prediction for lower-limb exoskeleton based on Deep Spatial-Temporal Model (DSTM). *2017 2nd International Conference on Advanced Robotics and Mechatronics (ICARM)*, 564–569. https://doi.org/10.1109/ICARM.2017.8273224

Louie, D. R., Eng, J. J., & Lam, T. (2015). Gait speed using powered robotic exoskeletons after spinal cord injury: a systematic review and correlational study. *Journal of NeuroEngineering and Rehabilitation*, *12*(1), 1. https://doi.org/10.1186/s12984-015-0074-9

Low, K. H. (2011). Robot-assisted gait rehabilitation: From exoskeletons to gait systems. *2011 Defense Science Research Conference and Expo (DSR)*, 1–10. https://doi.org/10.1109/DSR.2011.6026886

Luu, T. P., Low, K. H., Qu, X., Lim, H. B., & Hoon, K. H. (2014). An individual-specific gait pattern prediction model based on generalized regression neural networks. *Gait & Posture*, *39*(1), 443–448. https://doi.org/10.1016/j.gaitpost.2013.08.028

Makhsous, M., Rowles, D. M., Rymer, W. Z., Bankard, J., Nam, E. K., Chen, D., & Lin, F. (2007). Periodically relieving ischial sitting load to decrease the risk of pressure ulcers. *Archives of Physical Medicine and Rehabilitation*, *88*(7), 862–870. https://doi.org/10.1016/j.apmr.2007.03.017

Marchal-Crespo, L., & Reinkensmeyer, D. J. (2009). Review of control strategies for robotic movement training after neurologic injury. *Journal of NeuroEngineering and Rehabilitation*, *6*(1). https://doi.org/10.1186/1743-0003-6-20

Martin, A. E., & Schmiedeler, J. P. (2014). Predicting human walking gaits with a simple planar model. *Journal of Biomechanics*, *47*(6), 1416–1421. https://doi.org/10.1016/j.jbiomech.2014.01.035

Martinez, S. F., Kuzmicheva, O., & Gräser, A. (2016). Prediction of characteristic points of hip and knee joint trajectories during overground walking using IMUs and Artificial Neural Networks. *2016 IEEE International Symposium on Medical Measurements and Applications (MeMeA)*, 1–6. https://doi.org/10.1109/MeMeA.2016.7533795

Melis, E. H., Torres-Moreno, R., Barbeau, H., & Lemaire, E. D. (1999). Analysis of assisted-gait characteristics in persons with incomplete spinal cord injury. *Spinal Cord*, *37*(6), 430.

Menz, H. B., Lord, S. R., & Fitzpatrick, R. C. (2003). Age-related differences in walking stability. *Age and Ageing*, *32*(2), 137–142. https://doi.org/10.1093/ageing/32.2.137

Mertz, L. (2012). The next generation of exoskeletons: lighter, cheaper devices are in the works. *IEEE Pulse*, *3*(4), 56–61. https://doi.org/10.1109/MPUL.2012.2196836

Molinari, M. (2009). Plasticity properties of CPG circuits in humans: Impact on gait recovery. *Brain Research Bulletin*, *78*(1), 22–25. https://doi.org/10.1016/j.brainresbull.2008.02.030

Mooney, L. M., & Herr, H. M. (2016). Biomechanical walking mechanisms underlying the metabolic reduction caused by an autonomous exoskeleton. *Journal of NeuroEngineering and Rehabilitation*, *13*. https://doi.org/10.1186/s12984-016-0111-3

Mori, Y., Maejima, K., Inoue, K., Shiroma, N., & Fukuoka, Y. (2011). ABLE: A standing style transfer system for a person with disabled lower limbs (improvement of stability when traveling). *Industrial Robot*, *38*(3), 234–245.

Mori, Y., Okada, J., & Takayama, K. (2006). Development of a standing style transfer system “ABLE” for disabled lower limbs. *IEEE/ASME Transactions on Mechatronics*, *11*(4), 372–380.

Mori, Y., Takayama, K., & Zengo, T. (2008). Development of a standing style transfer system ABLE for a person with disabled lower limbs (design concept and experiments in a standing position). *Nihon Kikai Gakkai Ronbunshu, C Hen/Transactions of the Japan Society of Mechanical Engineers, Part C*, *74*(10), 2570–2576.

Moseley, A. M., Stark, A., Cameron, I. D., & Pollock, A. (2005). Treadmill training and body weight support for walking after stroke. *Cochrane Database of Systematic Reviews (Online)*, (4). Retrieved from http://www.scopus.com/inward/record.url?eid=2-s2.0-33644877651&partnerID=40&md5=394a863f38afb8a11e4259227f30c354

Mulroy, S. J., Farrokhi, S., Newsam, C. J., & Perry, J. (2004). Effects of spinal cord injury level on the activity of shoulder muscles during wheelchair propulsion: an electromyographic study. *Archives of Physical Medicine and Rehabilitation*, *85*(6), 925–934.

Murray, M. P., Kory, R. C., Clarkson, B. H., & Sepic, S. B. (1966). Comparison of free and fast speed walking patterns of normal men. *American Journal of Physical Medicine*, *45*(1), 8–23.

Murray, M. P., Mollinger, L. A., Gardner, G. M., & Sepic, S. B. (1984). Kinematic and EMG patterns during slow, free, and fast walking. *Journal of Orthopaedic Research*, *2*(3), 272–280. https://doi.org/10.1002/jor.1100020309

Murray, M. P., Spurr, G. B., Sepic, S. B., Gardner, G. M., & Mollinger, L. A. (1985). Treadmill vs. floor walking: kinematics, electromyogram, and heart rate. *Journal of Applied Physiology (Bethesda, Md.: 1985)*, *59*(1), 87–91. https://doi.org/10.1152/jappl.1985.59.1.87

Neuhaus, P. D. (2011). Design and evaluation of Mina: A robotic orthosis for paraplegics. *2011 IEEE International Conference on Rehabilitation Robotics*, 1–8.

Nolte, A., Augat, P., & Rasmussen, J. (2008). Analysis of the muscle and joint forces in the shoulder joint using the anybody simulation model. *Journal of Biomechanics*, *41*, 492. https://doi.org/10.1016/S0021-9290(08)70491-3

Nooijen, C., Ter Hoeve, N., & Field-Fote, E. (2009). Gait quality is improved by locomotor training in individuals with SCI regardless of training approach. *Journal of NeuroEngineering and Rehabilitation*, *6*(1). https://doi.org/10.1186/1743-0003-6-36

Noreau, L., Proulx, P., Gagnon, L., Drolet, M., & Laramée, M. T. (2000). Secondary impairments after spinal cord injury: a population-based study. *American Journal of Physical Medicine & Rehabilitation*, *79*(6), 526–535.

Nymark, J. R., Balmer, S. J., Melis, E. H., Lemaire, E. D., & Millar, S. (2005). Electromyographic and kinematic nondisabled gait differences at extremely slow overground and treadmill walking speeds. *Journal of Rehabilitation Research and Development*, *42*(4), 523–534.

Oberg, T., Karsznia, A., & Oberg, K. (1993). Basic gait parameters: reference data for normal subjects, 10-79 years of age. *Journal of Rehabilitation Research and Development*, *30*(2), 210–223.

Oberg, Tommy, & Karsznia, A. (1994). Joint angle parameters in gait: Reference data for normal subjects, 10-79 years of age. *Journal of Rehabilitation Research & Development*, *31*(3), 199.

Ohta, Y., Yano, H., Suzuki, R., Yoshida, M., Kawashima, N., & Nakazawa, K. (2007). A two-degree-of-freedom motor-powered gait orthosis for spinal cord injury patients. *Proceedings of the Institution of Mechanical Engineers, Part H: Journal of Engineering in Medicine*, *221*(6), 629–639. https://doi.org/10.1243/09544119JEIM55

Ong, C. F., Hicks, J. L., & Delp, S. L. (2016). Simulation-Based Design for Wearable Robotic Systems: An Optimization Framework for Enhancing a Standing Long Jump. *IEEE Transactions on Bio-Medical Engineering*, *63*(5), 894–903. https://doi.org/10.1109/TBME.2015.2463077

Opila, K. A., Nicol, A. C., & Paul, J. P. (1987). Upper limb loadings of gait with crutches. *Journal of Biomechanical Engineering*, *109*(4), 285–290.

Otter, A. R. D., Geurts, A. C. H., Mulder, T., & Duysens, J. (2004). Speed related changes in muscle activity from normal to very slow walking speeds. *Gait and Posture*, *19*(3), 270–278.

Pan, D., Gao, F., Miao, Y., & Cao, R. (2015). Co-simulation research of a novel exoskeleton-human robot system on humanoid gaits with fuzzy-PID/PID algorithms. *Advances in Engineering Software*, *79*, 36–46. https://doi.org/10.1016/j.advengsoft.2014.09.005

Pandy, M. G., & Andriacchi, T. P. (2010). Muscle and Joint Function in Human Locomotion. *Annual Review of Biomedical Engineering*, *12*(1), 401–433. https://doi.org/10.1146/annurev-bioeng-070909-105259

Parvataneni, K., Ploeg, L., Olney, S. J., & Brouwer, B. (2009). Kinematic, kinetic and metabolic parameters of treadmill versus overground walking in healthy older adults. *Clinical Biomechanics*, *24*(1), 95–100. https://doi.org/10.1016/j.clinbiomech.2008.07.002

Pentland, W. E., & Twomey, L. T. (1994). Upper limb function in persons with long term paraplegia and implications for independence: Part I. *Paraplegia*, *32*(4), 211–218. https://doi.org/10.1038/sc.1994.40

Pepin, A., Norman, K. E., & Barbeau, H. (2003). Treadmill walking in incomplete spinal-cord-injured subjects: 1. Adaptation to changes in speed. *Spinal Cord*, *41*(5), 257.

Perez-Rizo, E., Trincado-Alonso, F., Pérez-Nombela, S., Del, A.-E., Jiménez-Díaz, F., Lozano-Berrio, V., & Gil-Agudo, A. (2017). Application of a model to analyze shoulder biomechanics in adult patients with spinal cord injury when walking with crutches in two different gait patterns. *NeuroRehabilitation*, *40*(1), 129–140. https://doi.org/10.3233/NRE-161398

Perry, J., & Clark, D. (1997). Biomechanical abnormalities of post-polio patients and the implications for orthotic management. *NeuroRehabilitation*, *8*(2), 119–138. https://doi.org/10.3233/NRE-1997-8206

Perry, J., Fontaine, J. D., & Mulroy, S. (1995). Findings in post-poliomyelitis syndrome. Weakness of muscles of the calf as a source of late pain and fatigue of muscles of the thigh after poliomyelitis. *The Journal of Bone and Joint Surgery. American Volume*, *77*(8), 1148–1153.

Perry, J., Mulroy, S. J., & Renwick, S. E. (1993). The relationship of lower extremity strength and gait parameters in patients with post-polio syndrome. *Archives of Physical Medicine and Rehabilitation*, *74*(2), 165–169.

Perry, Jacquelin, & Burnfield, J. M. (Eds.). (2010). Gait Analysis: Normal and Pathological Function. *Journal of Sports Science & Medicine*, *9*(2), 353–353. Retrieved from PMC. (PMC3761742)

Ploeger, H. E., Bus, S. A., Brehm, M.-A., & Nollet, F. (2014). Ankle-foot orthoses that restrict dorsiflexion improve walking in polio survivors with calf muscle weakness. *Gait & Posture*, *40*(3), 391–398. https://doi.org/10.1016/j.gaitpost.2014.05.016

Quintero, H. A., Farris, R. J., & Goldfarb, M. (2011). Control and implementation of a powered lower limb orthosis to aid walking in paraplegic individuals. *IEEE International Conference on Rehabilitation Robotics*. Presented at the Rehab Week Zurich 2011 - 2011 IEEE International Conference on Rehabilitation Robotics, ICORR 2011. https://doi.org/10.1109/ICORR.2011.5975481

Ragnarsson, K. T. (2008). Functional electrical stimulation after spinal cord injury: current use, therapeutic effects and future directions. *Spinal Cord*, *46*(4), 255–274.

Rajasekaran, V. (2015). Adaptive control for wearable robots in human-centered rehabilitation tasks. *TDX (Tesis Doctorals En Xarxa)*. Retrieved from https://upcommons.upc.edu/handle/2117/96044

Rajasekaran, V., Aranda, J., & Casals, A. (2015a). Adaptive walking assistance based on human-orthosis interaction. *2015 IEEE/RSJ International Conference on Intelligent Robots and Systems (IROS)*, 6190–6195. https://doi.org/10.1109/IROS.2015.7354260

Rajasekaran, V., Aranda, J., & Casals, A. (2015b). Compliant gait assistance triggered by user intention. *2015 37th Annual International Conference of the IEEE Engineering in Medicine and Biology Society (EMBC)*, 3885–3888. https://doi.org/10.1109/EMBC.2015.7319242

Rajasekaran, V., Aranda, J., & Casals, A. (2016). User Intention Driven Adaptive Gait Assistance Using a Wearable Exoskeleton. In L. P. Reis, A. P. Moreira, P. U. Lima, L. Montano, & V. Muñoz-Martinez (Eds.), *Robot 2015: Second Iberian Robotics Conference* (pp. 289–301). Springer International Publishing.

Rajasekaran, V., López-Larraz, E., Trincado-Alonso, F., Aranda, J., Montesano, L., del-Ama, A. J., & Pons, J. L. (2018). Volition-adaptive control for gait training using wearable exoskeleton: preliminary tests with incomplete spinal cord injury individuals. *Journal of NeuroEngineering and Rehabilitation*, *15*(1). https://doi.org/10.1186/s12984-017-0345-8

Ramanujam, A., Momeni, K., Husain, S. R., Augustine, J., Garbarini, E., Barrance, P., … Forrest, G. F. (2018). Mechanisms for improving walking speed after longitudinal powered robotic exoskeleton training for individuals with spinal cord injury. *2018 40th Annual International Conference of the IEEE Engineering in Medicine and Biology Society (EMBC)*, 2805–2808. https://doi.org/10.1109/EMBC.2018.8512821

Rasmussen, J., Zee, M. D., Tørholm, S., & Damsgaard, M. (2007). Comparison of a musculoskeletal shoulder model with in-vivo joint forces. *International Society of Biomechanics 11th Congress: Abstracts*. Retrieved from http://vbn.aau.dk/en/publications/comparison-of-a-musculoskeletal-shoulder-model-with-invivo-joint-forces(87e44700-c030-11dc-a96e-000ea68e967b).html

Reinkensmeyer, D. J., Akoner, O. M., Ferris, D. P., & Gordon, K. E. (2009). Slacking by the human motor system: Computational models and implications for robotic orthoses. *2009 Annual International Conference of the IEEE Engineering in Medicine and Biology Society*, 2129–2132. https://doi.org/10.1109/IEMBS.2009.5333978

Requejo, P. S., Wahl, D. P., Bontrager, E. L., Newsam, C. J., Gronley, J. K., Mulroy, S. J., & Perry, J. (2005). Upper extremity kinetics during Lofstrand crutch-assisted gait. *Medical Engineering & Physics*, *27*(1), 19–29. https://doi.org/10.1016/j.medengphy.2004.08.008

Rex Bionics. (2017). Retrieved from Rex Bionics website: http://www.rexbionics.com/

Riley, P. O., Paolini, G., Della Croce, U., Paylo, K. W., & Kerrigan, D. C. (2007). A kinematic and kinetic comparison of overground and treadmill walking in healthy subjects. *Gait & Posture*, *26*(1), 17–24. https://doi.org/10.1016/j.gaitpost.2006.07.003

Sabes, P. N., Jordan, M. I., & Wolpert, D. M. (1998). The role of inertial sensitivity in motor planning. *The Journal of Neuroscience: The Official Journal of the Society for Neuroscience*, *18*(15), 5948–5957.

Saensook, W., Phonthee, S., Srisim, K., Mato, L., Wattanapan, P., & Amatachaya, S. (2014). Ambulatory assistive devices and walking performance in patients with incomplete spinal cord injury. *Spinal Cord*, *52*(3), 216–219. https://doi.org/10.1038/sc.2013.120

Safaeepour, Z., Esteki, A., Ghomshe, F. T., & Osman, N. A. A. (2014). Quantitative analysis of human ankle characteristics at different gait phases and speeds for utilizing in ankle-foot prosthetic design. *BioMedical Engineering OnLine*, *13*(1), 1–13. https://doi.org/10.1186/1475-925X-13-19

Salbach, N. M., O'Brien, K., Brooks, D., Irvin, E., Martino, R., Takhar, P., … Howe, J.-A. (2014). Speed and Distance Requirements for Community Ambulation: A Systematic Review. *Archives of Physical Medicine and Rehabilitation*, *95*(1), 117-128.e11. https://doi.org/10.1016/j.apmr.2013.06.017

Schablowski-Trautmann, M., & Gerner, H. J. (2006). State-space analysis of joint angle kinematics in normal treadmill walking. *Biomedizinische Technik. Biomedical Engineering*, *51*(5–6), 294–298. https://doi.org/10.1515/BMT.2006.060

Scheidt, R. A., Reinkensmeyer, D. J., Conditt, M. A., Rymer, W. Z., & Mussa-Ivaldi, F. A. (2000). Persistence of Motor Adaptation During Constrained, Multi-Joint, Arm Movements. *Journal of Neurophysiology*, *84*(2), 853–862.

Schmidt, R., & Bjork, R. (1992). New Conceptualizations of Practice: Common Principles in Three Paradigms Suggest New Concepts for Training. *Psychological Science*, *3*(4), 207–217. https://doi.org/10.1111/j.1467-9280.1992.tb00029.x

Schwartz, M. H., Rozumalski, A., & Trost, J. P. (2008). The effect of walking speed on the gait of typically developing children. *Journal of Biomechanics*, *41*(8), 1639–1650. https://doi.org/10.1016/j.jbiomech.2008.03.015

Sekiya, N., & Nagasaki, H. (1998). Reproducibility of the walking patterns of normal young adults: test-retest reliability of the walk ratio(step-length/step-rate). *Gait & Posture*, *7*(3), 225–227. https://doi.org/10.1016/S0966-6362(98)00009-5

Shemmell, J., Johansson, J., Portra, V., Gottlieb, G. L., Thomas, J. S., & Corcos, D. M. (2007). Control of interjoint coordination during the swing phase of normal gait at different speeds. *Journal of NeuroEngineering and Rehabilitation*, *4*(1), 10. https://doi.org/10.1186/1743-0003-4-10

Shi, P., Zhang, Y., & Yang, X. (2008). Lower Extremity Exoskeleton Control and Stability Analysis Based on Virtual Prototyping Technique. *2008 International Conference on Computer Science and Software Engineering*, *1*, 1131–1134. https://doi.org/10.1109/CSSE.2008.1105

Shourijeh, M. S., Jung, M., Ko, S.-T., McGrath, M., Stech, N., & Damsgaard, M. (2017). Simulating Physiological Discomfort of Exoskeletons Using Musculoskeletal Modelling. *Gait & Posture*. https://doi.org/10.1016/j.gaitpost.2017.06.301

Sie, I. H., Waters, R. L., Adkins, R. H., & Gellman, H. (1992). Upper extremity pain in the postrehabilitation spinal cord injured patient. *Archives of Physical Medicine and Rehabilitation*, *73*(1), 44–48.

Silder, A., Heiderscheit, B., & Thelen, D. G. (2008). Active and passive contributions to joint kinetics during walking in older adults. *Journal of Biomechanics*, *41*(7), 1520–1527. https://doi.org/10.1016/j.jbiomech.2008.02.016

Simpson, L. A., Eng, J. J., Hsieh, J. T. C., Wolfe, D. L., & Spinal Cord Injury Rehabilitation Evidence Scire Research Team. (2012). The health and life priorities of individuals with spinal cord injury: a systematic review. *Journal of Neurotrauma*, *29*(8), 1548–1555. https://doi.org/10.1089/neu.2011.2226

Sinitski, E. H., Lemaire, E. D., Baddour, N., Besemann, M., Dudek, N. L., & Hebert, J. S. (2015). Fixed and self-paced treadmill walking for able-bodied and transtibial amputees in a multi-terrain virtual environment. *Gait & Posture*, *41*(2), 568–573. https://doi.org/10.1016/j.gaitpost.2014.12.016

Slavens, B. A., Bhagchandani, N., Wang, M., Smith, P. A., & Harris, G. F. (2011). An upper extremity inverse dynamics model for pediatric Lofstrand crutch-assisted gait. *Journal of Biomechanics*, *44*(11), 2162–2167. https://doi.org/10.1016/j.jbiomech.2011.05.012

Slavens, B. A., Sturm, P. F., Bajournaite, R., & Harris, G. F. (2009). Upper extremity dynamics during Lofstrand crutch-assisted gait in children with myelomeningocele. *Gait & Posture*, *30*(4), 511–517. https://doi.org/10.1016/j.gaitpost.2009.07.125

Slavens, B. A., Sturm, P. F., & Harris, G. F. (2008). Upper extremity kinetics of children with myelomeningocele during Lofstrand crutch-assisted gait. *Conference Proceedings: ... Annual International Conference of the IEEE Engineering in Medicine and Biology Society. IEEE Engineering in Medicine and Biology Society. Annual Conference*, *2008*, 4583–4586. https://doi.org/10.1109/IEMBS.2008.4650233

Slavens, B. A., Sturm, P. F., & Harris, G. F. (2010). Upper extremity inverse dynamics model for crutch-assisted gait assessment. *Journal of Biomechanics*, *43*(10), 2026–2031. https://doi.org/10.1016/j.jbiomech.2010.03.026

Slavens, B. A., Sturm, P. F., Wang, M., & Harris, G. F. (2006). A Dynamic Model of the Upper Extremities for Quantitative Assessment of Lofstrand Crutch-Assisted Gait. *2006 International Conference of the IEEE Engineering in Medicine and Biology Society*, 1525–1528. https://doi.org/10.1109/IEMBS.2006.260646

Smidt, G. L., & Mommens, M. A. (1980). System of reporting and comparing influence of ambulatory aids on gait. *Physical Therapy*, *60*(5), 551–558.

Smith, A., Fournier, B., Lemaire, E., & Nantel, J. (2019). Estimating exoskeleton-human dynamics of persons with spinal cord injury walking with the assistance of a lower extremity powered exoskeleton prototype. *IEEE Transactions on Neural Systems and Rehabilitation Engineering*.

Smith, & Lemaire. (2018). Temporal-spatial gait parameter models of very slow walking. *Gait & Posture*, *61*, 125–129. https://doi.org/10.1016/j.gaitpost.2018.01.003

Smith, Lemaire, & Nantel. (2018). Lower Limb Sagittal Kinematic and Kinetic Modeling of Very Slow Walking for Gait Trajectory Scaling. *PLOS ONE*.

Srikanth, V. K., Fryer, J. L., Zhai, G., Winzenberg, T. M., Hosmer, D., & Jones, G. (2005). A meta-analysis of sex differences prevalence, incidence and severity of osteoarthritis. *Osteoarthritis and Cartilage*, *13*(9), 769–781. https://doi.org/10.1016/j.joca.2005.04.014

Stansfield, Hajarnis, & Sudarshan. (2015). Characteristics of very slow stepping in healthy adults and validity of the activPAL3™ activity monitor in detecting these steps. *Medical Engineering & Physics*, *37*(1), 42–47. https://doi.org/10.1016/j.medengphy.2014.10.003

Stansfield, Hawkins, Adams, & Bhatt. (2018). A mixed linear modelling characterisation of gender and speed related changes in spatiotemporal and kinematic characteristics of gait across a wide speed range in healthy adults. *Medical Engineering and Physics*, *60*, 94–102. https://doi.org/10.1016/j.medengphy.2018.07.015

Stansfield, Hawkins, Adams, & Church. (2018). Spatiotemporal and kinematic characteristics of gait initiation across a wide speed range. *Gait & Posture*, *61*, 331–338. https://doi.org/10.1016/j.gaitpost.2018.02.003

Stansfield, Hillman, Hazlewood, & Robb. (2006). Regression analysis of gait parameters with speed in normal children walking at self-selected speeds. *Gait & Posture*, *23*(3), 288–294. https://doi.org/10.1016/j.gaitpost.2005.03.005

Steinberg, N., Nemet, D., Pantanowitz, M., & Eliakim, A. (2018). Gait Pattern, Impact to the Skeleton and Postural Balance in Overweight and Obese Children: A Review. *Sports*, *6*(3), 75. https://doi.org/10.3390/sports6030075

Stoquart, G., Detrembleur, C., & Lejeune, T. (2008). Effect of speed on kinematic, kinetic, electromyographic and energetic reference values during treadmill walking. *Neurophysiologie Clinique/Clinical Neurophysiology*, *38*(2), 105–116. https://doi.org/10.1016/j.neucli.2008.02.002

Strausser, K. A., Swift, T. A., Zoss, A. B., & Kazerooni, H. (2010). Prototype medical exoskeleton for paraplegic mobility: First experimental results. *ASME 2010 Dynamic Systems and Control Conference, DSCC2010*, *1*, 453–458. Retrieved from http://www.scopus.com/inward/record.url?eid=2-s2.0-79958230320&partnerID=40&md5=1eae2f8441ebf8fc0ca12406dcabdc34

Strickland, E. (2012). Good-bye, wheelchair. *IEEE Spectrum*, *49*(1), 30–32.

Sup, F., Bohara, A., & Goldfarb, M. (2008). Design and Control of a Powered Transfemoral Prosthesis. *The International Journal of Robotics Research*, *27*(2), 263–273. https://doi.org/10.1177/0278364907084588

Sup, F., Varol, H. A., Mitchell, J., Withrow, T. J., & Goldfarb, M. (2009). Self-contained powered knee and ankle prosthesis: Initial evaluation on a transfemoral amputee. *2009 IEEE International Conference on Rehabilitation Robotics*, 638–644. https://doi.org/10.1109/ICORR.2009.5209625

Suzuki, K., Mito, G., Kawamoto, H., Hasegawa, Y., & Sankai, Y. (2007). Intention-based walking support for paraplegia patients with Robot Suit HAL. *Advanced Robotics*, *21*(12), 1441–1469. https://doi.org/10.1163/156855307781746061

Swift, T. A. (2011). *Control and Trajectory Generation of a Wearable Mobility Exoskeleton for Spinal Cord Injury Patients* (UC Berkeley). Retrieved from https://escholarship.org/uc/item/0xc9q3b6

Swift, T. A., Strausser, K. A., Zoss, A. B., & Kazerooni, H. (2010). Control and experimental results for post stroke gait rehabilitation with a prototype mobile medical exoskeleton. *ASME 2010 Dynamic Systems and Control Conference, DSCC2010*, *1*, 405–411. Retrieved from http://www.scopus.com/inward/record.url?eid=2-s2.0-79958210503&partnerID=40&md5=59e7ca375acf8fa30b8327371f504922

Szczesna, A., Blaszczyszyn, M., Pawlyta, M., & Michalczuk, A. (2018). Assessment of Gait Parameters in Virtual Environment. *2018 IEEE 20th International Conference on E-Health Networking, Applications and Services (Healthcom)*, 1–5. https://doi.org/10.1109/HealthCom.2018.8531159

Talaty, M., Esquenazi, A., & Briceno, J. E. (2013). Differentiating ability in users of the ReWalk(TM) powered exoskeleton: an analysis of walking kinematics. *IEEE ... International Conference on Rehabilitation Robotics: [Proceedings]*, *2013*, 6650469. https://doi.org/10.1109/ICORR.2013.6650469

Tamez-Duque, J., Cobian-Ugalde, R., Kilicarslan, A., Venkatakrishnan, A., Soto, R., & Contreras-Vidal, J. L. (2015). Real-time strap pressure sensor system for powered exoskeletons. *Sensors (Basel, Switzerland)*, *15*(2), 4550–4563. https://doi.org/10.3390/s150204550

Tanabe, S., Hirano, S., & Saitoh, E. (2013). Wearable Power-Assist Locomotor (WPAL) for supporting upright walking in persons with paraplegia. *NeuroRehabilitation*, *33*(1), 99–106. https://doi.org/10.3233/NRE-130932

Tanabe, S., Saitoh, E., Hirano, S., Katoh, M., Takemitsu, T., Uno, A., … Suzuki, T. (2013). Design of the Wearable Power-Assist Locomotor (WPAL) for paraplegic gait reconstruction. *Disability and Rehabilitation: Assistive Technology*, *8*(1), 84–91. https://doi.org/10.3109/17483107.2012.688238

Tsukahara, A., Hasegawa, Y., & Sankai, Y. (2009). Standing-up motion support for paraplegic patient with robot suit HAL. *2009 IEEE International Conference on Rehabilitation Robotics, ICORR 2009*, 211–217. https://doi.org/10.1109/ICORR.2009.5209567

Tsukahara, A., Kawanishi, R., Hasegawa, Y., & Sankai, Y. (2010). Sit-to-stand and stand-to-sit transfer support for complete paraplegic patients with robot suit HAL. *Advanced Robotics*, *24*(11), 1615–1638. https://doi.org/10.1163/016918610X512622

Tufekciler, N., van Asseldonk, E. H. F., & van der Kooij, H. (2011). Velocity-dependent reference trajectory generation for the LOPES gait training robot. *IEEE ... International Conference on Rehabilitation Robotics: [Proceedings]*, *2011*, 5975414. https://doi.org/10.1109/ICORR.2011.5975414

Turcato, A. M., Godi, M., Giardini, M., Arcolin, I., Nardone, A., Giordano, A., & Schieppati, M. (2018). Abnormal gait pattern emerges during curved trajectories in high-functioning Parkinsonian patients walking in line at normal speed. *PLOS ONE*, *13*(5), e0197264. https://doi.org/10.1371/journal.pone.0197264

Ulkar, B., Yavuzer, G., Guner, R., & Ergin, S. (2003). Energy expenditure of the paraplegic gait: comparison between different walking aids and normal subjects. *International Journal of Rehabilitation Research. Internationale Zeitschrift Fur Rehabilitationsforschung. Revue Internationale De Recherches De Readaptation*, *26*(3), 213–217. https://doi.org/10.1097/01.mrr.0000088447.78481.d1

Vallery, H., Asseldonk, E. H. F. van, Buss, M., & Kooij, H. van der. (2009). Reference Trajectory Generation for Rehabilitation Robots: Complementary Limb Motion Estimation. *IEEE Transactions on Neural Systems and Rehabilitation Engineering*, *17*(1), 23–30. https://doi.org/10.1109/TNSRE.2008.2008278

van den Bogert, A. J., & Su, A. (2008). A weighted least squares method for inverse dynamic analysis. *Computer Methods in Biomechanics and Biomedical Engineering*, *11*(1), 3–9. https://doi.org/10.1080/10255840701550865

van der Helm, F. C. (1994). A finite element musculoskeletal model of the shoulder mechanism. *Journal of Biomechanics*, *27*(5), 551–569.

van der Helm, F. C. T. (1997). A three-dimensional model of the shoulder and elbow. *Proceedings of the First Conference of the ISG*.

van Hedel, H. J. A., Tomatis, L., & Müller, R. (2006). Modulation of leg muscle activity and gait kinematics by walking speed and bodyweight unloading. *Gait & Posture*, *24*(1), 35–45. https://doi.org/10.1016/j.gaitpost.2005.06.015

Veneman, J., Ekkelenkamp, R., Kruidhof, R., van der Helm, F., & van der Kooij, H. (2006). A Series Elastic- and Bowden-Cable-Based Actuation System for Use as Torque Actuator in Exoskeleton-Type Robots. *The International Journal of Robotics Research*, *25*(3), 261–281. https://doi.org/10.1177/0278364906063829

Viteckova, S., Kutilek, P., & Jirina, M. (2013). Wearable lower limb robotics: A review. *Biocybernetics and Biomedical Engineering*, *33*(2), 96–105. https://doi.org/10.1016/j.bbe.2013.03.005

Wall, J. C., & Charteris, J. (1981). A kinematic study of long-term habituation to treadmill walking. *Ergonomics*, *24*(7), 531–542. https://doi.org/10.1080/00140138108924874

Waters, R. L., Yakura, J. S., Adkins, R., & Barnes, G. (1989). Determinants of gait performance following spinal cord injury. *Archives of Physical Medicine and Rehabilitation*, *70*(12), 811–818.

Wilken, J. M., Rodriguez, K. M., Brawner, M., & Darter, B. J. (2012). Reliability and minimal detectible change values for gait kinematics and kinetics in healthy adults. *Gait & Posture*, *35*(2), 301–307. https://doi.org/10.1016/j.gaitpost.2011.09.105

Winchester, P., McColl, R., Querry, R., Foreman, N., Mosby, J., Tansey, K., & Williamson, J. (2005). Changes in supraspinal activation patterns following robotic locomotor therapy in motor-incomplete spinal cord injury. *Neurorehabilitation and Neural Repair*, *19*(4), 313–324. https://doi.org/10.1177/1545968305281515

Winter, D. A. (1984). Kinematic and kinetic patterns in human gait: Variability and compensating effects. *Human Movement Science*, *3*(1–2), 51–76. https://doi.org/10.1016/0167-9457(84)90005-8

Winter, D. A. (1992). Foot Trajectory in Human Gait: A Precise and Multifactorial Motor Control Task. *Physical Therapy*, *72*(1), 45–53. https://doi.org/10.1093/ptj/72.1.45

Winter, D. A. (1995). Human balance and posture control during standing and walking. *Gait & Posture*, *3*(4), 193–214. https://doi.org/10.1016/0966-6362(96)82849-9

Winter, D. A., Patla, A. E., Frank, J. S., & Walt, S. E. (1990). Biomechanical Walking Pattern Changes in the Fit and Healthy Elderly. *Physical Therapy*, *70*(6), 340–347.

Wolpert, D. M., Ghahramani, Z., & Jordan, M. I. (1995). Are arm trajectories planned in kinematic or dynamic coordinates? An adaptation study. *Experimental Brain Research*, *103*(3), 460–470. https://doi.org/10.1007/BF00241505

Wu, G., van der Helm, F. C. T., (DirkJan) Veeger, H. E. J., Makhsous, M., Van Roy, P., Anglin, C., … Buchholz, B. (2005). ISB recommendation on definitions of joint coordinate systems of various joints for the reporting of human joint motion—Part II: shoulder, elbow, wrist and hand. *Journal of Biomechanics*, *38*(5), 981–992. https://doi.org/10.1016/j.jbiomech.2004.05.042

Yan, T., Cempini, M., Oddo, C. M., & Vitiello, N. (2015). Review of assistive strategies in powered lower-limb orthoses and exoskeletons. *Robotics and Autonomous Systems*, *64*, 120–136. https://doi.org/10.1016/j.robot.2014.09.032

Yang, A., Asselin, P., Knezevic, S., Kornfeld, S., & Spungen, A. M. (2015). Assessment of In-Hospital Walking Velocity and Level of Assistance in a Powered Exoskeleton in Persons with Spinal Cord Injury. *Topics in Spinal Cord Injury Rehabilitation*, *21*(2), 100–109. https://doi.org/10.1310/sci2102-100

Yang, M., Xu, Z., Liu, Y., He, Y., & Xu, Y. (2013). Perceiving and predicting the intended motion with human-machine interaction force for walking assistive exoskeleton robot. *2013 IEEE International Conference on Mechatronics and Automation (ICMA)*, 805–810. https://doi.org/10.1109/ICMA.2013.6618019

Zeilig, G., Weingarden, H., Zwecker, M., Dudkiewicz, I., Bloch, A., & Esquenazi, A. (2012). Safety and tolerance of the ReWalk^{TM} exoskeleton suit for ambulation by people with complete spinal cord injury: A pilot study. *The Journal of Spinal Cord Medicine*, *35*(2), 96–101. https://doi.org/10.1179/2045772312Y.0000000003

Zörner, B., Blanckenhorn, W. U., Dietz, V., EM-SCI Study Group, & Curt, A. (2010). Clinical algorithm for improved prediction of ambulation and patient stratification after incomplete spinal cord injury. *Journal of Neurotrauma*, *27*(1), 241–252. https://doi.org/10.1089/neu.2009.0901

Chapter 8. Appendices

Table 8-1 Stride parameters. Standard deviation (SD), Confidence interval (CI), coefficient of variation (CV), self-pace (SP). Supporting material Chapter 3.

Parameter	Speed (m/s)	Mean	SD	Max	Min	CV	95% CI
Stride-time (s)	0.20	2.91	0.56	4.25	1.51	0.19	2.71-3.11
	0.30	2.28	0.78	3.22	2.31	0.34	1.99-2.56
	0.40	1.91	0.65	2.43	1.94	0.34	1.67-2.15
	0.50	1.69	0.57	2.05	1.73	0.34	1.48-1.89
	0.60	1.52	0.51	1.82	1.55	0.33	1.34-1.71
	0.70	1.41	0.46	1.76	1.44	0.33	1.24-1.58
	0.80	1.33	0.43	1.55	1.35	0.33	1.17-1.48
	SP	1.05	0.34	1.21	1.06	0.32	0.93-1.17
Step-time (s)	0.20	1.44	0.28	2.18	0.75	0.19	1.34-1.54
	0.30	1.13	0.15	1.60	0.78	0.13	1.07-1.19
	0.40	0.95	0.10	1.15	0.69	0.11	0.91-0.98
	0.50	0.84	0.08	1.00	0.66	0.10	0.81-0.87
	0.60	0.75	0.07	0.92	0.61	0.09	0.73-0.78
	0.70	0.70	0.06	0.86	0.60	0.09	0.68-0.73
	0.80	0.66	0.05	0.77	0.59	0.07	0.64-0.68
	SP	0.53	0.03	0.59	0.48	0.06	0.51-0.54
Stance-time (s)	0.20	2.31	0.51	3.73	1.17	0.22	2.12-2.50
	0.30	1.70	0.26	2.40	1.15	0.15	1.61-1.80
	0.40	1.38	0.18	1.83	0.97	0.13	1.31-1.44
	0.50	1.17	0.13	1.48	0.90	0.11	1.12-1.22
	0.60	1.04	0.10	1.27	0.86	0.10	1.00-1.07
	0.70	0.94	0.09	1.18	0.79	0.09	0.91-0.97
	0.80	0.87	0.07	1.05	0.73	0.08	0.85-0.90
	SP	0.64	0.07	0.79	0.55	0.10	0.62-0.66
Swing-time (s)	0.20	0.60	0.13	1.06	0.34	0.22	0.55-0.65
	0.30	0.58	0.09	0.83	0.38	0.15	0.54-0.61
	0.40	0.54	0.05	0.65	0.41	0.10	0.52-0.56
	0.50	0.51	0.06	0.69	0.40	0.13	0.49-0.54
	0.60	0.48	0.06	0.66	0.34	0.13	0.46-0.51
	0.70	0.47	0.05	0.61	0.39	0.12	0.45-0.49
	0.80	0.45	0.04	0.55	0.38	0.09	0.44-0.47
	SP	0.41	0.02	0.45	0.35	0.05	0.40-0.42
Double-leg-support-time (s)	0.20	0.84	0.24	1.66	0.41	0.29	0.75-0.93
	0.30	0.55	0.11	0.82	0.37	0.20	0.51-0.59
	0.40	0.41	0.07	0.57	0.27	0.17	0.38-0.44
	0.50	0.32	0.05	0.46	0.24	0.16	0.30-0.34
	0.60	0.27	0.04	0.37	0.20	0.14	0.26-0.28
	0.70	0.23	0.04	0.33	0.15	0.16	0.22-0.25
	0.80	0.21	0.03	0.28	0.15	0.15	0.19-0.22
	SP	0.12	0.03	0.19	0.07	0.27	0.11-0.13

Parameter	Speed (m/s)	Mean	SD	Max	Min	CV	95% CI
Single-leg-support-time (s)	0.20	0.63	0.13	1.05	0.34	0.21	0.58-0.68
	0.30	0.59	0.09	0.83	0.37	0.15	0.56-0.62
	0.40	0.55	0.07	0.75	0.40	0.12	0.53-0.58
	0.50	0.53	0.08	0.71	0.40	0.14	0.50-0.56
	0.60	0.50	0.06	0.66	0.41	0.12	0.47-0.52
	0.70	0.48	0.06	0.66	0.38	0.13	0.46-0.50
	0.80	0.46	0.05	0.57	0.39	0.10	0.45-0.48
	SP	0.41	0.02	0.46	0.37	0.05	0.40-0.42
Stride-Length (m)	0.20	0.58	0.11	0.83	0.31	0.18	0.54-0.61
	0.30	0.68	0.09	0.95	0.45	0.14	0.64-0.71
	0.40	0.75	0.08	0.90	0.54	0.11	0.72-0.78
	0.50	0.83	0.09	1.00	0.64	0.10	0.80-0.86
	0.60	0.90	0.08	1.07	0.73	0.09	0.87-0.93
	0.70	0.97	0.09	1.23	0.82	0.09	0.94-1.00
	0.80	1.05	0.08	1.25	0.93	0.08	1.02-1.08
	SP	1.40	0.15	1.81	1.09	0.11	1.34-1.45
Step-Length (m)	0.20	0.29	0.06	0.43	0.15	0.19	0.27-0.31
	0.30	0.34	0.04	0.48	0.24	0.13	0.32-0.35
	0.40	0.38	0.04	0.45	0.26	0.10	0.36-0.39
	0.50	0.41	0.04	0.50	0.31	0.11	0.40-0.43
	0.60	0.45	0.04	0.53	0.37	0.10	0.43-0.46
	0.70	0.49	0.05	0.64	0.41	0.09	0.47-0.50
	0.80	0.52	0.04	0.65	0.45	0.08	0.51-0.54
	SP	0.70	0.08	0.91	0.56	0.11	0.68-0.73
Step-frequency (steps/s)	0.20	0.73	0.17	1.34	0.46	0.23	0.67-0.79
	0.30	0.90	0.12	1.28	0.63	0.14	0.86-0.95
	0.40	1.08	0.12	1.46	0.87	0.11	1.03-1.12
	0.50	1.21	0.13	1.53	1.00	0.10	1.16-1.25
	0.60	1.34	0.12	1.64	1.09	0.09	1.29-1.38
	0.70	1.43	0.12	1.66	1.16	0.08	1.39-1.48
	0.80	1.53	0.11	1.69	1.29	0.07	1.49-1.57
	SP	1.91	0.05	2.09	1.69	0.02	1.89-1.93

Table 8-2 Maximum sagittal plane kinematics and kinetics parameter regression equations for cadence.(c). Supporting information for Chapter 4.

Parameter	Peak	Linear Equation	R^2	Quadratic Equation 2nd Order	R^2	Quadratic Equation 3rd Order	R^2
Ankle Angle	AAx1	$y = 2.10c + -9.7$	0.36	$y = 5.24c^2 - 8.28c - 5.03$	0.29	$y = -15.85c^3 + 51.69c^2 - 51.03c + 7.34$	0.30
	AAx2	$y = -2.76c + 14.95$	0.43	$y = -3.53c^2 + 4.22c + 11.80$	0.48	$y = 22.2c^3 - 68.59c^2 + 64.1c - 5.52$	0.56
	AAx3	$y = 12.62c + -21.46$	0.65	$y = -24.70c^2 + 61.55c - 43.50$	0.75	$y = 59.35c^3 - 198.64c^2 + 221.62c - 89.82$	0.76
	AAx4	$y = 4.14c + -0.45$	0.55	$y = 0.3c^2 + 3.56c - 0.18$	0.53	$y = -24.61c^3 + 72.41c^2 - 62.81c + 19.02$	0.56
	AAxRG	$y = -11.04c + 35$	0.69	$y = 14.75c^2 - 40.26c + 48.16$	0.73	$y = -29.76c^3 + 101.97c^2 - 120.53c + 71.38$	0.73
Knee Angle	KAx1	$y = 3.65c + -1.75$	0.37	$y = 10.11c^2 - 16.37c + 7.27$	0.38	$y = -30.25c^3 + 98.76c^2 - 97.96c + 30.88$	0.41
	KAx2	$y = -7.96c + 14.71$	0.48	$y = 34.75c^2 - 76.8c + 45.71$	0.68	$y = -75.01c^3 + 254.58c^2 - 279.1c + 104.25$	0.72
	KAx3	$y = -2.86c + 3.21$	0.42	$y = 6.81c^2 - 16.35c + 9.29$	0.50	$y = -13.75c^3 + 47.11c^2 - 53.43c + 20.02$	0.51
	KAx4	$y = -16.47c + 69.8$	0.82	$y = 17.04c^2 - 50.22c + 85$	0.83	$y = -14.15c^3 + 58.52c^2 - 88.39c + 96.05$	0.84
	KAxRG	$y = -19.03c + 74.81$	0.86	$y = 16.42c^2 - 51.55c + 89.46$	0.86	$y = 0.95c^3 + 13.62c^2 - 48.98c + 88.72$	0.87
Hip Angle	HAx1	$y = -7.42c + 23.18$	0.67	$y = 13.24c^2 - 33.65c + 35$	0.77	$y = -30.3c^3 + 102.03c^2 - 115.36c + 58.64$	0.80
	HAx2	$y = 7.29c + -18.02$	0.69	$y = -16.95c^2 + 40.87c - 33.14$	0.81	$y = 42.07c^3 - 140.25c^2 + 154.34c - 65.97$	0.84
	HAx3	$y = -6.82c + 25.52$	0.67	$y = 11.04c^2 - 28.70c + 35.37$	0.74	$y = -9.62c^3 + 39.25c^2 - 54.66c + 42.88$	0.74
	HAxRG	$y = -14.14c + 43.68$	0.78	$y = 28.06c^2 - 69.71c + 68.71$	0.90	$y = -52.35c^3 + 181.48c^2 - 210.91c + 109.57$	0.91
Ankle Moment	AMx1	$y = 0.16c + -0.25$	0.75	$y = -0.33c^2 + 0.81c - 0.54$	0.86	$y = 0.75c^3 - 2.53c^2 + 2.84c - 1.12$	0.88
	AMx2	$y = -0.78c + 1.7$	0.87	$y = 1.28c^2 - 3.32c + 2.85$	0.94	$y = -2.1c^3 + 7.44c^2 - 8.98c + 4.49$	0.94
Knee Moment	KMx1	$y = 0.18c + -0.32$	0.66	$y = -0.37c^2 + 0.91c - 0.65$	0.77	$y = 0.55c^3 - 1.98c^2 + 2.40c - 1.08$	0.78
	KMx2	$y = -0.48c + 0.62$	0.59	$y = 1.50c^2 - 3.45c + 1.95$	0.83	$y = -3.73c^3 + 12.43c^2 - 13.51c + 4.86$	0.88
	KMx3	$y = 0.11c + -0.36$	0.43	$y = -0.30c^2 + 0.71c - 0.63$	0.51	$y = 0.76c^3 - 2.53c^2 + 2.76c - 1.23$	0.54
	KMx4	$y = -0.1c + 0.19$	0.58	$y = 0.25c^2 - 0.60c + 0.41$	0.72	$y = -0.54c^3 + 1.83c^2 - 2.05c + 0.83$	0.73
Hip Moment	HMx1	$y = -0.56c + 0.85$	0.70	$y = 1.49c^2 - 3.52c + 2.18$	0.91	$y = -3.42c^3 + 11.53c^2 - 12.75c + 4.86$	0.94
	HMx2	$y = 0.52c + -0.84$	0.75	$y = -1.22c^2 + 2.92c - 1.92$	0.92	$y = 2.89c^3 - 9.69c^2 + 10.72c - 4.18$	0.95
	HMx3	$y = -0.3c + 0.42$	0.73	$y = 0.74c^2 - 1.77c + 1.08$	0.91	$y = -1.45c^3 + 5.00c^2 - 5.68c + 2.21$	0.93
Ankle Power	APx1	$y = 0.40c + -0.52$	0.62	$y = -1.19c^2 + 2.77c - 1.58$	0.88	$y = 3.27c^3 - 10.78c^2 + 11.59c - 4.14$	0.95
	APx2	$y = 0.80c + -1.26$	0.84	$y = -0.75c^2 + 2.29c - 1.93$	0.84	$y = -1.27c^3 + 2.98c^2 - 1.15c - 0.94$	0.87
	APx3	$y = -3.07c + 3.94$	0.73	$y = 8.10c^2 - 19.12c + 11.16$	0.95	$y = -17.89c^3 + 60.52c^2 - 67.36c + 25.12$	0.98
Knee Power	KPx1	$y = -0.42c + 0.5$	0.60	$y = 1.31c^2 - 3.00c + 1.67$	0.86	$y = -3.13c^3 + 10.48c^2 - 11.45c + 4.11$	0.90
	KPx2	$y = 0.65c + -0.79$	0.50	$y = -2.39c^2 + 5.38c - 2.92$	0.82	$y = 6.81c^3 - 22.35c^2 + 23.75c - 8.24$	0.92
	KPx3	$y = -0.47c + 0.69$	0.70	$y = 1.14c^2 - 2.73c + 1.70$	0.85	$y = -2.36c^3 + 8.06c^2 - 9.10c + 3.54$	0.87
	KPx4	$y = 0.74c + -1.03$	0.71	$y = -1.87c^2 + 4.45c - 2.70$	0.89	$y = 4.53c^3 - 15.14c^2 + 16.67c - 6.23$	0.93
Hip Power	HPx1	$y = -0.57c + 0.79$	0.68	$y = 1.37c^2 - 3.28c + 2.01$	0.82	$y = -2.92c^3 + 9.93c^2 - 11.16c + 4.29$	0.84
	HPx2	$y = 0.42c + -0.56$	0.62	$y = -1.23c^2 + 2.86c - 1.66$	0.87	$y = 3.6c^3 - 11.80c^2 + 12.58c - 4.48$	0.96
	HPx3	$y = -0.72c + 1$	0.75	$y = 1.76c^2 - 4.20c + 2.56$	0.92	$y = -3.99c^3 + 13.45c^2 - 14.97c + 5.68$	0.95

Table 8-3 Maximum sagittal plane kinematics and kinetics parameter regression equations for stride-length (l).

Parameter	Peak	Linear Equation	R^2	Quadratic Equation 2nd Order	R^2	Quadratic Equation 3rd Order	R^2
Ankle Angle	AAx1	$y = -1.18l - 6.81$	0.37	$y = 10.4l^2 - 21.82l + 2.73$	0.30	$y = -12.58l^3 + 47.46l^2 - 56.39l + 12.97$	0.30
	AAx2	$y = 1.97l + 10.77$	0.38	$y = -11.86l^2 + 25.51l - 0.12$	0.54	$y = -4.89l^3 + 2.53l^2 + 12.08l + 3.86$	0.57
	AAx3	$y = -17.05l + 4.84$	0.72	$y = -4.05l^2 - 9.02l + 1.13$	0.76	$y = 7.49l^3 - 26.09l^2 + 11.55l - 4.96$	0.75
	AAx4	$y = -3.74l + 6.53$	0.51	$y = 13l^2 - 29.54l + 18.46$	0.52	$y = 23.49l^3 - 56.2l^2 + 35.03l - 0.65$	0.56
	AAxRG	$y = 13.66l + 13.11$	0.72	$y = -4.92l^2 + 23.43l + 8.59$	0.73	$y = 2.63l^3 - 12.67l^2 + 30.65l + 6.45$	0.73
Knee Angle	KAx1	$y = -1.88l + 3.13$	0.36	$y = 19.44l^2 - 40.46l + 20.97$	0.41	$y = -17.58l^3 + 71.22l^2 - 88.77l + 35.27$	0.41
	KAx2	$y = 13.93l - 4.72$	0.58	$y = 23.13l^2 - 31.97l + 16.51$	0.72	$y = -42.48l^3 + 148.25l^2 - 148.71l + 51.07$	0.72
	KAx3	$y = 4.04l - 2.9$	0.47	$y = 1.81l^2 + 0.44l - 1.24$	0.52	$y = -7.61l^3 + 24.22l^2 - 20.47l + 4.95$	0.52
	KAx4	$y = 19.15l + 38.25$	0.82	$y = -17.63l^2 + 54.12l + 22.08$	0.83	$y = -24.98l^3 + 55.95l^2 - 14.53l + 42.4$	0.84
	KAxRG	$y = 21.42l + 38.99$	0.84	$y = -25.72l^2 + 72.45l + 15.39$	0.85	$y = -34.27l^3 + 75.21l^2 - 21.73l + 43.26$	0.87
Hip Angle	HAx1	$y = 9.78l + 7.94$	0.76	$y = 1.14l^2 + 7.52l + 8.98$	0.80	$y = 3.22l^3 - 8.34l^2 + 16.37l + 6.37$	0.81
	HAx2	$y = -10.38l - 2.34$	0.79	$y = -6.56l^2 + 2.65l - 8.37$	0.85	$y = -4.61l^3 + 7.02l^2 - 10.03l - 4.62$	0.85
	HAx3	$y = 8.54l + 11.91$	0.72	$y = -3.39l^2 + 15.27l + 8.8$	0.74	$y = -18.69l^3 + 51.64l^2 - 36.09l + 24$	0.74
	HAxRG	$y = 18.95l + 14.34$	0.87	$y = 3.32l^2 + 12.37l + 17.39$	0.92	$y = -13.29l^3 + 42.45l^2 - 24.14l + 28.2$	0.92
Ankle Moment	AMx1	$y = -0.22l + 0.09$	0.84	$y = -0.07l^2 - 0.08l + 0.03$	0.89	$y = -0.01l^3 - 0.05l^2 - 0.09l + 0.03$	0.89
	AMx2	$y = 1l + 0.13$	0.93	$y = -0.17l^2 + 1.33l - 0.03$	0.94	$y = -0.51l^3 + 1.33l^2 - 0.07l + 0.39$	0.94
Knee Moment	KMx1	$y = -0.25l + 0.06$	0.73	$y = -0.02l^2 - 0.2l + 0.04$	0.77	$y = 0.28l^3 - 0.84l^2 + 0.56l - 0.19$	0.77
	KMx2	$y = 0.75l - 0.47$	0.72	$y = 0.86l^2 - 0.96l + 0.32$	0.89	$y = -0.41l^3 + 2.06l^2 - 2.08l + 0.65$	0.89
	KMx3	$y = -0.16l - 0.12$	0.48	$y = -0.18l^2 + 0.19l - 0.28$	0.54	$y = -0.29l^3 + 0.68l^2 - 0.61l - 0.05$	0.54
	KMx4	$y = 0.14l - 0.02$	0.66	$y = 0.09l^2 - 0.04l + 0.06$	0.73	$y = -0.2l^3 + 0.69l^2 - 0.6l + 0.23$	0.73
Hip Moment	HMx1	$y = 0.82l - 0.38$	0.82	$y = 0.66l^2 - 0.49l + 0.23$	0.94	$y = -0.21l^3 + 1.28l^2 - 1.07l + 0.41$	0.94
	HMx2	$y = -0.73l + 0.27$	0.87	$y = -0.45l^2 + 0.16l - 0.15$	0.95	$y = -0.11l^3 - 0.14l^2 - 0.13l - 0.06$	0.96
	HMx3	$y = 0.42l - 0.22$	0.84	$y = 0.25l^2 - 0.08l + 0.01$	0.93	$y = -0.4l^3 + 1.42l^2 - 1.17l + 0.33$	0.93
Ankle Power	APx1	$y = -0.62l + 0.39$	0.77	$y = -0.73l^2 + 0.83l - 0.28$	0.95	$y = -0.71l^3 + 1.35l^2 - 1.11l + 0.3$	0.95
	APx2	$y = -0.89l + 0.24$	0.81	$y = 1.25l^2 - 3.37l + 1.39$	0.84	$y = 3.01l^3 - 7.63l^2 + 4.92l - 1.07$	0.88
	APx3	$y = 4.49l - 2.77$	0.86	$y = 3.31l^2 - 2.09l + 0.27$	0.98	$y = -3.69l^3 + 14.19l^2 - 12.24l + 3.28$	0.98
Knee Power	KPx1	$y = 0.65l - 0.44$	0.72	$y = 0.73l^2 - 0.79l + 0.22$	0.90	$y = -0.6l^3 + 2.5l^2 - 2.45l + 0.71$	0.90
	KPx2	$y = -1.1l + 0.76$	0.64	$y = -1.79l^2 + 2.46l - 0.88$	0.91	$y = -0.91l^3 + 0.9l^2 - 0.05l - 0.14$	0.93
	KPx3	$y = 0.67l - 0.33$	0.80	$y = 0.39l^2 - 0.1l + 0.03$	0.87	$y = 0l^3 + 0.39l^2 - 0.1l + 0.03$	0.87
	KPx4	$y = -1.08l + 0.59$	0.83	$y = -0.78l^2 + 0.46l - 0.13$	0.93	$y = 0.26l^3 - 1.54l^2 + 1.17l - 0.34$	0.93
Hip Power	HPx1	$y = 0.81l - 0.44$	0.77	$y = 0.47l^2 - 0.13l - 0.01$	0.84	$y = 0.07l^3 + 0.26l^2 + 0.07l - 0.06$	0.84
	HPx2	$y = -0.65l + 0.39$	0.77	$y = -0.79l^2 + 0.91l - 0.33$	0.95	$y = -0.9l^3 + 1.88l^2 - 1.57l + 0.4$	0.96
	HPx3	$y = 1.03l - 0.56$	0.87	$y = 0.63l^2 - 0.22l + 0.02$	0.95	$y = -0.49l^3 + 2.06l^2 - 1.55l + 0.41$	0.95

Table 8-4 Kinematic parameters. Standard deviation (SD), coefficient of variation (CV), self-pace (SP). Slow walking kinematics Chapter 4.

	Speed (m/s)	Mean	SD	Max	Min	CV
Ankle angle peak 1 (degrees)	0.20	-6.27	5.54	2.26	-19.72	0.88
	0.30	-7.29	4.86	-1.25	-7.04	0.67
	0.40	-7.95	4.47	-3.13	-8.05	0.56
	0.50	-8.37	4.08	-3.18	-8.71	0.49
	0.60	-8.61	4.22	-3.67	-8.98	0.49
	0.70	-8.46	4.87	-1.40	-8.56	0.58
	0.80	-8.49	4.76	-0.84	-8.65	0.56
	SP	-7.49	5.27	0.87	-7.46	0.70
Ankle angle peak 2 (degrees)	0.20	10.81	4.78	15.26	-5.83	0.44
	0.30	11.57	4.69	16.04	-4.23	0.40
	0.40	12.34	4.80	16.69	-3.96	0.39
	0.50	12.84	4.80	17.55	-3.69	0.37
	0.60	13.18	5.13	17.97	-4.68	0.39
	0.70	13.62	5.24	18.47	-4.65	0.38
	0.80	13.57	5.18	18.92	-5.67	0.38
	SP	12.32	5.51	17.75	-6.70	0.45
Ankle angle peak 3 (degrees)	0.20	-5.39	9.29	6.78	-27.77	1.72
	0.30	-7.17	8.70	5.46	-27.91	1.21
	0.40	-8.00	9.88	4.06	-31.51	1.23
	0.50	-8.68	8.10	0.49	-26.95	0.93
	0.60	-10.30	8.12	-2.19	-30.87	0.79
	0.70	-11.14	8.56	0.59	-32.18	0.77
	0.80	-13.29	8.27	-3.73	-34.29	0.62
	SP	-19.37	7.78	-4.96	-42.04	0.40
Ankle angle peak 4 (degrees)	0.20	5.32	5.36	12.75	-14.57	1.01
	0.30	4.61	4.84	12.24	-12.75	1.05
	0.40	3.95	4.63	10.18	-12.51	1.17
	0.50	3.19	5.36	10.81	-17.11	1.68
	0.60	2.36	5.16	9.34	-17.84	2.19
	0.70	1.87	5.20	8.47	-18.51	2.78
	0.80	1.44	5.12	8.77	-19.10	3.55
	SP	2.71	5.65	8.55	-19.24	2.08
Ankle angle range (degrees)	0.20	20.43	5.82	31.49	11.26	0.29
	0.30	22.25	5.29	33.25	12.37	0.24
	0.40	23.78	6.93	48.20	14.37	0.29
	0.50	24.36	5.55	40.33	13.87	0.23
	0.60	25.62	5.80	38.73	14.70	0.23
	0.70	26.68	6.03	40.38	17.70	0.23
	0.80	27.81	6.05	43.63	16.39	0.22
	SP	31.74	5.32	43.90	22.55	0.17

	Speed (m/s)	Mean	SD	Max	Min	CV
Knee angle peak 1 (degrees)	0.20	4.30	4.93	20.83	-2.81	1.15
	0.30	2.57	4.55	15.80	-4.15	1.77
	0.40	0.90	4.13	10.78	-4.64	4.59
	0.50	0.63	4.15	9.38	-6.14	6.59
	0.60	0.48	3.98	9.23	-4.93	8.35
	0.70	0.27	4.33	9.32	-7.23	16.28
	0.80	0.05	3.40	6.26	-8.67	66.28
	SP	2.36	3.36	8.26	-5.24	1.42
Knee angle peak 2 (degrees)	0.20	6.32	5.89	29.30	-1.02	0.93
	0.30	5.40	5.72	23.84	-2.49	1.06
	0.40	4.76	5.76	18.92	-4.42	1.21
	0.50	5.55	5.97	18.20	-5.36	1.08
	0.60	6.37	5.89	18.66	-3.55	0.93
	0.70	7.37	6.31	18.95	-5.70	0.86
	0.80	9.30	5.75	19.54	-6.12	0.62
	SP	16.87	3.80	26.72	7.35	0.23
Knee angle peak 3 (degrees)	0.20	-0.30	4.25	12.69	-8.15	14.39
	0.30	-0.06	4.06	10.48	-7.54	63.38
	0.40	-0.09	4.08	10.34	-7.68	47.08
	0.50	0.49	3.97	10.15	-7.18	8.03
	0.60	0.44	4.00	10.72	-8.27	9.01
	0.70	0.83	4.03	10.32	-6.62	4.88
	0.80	1.48	3.69	9.71	-6.60	2.49
	SP	2.88	3.36	10.17	-4.15	1.16
Knee angle peak 4 (degrees)	0.20	47.77	6.76	64.80	35.76	0.14
	0.30	50.92	4.83	64.03	43.84	0.09
	0.40	52.39	5.05	65.18	44.63	0.10
	0.50	54.22	4.84	66.41	44.04	0.09
	0.60	56.49	4.20	67.79	49.19	0.07
	0.70	58.26	4.77	70.63	50.71	0.08
	0.80	59.92	4.73	72.34	52.59	0.08
	SP	63.17	4.11	71.12	54.83	0.07
Knee angle range (degrees)	0.20	49.18	6.93	64.97	34.44	0.14
	0.30	52.77	5.23	63.47	42.59	0.10
	0.40	54.78	5.36	64.87	45.64	0.10
	0.50	57.06	5.15	66.07	45.45	0.09
	0.60	59.85	4.61	68.44	50.05	0.08
	0.70	61.75	4.54	72.25	51.82	0.07
	0.80	63.67	4.50	72.99	53.18	0.07
	SP	66.23	4.30	72.48	58.50	0.06

	Speed (m/s)	Mean	SD	Max	Min	CV
Hip angle peak 1 (degrees)	0.20	13.67	3.43	20.38	8.16	0.25
	0.30	14.63	3.61	22.21	7.37	0.25
	0.40	15.52	3.40	22.50	9.19	0.22
	0.50	15.75	3.54	21.80	9.46	0.22
	0.60	16.75	3.95	24.17	9.57	0.24
	0.70	17.45	4.00	24.12	10.57	0.23
	0.80	18.03	4.15	25.50	10.66	0.23
	SP	21.77	5.69	32.68	8.00	0.26
Hip angle peak 2 (degrees)	0.20	-8.99	4.36	-0.75	-18.96	0.48
	0.30	-9.50	4.39	-0.36	-19.35	0.46
	0.40	-10.35	4.36	-0.67	-18.98	0.42
	0.50	-10.72	4.51	-1.58	-20.67	0.42
	0.60	-11.30	4.48	-2.35	-20.27	0.40
	0.70	-11.78	4.43	-4.04	-20.91	0.38
	0.80	-12.87	4.70	-4.24	-24.65	0.37
	SP	-17.55	6.11	-4.63	-34.50	0.35
Hip angle peak 3 (degrees)	0.20	16.82	3.53	25.90	10.65	0.21
	0.30	17.40	3.68	25.62	10.05	0.21
	0.40	18.20	3.58	26.72	11.51	0.20
	0.50	18.72	3.77	26.82	11.58	0.20
	0.60	19.86	3.93	27.93	12.74	0.20
	0.70	20.69	4.06	28.85	13.66	0.20
	0.80	21.27	3.89	30.14	13.64	0.18
	SP	23.43	5.66	33.09	9.55	0.24
Hip angle range (degrees)	0.20	25.92	4.61	40.03	17.10	0.18
	0.30	27.02	4.22	39.80	20.90	0.16
	0.40	28.69	4.05	41.18	22.57	0.14
	0.50	29.56	4.16	40.32	21.45	0.14
	0.60	31.27	3.64	39.93	25.54	0.12
	0.70	32.59	3.94	42.68	27.17	0.12
	0.80	34.26	3.40	43.25	28.57	0.10
	SP	41.14	3.43	46.82	32.84	0.08

Table 8-5 Kinetic parameters. Standard deviation (SD), coefficient of variation (CV), self-pace (SP). Slow walking kinetics Chapter 4.

	Speed (m/s)	**Mean**	**SD**	**Max**	**Min**	**CV**
Ankle moment peak 1 (Nm/kg)	0.20	-0.04	0.02	0.00	-0.09	0.57
	0.30	-0.06	0.03	-0.01	-0.06	0.53
	0.40	-0.08	0.04	-0.02	-0.08	0.49
	0.50	-0.09	0.06	-0.02	-0.09	0.64
	0.60	-0.10	0.05	-0.04	-0.10	0.53
	0.70	-0.12	0.06	-0.05	-0.13	0.47
	0.80	-0.13	0.07	-0.05	-0.14	0.51
	SP	-0.22	0.07	-0.06	-0.23	0.32
Ankle moment peak 2 (Nm/kg)	0.20	0.70	0.16	1.00	0.42	0.23
	0.30	0.79	0.16	1.11	0.54	0.21
	0.40	0.86	0.18	1.14	0.46	0.21
	0.50	0.96	0.18	1.24	0.60	0.18
	0.60	1.04	0.17	1.34	0.67	0.16
	0.70	1.11	0.16	1.39	0.76	0.15
	0.80	1.19	0.14	1.43	0.85	0.12
	SP	1.51	0.18	2.03	1.11	0.12
Knee moment peak 1 (Nm/kg)	0.20	-0.09	0.04	-0.02	-0.18	0.40
	0.30	-0.10	0.04	-0.03	-0.25	0.39
	0.40	-0.13	0.05	-0.03	-0.25	0.36
	0.50	-0.14	0.05	-0.01	-0.22	0.36
	0.60	-0.16	0.07	-0.06	-0.33	0.43
	0.70	-0.19	0.06	-0.05	-0.31	0.34
	0.80	-0.20	0.07	-0.03	-0.35	0.34
	SP	-0.29	0.13	0.04	-0.70	0.45
Knee moment peak 2 (Nm/kg)	0.20	0.06	0.17	0.82	-0.14	3.10
	0.30	0.06	0.14	0.60	-0.19	2.21
	0.40	0.08	0.15	0.54	-0.16	1.86
	0.50	0.11	0.16	0.51	-0.13	1.45
	0.60	0.13	0.17	0.54	-0.15	1.28
	0.70	0.21	0.21	0.78	-0.11	0.99
	0.80	0.26	0.20	0.74	-0.09	0.77
	SP	0.66	0.18	1.02	0.39	0.28
Knee moment peak 3 (Nm/kg)	0.20	-0.23	0.15	0.03	-0.57	0.63
	0.30	-0.23	0.15	0.05	-0.58	0.66
	0.40	-0.24	0.14	0.01	-0.56	0.59
	0.50	-0.25	0.14	0.02	-0.55	0.57
	0.60	-0.27	0.15	-0.01	-0.60	0.57
	0.70	-0.26	0.15	0.03	-0.62	0.56
	0.80	-0.27	0.14	-0.01	-0.62	0.51
	SP	-0.37	0.14	-0.08	-0.67	0.39

	Speed (m/s)	Mean	SD	Max	Min	CV
Knee moment peak 4 (Nm/kg)	0.20	0.07	0.03	0.14	0.01	0.47
	0.30	0.08	0.03	0.13	0.03	0.36
	0.40	0.08	0.04	0.20	0.04	0.47
	0.50	0.09	0.03	0.20	0.05	0.38
	0.60	0.10	0.03	0.18	0.05	0.33
	0.70	0.11	0.04	0.20	0.05	0.35
	0.80	0.12	0.04	0.22	0.05	0.36
	SP	0.18	0.05	0.32	0.09	0.29
Hip moment peak 1 (Nm/kg)	0.20	0.18	0.07	0.36	0.02	0.42
	0.30	0.20	0.07	0.37	0.05	0.34
	0.40	0.23	0.07	0.37	0.03	0.31
	0.50	0.27	0.07	0.38	0.07	0.27
	0.60	0.33	0.11	0.56	0.12	0.32
	0.70	0.40	0.10	0.61	0.17	0.25
	0.80	0.44	0.12	0.72	0.15	0.27
	SP	0.84	0.25	1.57	0.45	0.29
Hip moment peak 2 (Nm/kg)	0.20	-0.20	0.09	-0.05	-0.39	0.44
	0.30	-0.24	0.10	-0.05	-0.50	0.41
	0.40	-0.28	0.10	-0.12	-0.52	0.34
	0.50	-0.33	0.11	-0.12	-0.58	0.33
	0.60	-0.36	0.10	-0.19	-0.60	0.28
	0.70	-0.42	0.11	-0.22	-0.66	0.25
	0.80	-0.47	0.12	-0.22	-0.69	0.25
	SP	-0.80	0.17	-0.51	-1.12	0.21
Hip moment peak 3 (Nm/kg)	0.20	0.06	0.04	0.17	0.01	0.70
	0.30	0.06	0.05	0.20	0.01	0.70
	0.40	0.09	0.05	0.23	0.01	0.58
	0.50	0.11	0.05	0.26	0.03	0.46
	0.60	0.14	0.06	0.30	0.07	0.40
	0.70	0.18	0.05	0.28	0.07	0.29
	0.80	0.21	0.05	0.35	0.11	0.24
	SP	0.39	0.11	0.68	0.19	0.27
Ankle power peak 1 (W/kg)	0.20	-0.04	0.02	-0.01	-0.12	0.55
	0.30	-0.05	0.03	-0.02	-0.13	0.49
	0.40	-0.07	0.03	-0.03	-0.18	0.45
	0.50	-0.11	0.06	-0.03	-0.35	0.58
	0.60	-0.13	0.06	-0.04	-0.31	0.47
	0.70	-0.17	0.08	-0.05	-0.37	0.46
	0.80	-0.19	0.10	-0.06	-0.45	0.52
	SP	-0.56	0.26	-0.18	-1.29	0.47

	Speed (m/s)	Mean	SD	Max	Min	CV
Ankle power peak 2 (W/kg)	0.20	-0.20	0.05	-0.09	-0.30	0.24
	0.30	-0.29	0.08	-0.17	-0.51	0.26
	0.40	-0.40	0.10	-0.26	-0.76	0.25
	0.50	-0.52	0.14	-0.33	-1.07	0.26
	0.60	-0.62	0.16	-0.37	-1.20	0.25
	0.70	-0.75	0.21	-0.37	-1.42	0.28
	0.80	-0.81	0.23	-0.44	-1.71	0.29
	SP	-0.87	0.28	-0.43	-1.53	0.33
Ankle power peak 3 (W/kg)	0.20	0.23	0.09	0.45	0.07	0.37
	0.30	0.37	0.14	0.72	0.16	0.38
	0.40	0.53	0.20	1.19	0.26	0.38
	0.50	0.76	0.24	1.41	0.47	0.32
	0.60	1.07	0.28	1.91	0.69	0.26
	0.70	1.42	0.34	2.35	0.97	0.24
	0.80	1.78	0.34	2.60	1.14	0.19
	SP	3.83	0.73	5.59	2.21	0.19
Knee power peak 1 (W/kg)	0.20	0.01	0.02	0.07	-0.04	1.21
	0.30	0.02	0.02	0.06	-0.01	0.83
	0.40	0.03	0.02	0.08	0.00	0.75
	0.50	0.06	0.05	0.28	0.00	0.94
	0.60	0.09	0.09	0.47	-0.04	1.00
	0.70	0.14	0.11	0.40	0.00	0.74
	0.80	0.20	0.15	0.64	0.01	0.76
	SP	0.53	0.30	1.42	0.11	0.57
Knee power peak 2 (W/kg)	0.20	-0.05	0.08	-0.01	-0.44	1.54
	0.30	-0.04	0.04	0.00	-0.18	0.87
	0.40	-0.06	0.04	0.00	-0.16	0.70
	0.50	-0.09	0.06	0.00	-0.29	0.69
	0.60	-0.12	0.09	-0.01	-0.46	0.77
	0.70	-0.19	0.16	-0.01	-0.73	0.82
	0.80	-0.26	0.25	-0.03	-0.96	0.96
	SP	-0.96	0.42	-0.33	-2.12	0.44
Knee power peak 3 (W/kg)	0.20	0.11	0.09	0.51	0.02	0.82
	0.30	0.13	0.08	0.34	0.12	0.67
	0.40	0.17	0.10	0.45	0.15	0.62
	0.50	0.21	0.09	0.49	0.19	0.42
	0.60	0.26	0.12	0.64	0.24	0.47
	0.70	0.30	0.11	0.64	0.27	0.38
	0.80	0.34	0.14	0.72	0.31	0.42
	SP	0.65	0.20	1.07	0.67	0.30

	Speed (m/s)	Mean	SD	Max	Min	CV
Hip power peak 1 (W/kg)	0.20	0.09	0.04	0.19	0.01	0.47
	0.30	0.12	0.06	0.30	0.02	0.49
	0.40	0.16	0.07	0.37	0.01	0.42
	0.50	0.21	0.09	0.41	0.02	0.44
	0.60	0.28	0.13	0.67	0.05	0.47
	0.70	0.34	0.15	0.61	0.07	0.45
	0.80	0.36	0.19	0.76	0.06	0.52
	SP	0.75	0.32	1.76	0.27	0.44
Hip power peak 2 (W/kg)	0.20	-0.06	0.04	-0.01	-0.17	0.73
	0.30	-0.08	0.06	0.00	-0.23	0.73
	0.40	-0.11	0.07	-0.02	-0.30	0.66
	0.50	-0.13	0.08	-0.01	-0.33	0.58
	0.60	-0.15	0.09	-0.03	-0.39	0.61
	0.70	-0.19	0.10	-0.04	-0.44	0.52
	0.80	-0.23	0.11	-0.06	-0.48	0.48
	SP	-0.61	0.19	-0.28	-0.94	0.32
Hip power peak 3 (W/kg)	0.20	0.11	0.04	0.20	0.05	0.33
	0.30	0.16	0.05	0.29	0.08	0.30
	0.40	0.20	0.05	0.30	0.10	0.26
	0.50	0.26	0.06	0.38	0.14	0.24
	0.60	0.33	0.08	0.52	0.17	0.24
	0.70	0.41	0.08	0.62	0.22	0.21
	0.80	0.50	0.14	0.88	0.22	0.27
	SP	0.95	0.26	1.64	0.43	0.27